Hydrodynamics of soft active matter

M. C. Marchetti*

Physics Department and Syracuse Biomaterials Institute, Syracuse University, Syracuse, New York 13244, USA

J. F. Joanny

Physicochimie Curie (CNRS-UMR168 and Université Pierre et Marie Curie), Institut Curie Section de Recherche, 26 rue d'Ulm, 75248 Paris Cedex, 05 France

S. Ramaswamy

Department of Physics, Indian Institute of Science, Bangalore, 560 12 India and TIFR Centre for Interdisciplinary Sciences, Tata Institute of Fundamental Research, 21 Brundavan Colony Narsingi, Hyderabad 500 075 India

T. B. Liverpool

School of Mathematics, University of Bristol, Bristol, BS8 1TW United Kingdom

J. Prost

Physicochimie Curie (CNRS-UMR168 and Université Pierre et Marie Curie), Institut Curie Section de Recherche 26 rue d'Ulm, 75248 Paris Cedex, 05 France and E.S.P.C.I, 10 rue Vauquelin, 75231 Paris Cedex 05 France

Madan Rao

Raman Research Institute, Bangalore, 560 080 India and National Centre for Biological Sciences (TIFR), Bangalore, 560065 India

R. Aditi Simha

Department of Physics, Indian Institute of Technology Madras, Chennai 600 036 India

(published 19 July 2013)

This review summarizes theoretical progress in the field of active matter, placing it in the context of recent experiments. This approach offers a unified framework for the mechanical and statistical properties of living matter: biofilaments and molecular motors *in vitro* or *in vivo*, collections of motile microorganisms, animal flocks, and chemical or mechanical imitations. A major goal of this review is to integrate several approaches proposed in the literature, from semimicroscopic to phenomenological. In particular, first considered are "dry" systems, defined as those where momentum is not conserved due to friction with a substrate or an embedding porous medium. The differences and similarities between two types of orientationally ordered states, the nematic and the polar, are clarified. Next, the active hydrodynamics of suspensions or "wet" systems is discussed and the relation with and difference from the dry case, as well as various large-scale instabilities of these nonequilibrium states of matter, are highlighted. Further highlighted are various large-scale instabilities of these nonequilibrium states of matter. Various semimicroscopic derivations of the continuum theory are discussed and connected, highlighting the unifying and generic nature of the continuum model. Throughout the review, the experimental relevance of these theories for describing bacterial swarms and suspensions, the cytoskeleton of living cells, and vibrated granular material is discussed. Promising extensions toward greater realism in specific contexts from cell biology to animal behavior are suggested, and remarks are given on some exotic active-matter analogs. Last, the outlook for a quantitative understanding of active matter, through the interplay of detailed theory with controlled experiments on simplified systems, with living or artificial constituents, is summarized.

DOI: 10.1103/RevModPhys.85.1143 PACS numbers: 05.65.+b, 87.18.Hf, 82.70.−y, 87.16.Ln

CONTENTS

*mcm@phy.syr.edu

I. INTRODUCTION

The goal of this article is to introduce the reader to a general framework and viewpoint for the study of the mechanical and statistical properties of living matter and of some remarkable nonliving imitations on length scales from subcellular to oceanic. The ubiquitous nonequilibrium condensed systems that this review is concerned with (Toner, Tu, and Ramaswamy, 2005; Jülicher *et al.*, 2007; Joanny and Prost, 2009a; Ramaswamy, 2010) have come to be known as *active matter*. Their unifying characteristic is that they are composed of self-driven units, active particles, each capable of converting stored or ambient free energy into systematic movement (Schweitzer, 2003). The interaction of active particles with each other, and with the medium they live in, gives rise to highly correlated collective motion and mechanical stress. Active particles are generally elongated and their direction of self-propulsion is set by their own anisotropy, rather than fixed by an external field. Orientational order is thus a theme that runs through much of the active-matter narrative as can be seen, for instance, in the image of a swarm of myxobacteria, shown in Fig. 1. The biological systems of interest to us include *in vitro* mixtures of cell extracts of biofilaments and associated motor proteins (see Fig. 2), the whole cytoskeleton of living cells, bacterial suspensions (see Fig. 3), cell layers (see Fig. 4), and terrestrial, aquatic (see Fig. 5), and aerial flocks. Nonliving active matter arises in layers of vibrated granular rods, colloidal or nanoscale particles propelled through a fluid by catalytic activity at their surface (see Fig. 6), and collections of robots. A distinctive, indeed, defining feature of active systems compared to more familiar nonequilibrium systems is the fact that the energy input that drives the system out of equilibrium is local, for example, at the level of each particle, rather than at the

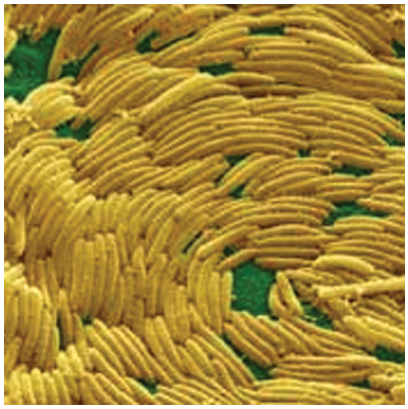

FIG. 1 (color). Liquid-crystalline order in a myxobacterial flock. Figure from Gregory Velicer (Indiana University Bloomington) and Juergen Bergen (Max-Planck Institute for Developmental Biology).

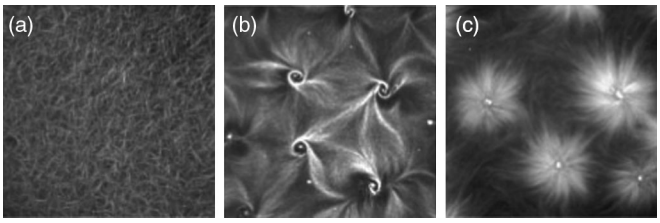

FIG. 2. Patterns organized *in vitro* by the action of multimeric kinesin complexes on microtubules, imaged by dark-field microscopy. The concentration of motor proteins increases from left to right. (a) A disordered array of microtubules. The other two images display motor-induced organization in (b) spiral and (c) aster patterns. The bright spots in the images correspond to the minus end of microtubules. These remarkable experiments from Surrey *et al.* (2001) led the way to the study of pattern formation in active systems. Adapted from Surrey *et al.*, 2001.

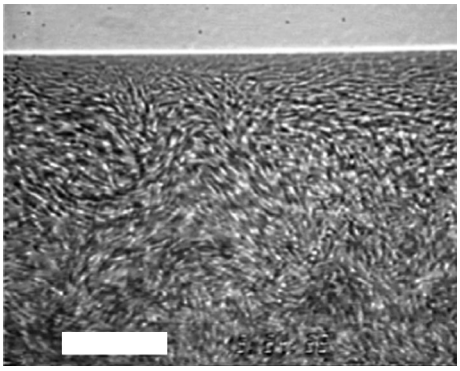

FIG. 3. Bacterial "turbulence" in a sessile drop of *Bacillus subtilis* viewed from below through the bottom of a petri dish. Gravity is perpendicular to the plane of the picture, and the horizontal white line near the top is the air-water-plastic contact line. The central fuzziness is due to collective motion, not quite captured at the frame rate of 1/30 s. The scale bar is 35 μm. Adapted from Dombrowski *et al.*, 2004.

system's boundaries as in a shear flow. Each active particle consumes and dissipates energy going through a cycle that fuels internal changes, generally leading to motion. Active systems exhibit a wealth of intriguing nonequilibrium properties, including emergent structures with collective behavior qualitatively different from that of the individual constituents, bizarre fluctuation statistics, nonequilibrium order-disorder transitions, pattern formation on mesoscopic scales, unusual mechanical and rheological properties, and wave propagation and sustained oscillations even in the absence of inertia in the strict sense.

Living systems, of course, provide the preeminent example of active matter, exhibiting extraordinary properties such as reproduction, adaptation, spontaneous motion, and dynamical organization, including the ability to generate and to respond in a calibrated manner to forces.

A theoretical description of the general properties of living matter is not currently achievable because of its overall complexity, with the detailed state of a cell determined by a hopelessly large number of variables. In a given living organism there are at most 300 different cell types, which may appear as a relatively small number. The behavior of each cell is, however, affected by a myriad of internal and external

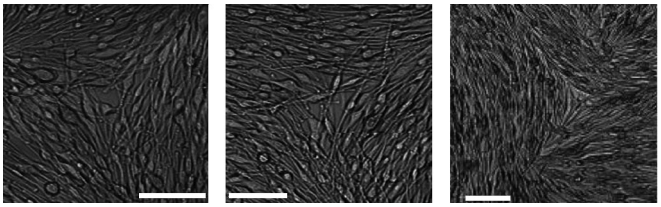

FIG. 4. A disclination defect of strength $m = -1/2$ formed by human melanocytes on a plastic surface. The bars are 100 μm. The three images show three different situations: (i) the core of the defect is an area free of cells (left), (ii) the core of the disclination is an area with isotropically distributed cells (center), and (iii) the core of the defect is occupied by a star-shaped cell (right). The cells that form the nematoid order are in an elongated state. From Kemkemer *et al.*, 2000.

FIG. 5 (color). A remarkable demonstration of polar order in a sardine school. Figure from Jon Bertsch, from underwater images from the Sea of Cortez: http://www.thalassagraphics.com/blog/?p=167.

signals and stimuli, rendering the accessible parameter space immense. Perhaps, therefore, global principles such as conservation laws and symmetries constrain the possible dynamical behaviors of cells or, indeed, of organisms and populations, such as collections of bacteria (see Fig. 3), fish schools (see Fig. 5), and bird flocks. Quantifying the spontaneous dynamical organization and motion of living systems is the first step toward understanding in a generic way some of these principles, by focusing on specific questions that are accessible to theory. This has proven to be the case for the long-wavelength behavior of active membranes (Prost and Bruinsma, 1996; Ramaswamy, Toner, and Prost, 2000; Manneville *et al.*, 2001; Ramaswamy and Rao, 2001), the general theory of flocking (Toner and Tu, 1995, 1998; Toner, Tu, and Ramaswamy, 2005), and the macroscopic mechanical properties of the cytoskeleton as an active gel (Kruse *et al.*, 2005; Jülicher *et al.*, 2007). Agent-based models offer a minimal approach to the study of active systems, with an emphasis on order and fluctuations rather than forces and mechanics. In such a setting, seminal studies of flocking as a phase transition were first carried out by Vicsek *et al.* (1995) [see also the computer-animation work of Reynolds (1987)], with important modifications and extensions by Grégoire and Chaté (2004), Chaté, Ginelli, and Montagne (2006), and Chaté, Ginelli, Grégoire, Peruani, and Raynaud (2008). These models describe point particles with fixed speed moving on an inert background. The direction of motion changes according to a noisy local rule that requires particles to align with their neighbors at each time step. This family of models displays a well-defined transition from a disordered to an ordered phase with decreasing noise strength or increasing density. In the context of the cytoskeleton activated by motor proteins, detailed simulations of ensembles of semiflexible filaments on which motor bundles can exert force dipoles have also been carried out by several authors (Mogilner and Oster, 1996; Nédélec *et al.*, 1997; Pinot *et al.*, 2009; Head, Briels, and Gompper, 2011).

In this article we will not review the agent-based models and the wealth of results obtained by numerical simulations, but rather focus on identifying generic aspects of the large-scale behavior of active systems and characterizing their material properties. Many of the macroscopic properties

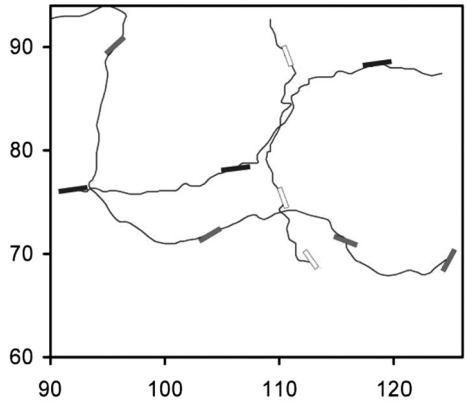

FIG. 6. Colloids that swim: Hydrogen peroxide is oxidized to generate protons in solution and electrons in the wire on the platinum end of micron-sized gold-platinum wires. The protons and electrons are then consumed with the reduction of H_2O_2 on the gold end. The resulting ion flux induces an electric field and motion of the particle relative to the fluid, propelling the particle toward the platinum end at speeds of tens of microns a second. On longer time scales the rods tumble due to thermal or other noise; the resulting motion is thus a persistent random walk. From Paxton *et al.*, 2004.

of active systems are universal, in the sense that systems operating at widely differing length scales, with significant differences in their detailed dynamics at the microscopic level, display broadly similar properties. Visually similar flocking phenomena are seen in fish shoals (Parrish and Hamner, 1997) and collections of keratocytes (Szabó *et al.*, 2006). Contractile stresses are evident on a subcellular scale in the cytoskeleton (see Fig. 7) (Bendix *et al.*, 2008; Joanny and Prost, 2009a), as well as on a scale of many cells in swimming algae (Rafaï, Jibuti, and Peyla, 2010). The hope is to be able to classify active matter in a small number of

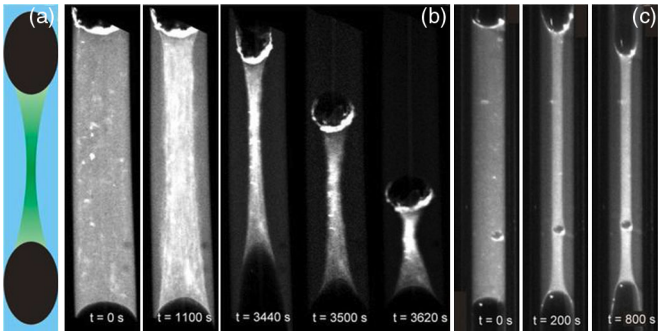

FIG. 7 (color online). Measurement of contractile stresses in cell (Xenopus oocyte) extracts and a reconstituted actomyosin gel made using skeletal muscle myosin II thick filaments: (a) Schematic of active gel in a narrow glass capillary (inner diameter, 400 μm) sandwiched between two oil droplets. (b) Confocal fluorescence images of the network at five different time points show that the active gel first pulls away from the capillary walls and deforms the oil droplets as it contracts before reaching a breaking point when the gel collapses. (c) Dark-field images of contracting cell extract shows the same behavior. Analysis of the deformation of the oil droplet gives an estimate of the contractile force exerted by the actin gel, which consists of bundles of actin filaments cross-linked by α-actinin. This force is around 1 μN or 100 pN per actin bundle. Adapted from Bendix *et al.*, 2008.

universality classes, based on considerations of symmetry and conservation laws, each with a well-defined macroscopic behavior. We consider here four classes of active matter according to the nature of the broken symmetry of the ordered phase and the type of momentum damping. First the broken symmetry: elongated self-propelled objects are in general polar entities with distinct heads and tails, which can cooperatively order either in a polar (ferromagnetic) phase or in a nematic phase. In a polar phase, all the microscopic objects are on average aligned in the same direction; this is the case for bacteria or fish. The polar order is described by a vector order parameter $\mathbf{p}$, known as the polarization. Nematic ordering can be obtained in two ways, either in systems where polar self-propelled objects are parallel but with random head-tail orientations or in systems where the self-propelled particles are themselves head-tail symmetric such as the melanocytes that distribute pigment in the skin. Nematic order is described by a tensor order parameter $\mathbf{Q}$, known as the alignment tensor. The polar-apolar distinction in the context of living matter is brought out clearly by contrasting the pattern of microtubules and kinesin shown in Fig. 2 to those formed by melanocytes shown in Fig. 4. Next, the nature of damping: in a bulk fluid, active or otherwise, viscosity damps the relative motion of neighboring regions, which means that the total momentum of the system is conserved. In systems in contact with a substrate, e.g., restricted to lie on a surface or between two closely spaced walls, or moving through a porous medium, the drag due to the substrate dominates, simply either through no slip or through binding and unbinding of constituents of the systems to the confining medium, and the momentum of the fluid is not conserved.[1] Active particles in a viscous fluid of viscosity η and experiencing a frictional drag γ can in general be described as a system with or without momentum conservation, depending on the physical parameters, such as the density of active particles, and the length scales of interest. If the fluid can be treated as an inert medium, providing only friction, then the collection of active particles that transfer momentum to the fluid can be modeled as a system with overdamped dynamics and no momentum conservation. We refer below to systems that can be described by models with no momentum conservation as "dry." In contrast, when solvent-mediated hydrodynamic interactions are important, the dynamics of the suspending fluid must be incorporated in the model and one must develop a description of the suspension of active particles and fluid, with conserved total momentum. We refer to systems described by models with momentum conservation, where fluid flow is important, as "wet." Although below we often refer to various systems as wet or dry, we stress that this distinction refers to the model used, rather than to the system itself, and also to the length scales of interest, as in general hydrodynamic flows can be neglected only on length scales larger than $\sqrt{\eta/\gamma}$. For instance, actin filaments in motility assays as in the experiments by Schaller *et al.* (2010) have been described as dry systems, where momentum is not conserved, as the filaments exchange momentum with the cover slip, but hydrodynamic

[1]Of course the momentum of the entire system consisting of fluid plus substrate is always conserved.

TABLE I. Examples of active systems classified according to symmetry and to the relevance of momentum conservation (wet or dry).

	Nematic	Polar
Dry	Melanocytes (Kemkemer *et al.*, 2000) Vibrated granular rods (Narayan, Ramaswamy, and Menon, 2007)	Migrating animal herds (Parrish and Hamner, 1997) Migrating cell layers (Serra-Picamal *et al.*, 2012) Vibrated asymmetric granular particles (Kudrolli *et al.*, 2008) Films of cytoskeletal extracts (Surrey *et al.*, 2001)
Wet	Suspensions of catalytic colloidal rods (Paxton *et al.*, 2004)	Cell cytoskeleton and cytoskeletal extracts in bulk suspensions (Bendix *et al.*, 2008) Swimming bacteria in bulk (Dombrowski *et al.*, 2004) Pt catalytic colloids (Palacci *et al.*, 2010)

interactions may be important on some length scales (Schaller, Weber, Frey, and Bausch, 2011). Conversely, it was recently argued that the complex turbulent flows of dense bacterial suspensions are well described by a model of an incompressible fluid with overdamped dynamics, effectively equivalent to what is referred to as a dry model in this review (Wensink *et al.*, 2012). Table I summarizes various examples of active systems classified according to symmetry and to whether they may be described by models with or without momentum conservation (wet or dry).

A useful theoretical framework to describe the macroscopic properties of active matter is provided by the methods of nonequilibrium statistical mechanics. In a generalized hydrodynamic approach,[2] a coarse-grained description of the large-scale, long-time behavior of the system is given in terms of a small number of continuum fields. The evolution of these fields is written in terms of a set of continuum or hydrodynamic equations that modify the well-known liquid-crystal hydrodynamics (Martin, Parodi, and Pershan, 1972; de Gennes and Prost, 1993) to include new nonequilibrium terms that arise from the activity. Generalized hydrodynamic theories have been very successful in the description of many condensed matter systems, such as superfluids (Dzyaloshinskii and Volovick, 1980), liquid crystals (Martin, Parodi, and Pershan, 1972), polymers (Milner, 1993), as well as, of course, simple fluids.

One approach to obtain a hydrodynamic theory of active systems is to start from a microscopic model and use the tools of statistical physics to coarse grain the model and obtain the long-wavelength, long-time scale equations (Kruse and Jülicher, 2003; Liverpool, 2003; Ahmadi, Marchetti, and Liverpool, 2005; Aranson and Tsimring, 2005; Ahmadi, Marchetti, and Liverpool, 2006). This task is difficult if the microscopic description is realistic and it can be carried out only at the cost of approximations, such as low-density or weak interactions. It allows one to relate the parameters in the macroscopic equations to specific physical mechanisms (albeit in a model-dependent manner) and to estimate them in terms of experimentally accessible quantities. The low-density limit has been worked out for several models, initially without and later including the effect of the embedding solvent. Some specific examples are discussed in Sec. IV.D.

An alternative, more pragmatic approach is to directly write hydrodynamic equations for the macroscopic fields including all terms allowed by symmetry as pioneered for dry flocks by Toner and Tu (1995, 1998) and extended to the case of self-propelled particles suspended in a fluid by Simha and Ramaswamy (2002a) and more generally to active-filament solutions (Hatwalne *et al.*, 2004). As one might expect in hindsight, novel terms, of a form ruled out for thermal equilibrium systems, appear in these "pure-thought" versions of the equations of active hydrodynamics.

A more systematic implementation of the phenomenological hydrodynamic approach is to treat the nonequilibrium steady state of an active system as arising through the imposition of a nonvanishing but small driving force on a well-defined parent *thermal equilibrium* state whose existence is not in question (de Groot and Mazur, 1984). For example, in the biological case of systems composed of cytoskeletal filaments and motor proteins, such as the cell cytoskeleton, the driving force is the difference $\Delta\mu$ between adenosine triphosphate (ATP) and its hydrolysis products. If $\Delta\mu$ is assumed to be small, the macroscopic hydrodynamic equations can be derived in a systematic way following the Onsager procedure. One identifies thermodynamic fluxes and forces and writes the most general linear relation between them that respects the symmetries of the problem. The novel terms mentioned above that arose by directly writing down the hydrodynamic equations of active matter are then seen to be a consequence of off-diagonal Onsager coefficients and an imposed constant nonzero $\Delta\mu$. Generalized hydrodynamic theories have been very successful in the description of complex and simple fluids (Martin, Parodi, and Pershan, 1972). The advantage is that the equations are expanded around a well-defined state. The drawback is that many active systems, biological ones being particularly pertinent examples, are far from equilibrium and one might, for example, miss some important physics by the restriction to the linear nonequilibrium regime. This phenomenological approach can, however, be very useful, especially when coupled to microscopic derivations for specific model systems.

Regardless of the choice of hydrodynamic framework, the reasons for the choice of variables remain the same. When an extended system is disturbed from equilibrium by an external

[2]In this review the word "hydrodynamics" refers to any continuum model where a system of many interacting constituents can be described at large scales in terms of the dynamics of a small number of fields, generally corresponding to conserved variables and, when applicable, broken-symmetry fields, but possibly amplified to include the amplitude of the order parameters (Chaikin and Lubensky, 2000). This general approach holds for both systems with overdamped dynamics and with momentum conservation.

perturbation, its relaxation is controlled by the microscopic interactions among constituents. It is useful to divide the relaxation processes into fast and slow, and to build a theory of the slow dynamics in which the fast processes enter as noise and damping. Such a division is unambiguous when there are collective excitations with relaxation rates $\omega(q)$ that vanish as the wave vector q goes to zero; these are the hydrodynamic modes of the systems (Martin, Parodi, and Pershan, 1972; Forster, 1975). Familiar examples are diffusion and sound waves in fluids. A formulation in terms of hydrodynamic fields provides a generic description of the nonequilibrium large-scale physics that relies only on general properties and local thermodynamics, and does not depend strongly on microscopic details of the interactions. In order to build a hydrodynamic theory, whether phenomenologically or by deriving it from a microscopic model, the first task is to identify the slow variables, which are the local densities of conserved quantities, the ''broken-symmetry'' variables which have no restoring force at zero wave number, and, in the vicinity of a continuous phase transition, the order parameter (Martin, Parodi, and Pershan, 1972; Forster, 1975). From there on, the procedure is well defined and systematic. Conserved quantities are fairly easy to identify. Momentum conservation for wet systems means that the momentum density is a slow, conserved variable, while for dry systems it is a fast variable. Identifying the type of order (polar or nematic, in the cases that we will examine) yields both the nature of the order parameter and the broken-symmetry modes.

Several useful reviews on various aspects of the behavior of flocks and active systems have appeared in the recent literature (Toner, Tu, and Ramaswamy, 2005; Jülicher *et al.*, 2007; Joanny and Prost, 2009a; Ramaswamy, 2010; Romanczuk *et al.*, 2012), as well as on the properties of swimmers (Ishikawa, 2009; Lauga and Powers, 2009; Koch and Subramanian, 2011) and bacterial suspensions and colonies (Ben-Jacob, Cohen, and Levine, 2000; Murray, 2003; Cates, 2012). This review aims at highlighting the unity of various approaches and at providing a classification of active systems. It demonstrates the link between microscopic derivations and continuum models, showing that the hydrodynamic equations derived from different microscopic models with the same general symmetry have the same structure and only differ in the details of parameter values, and that the continuum models proposed and used in the literature can all be formulated in a unified manner. It is hoped that this review will provide a useful and self-contained starting point for new researchers entering the field.

This review is organized as follows. We first consider dry active systems focusing on the ordering transition, the properties of the ordered phase, and the differences between polar and nematic active matter. We also discuss in Sec. II a system first analyzed theoretically by Baskaran and Marchetti (2008a, 2008b), where the self-propelled particles are polar in their movement but nematic in their interaction and hence in the nature of their macroscopic order. In Sec. III we discuss orientable active particles suspended in a fluid, or active gels, for short. We give a systematic derivation of the constitutive equations of a nematic active gel, for a system weakly out of equilibrium, and dwell briefly on the effects of polar order, viscoelasticity, and the presence of multiple components. In Sec. IV we present some applications of the hydrodynamic theory of active matter to specific geometries that could arise in experiments. We focus on instabilities of thin films and on the rheological properties of active matter. Section IV.D gives a brief account of microscopic theories of active matter. We offer examples to show how microscopic theories allow one to determine in principle the phenomenological transport parameters introduced in the hydrodynamic theories and to estimate their order of magnitude. The concluding Sec. VI presents open questions related to hydrodynamic theories of active matter and gives some perspectives.

II. DRY ACTIVE MATTER

In this section we consider active systems with no momentum conservation. This class includes bacteria gliding on a rigid surface (Wolgemuth *et al.*, 2002), animal herds on land (Toner and Tu, 1998), or, in the artificial realm, vibrated granular particles on a plate (Ramaswamy, Simha, and Toner, 2003; Yamada, Hondou, and Sano, 2003; Aranson and Tsimring, 2006; Narayan, Ramaswamy, and Menon, 2007; Kudrolli *et al.*, 2008; Deseigne, Dauchot, and Chaté, 2010) in all of which momentum is damped by friction with the substrate. It is also plausible that models without an explicit ambient fluid contain the main physics of concentrated collections of swimming bacteria (Drescher *et al.*, 2011) and motor-filament suspensions (Liverpool, 2003), where steric and stochastic effects could for most purposes overwhelm hydrodynamic interactions. Minimal flocking models have also been employed to interpret observations on aerial displays by large groups of birds where, despite the much lower concentration in comparison to bacterial suspensions (presumably inertial), long-range interactions seem negligible (Ballerini *et al.*, 2008) and metric-free interactions, as investigated by Ginelli and Chaté (2010), may dominate.

We refer to these systems as dry active systems. In this case the only conserved quantity is the number of particles (neglecting, of course, division and death) and the associated hydrodynamic field is the local density of active units. Overdamped active particles that can order in states with polar and nematic symmetries are described below. The first class consists of polar or self-propelled units with interactions that tend to promote polar order, i.e., explicitly align the particles head to head and tail to tail, as in the classic Vicsek model (Vicsek *et al.*, 1995). The second class consists of active particles that may themselves be apolar, such as melanocytes, the cells that distribute pigments in the skin, where activity induces nondirected motion on each cell (Gruler, Dewald, and Eberhardt, 1999) or polar, such as self-propelled hard rods (Peruani, Deutsch, and Bär, 2006; Baskaran and Marchetti, 2008b; Yang, Marceau, and Gompper, 2010), but with interactions that tend to align particles regardless of their polarity, so that the ordered state, if present, has nematic symmetry. A cartoon of the different cases is shown in Fig. 8.

A. Polar active systems: Toner and Tu continuum model of flocking

A continuum effective theory for the flocking model of Vicsek *et al.* (1995) was proposed in 1995 by Toner and Tu

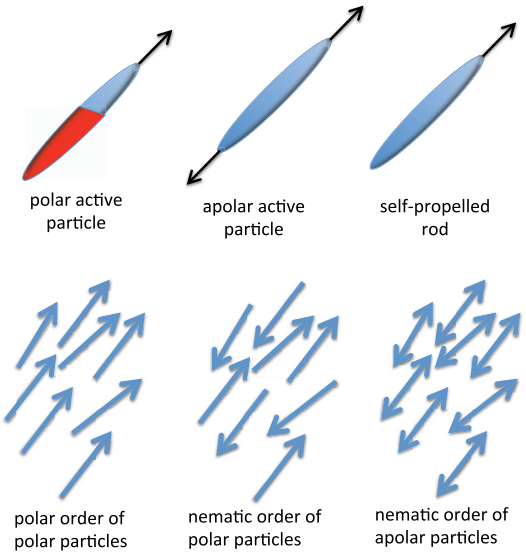

FIG. 8 (color online). Schematic of the various types of active particles and orientationally ordered states. Polar active particles (top left image), such as bacteria or birds, have a head and a tail and are generally self-propelled along their long axis. They can order in polar states (bottom left) or nematic states (bottom center). The polar state is also a moving state with a nonzero mean velocity. Apolar active particles (top center image) are head-tail symmetric and can order in nematic states (bottom right). Self-propelled rods (top right image) are head-tail symmetric, but each rod is self-propelled in a specific direction along its long axis. The self-propulsion renders the particles polar, but for exclusively apolar interactions (such as steric effects), self-propelled rods can order only in nematic states (bottom center).

(1995, 1998) [see also Toner, Tu, and Ramaswamy (2005)]. The Vicsek model describes a collection of self-propelled particles with fixed speed and noisy polar aligning interactions and displays a nonequilibrium phase transition from a disordered state at low density or high noise to an ordered, coherently moving state at high density or low noise strength. Toner and Tu formulated the continuum model phenomenologically solely on the basis of symmetry considerations. Recently, the Toner-Tu model was derived by Bertin, Droz, and Grégoire (2006, 2009) and Ihle (2011) by coarse graining the microscopic Vicsek model. These derivations provide a microscopic basis for the hydrodynamic theory, yielding explicit values for essentially all the parameters in the Toner-Tu model, except for the noise strength in the latter. The Boltzmann-equation approach of Bertin, Droz, and Grégoire (2006) and Ihle (2011) leads to a deterministic coarse-grained description, with the stochasticity of the Vicsek model reflected in an average sense through the diffusion and relaxation terms. In this section we introduce the continuum equations in their simplest form and analyze their consequences.

Since the particles are moving on a frictional substrate, the only conserved field is the number density $\rho(\mathbf{r}, t)$ of active particles. In addition, to describe the possibility of states with polar orientational order, one must consider the dynamics of a polarization vector field $\mathbf{p}(\mathbf{r}, t)$. These continuum fields can be defined in terms of the position $\mathbf{r}_n(t)$ of each active particle and a unit vector $\hat{\boldsymbol{\nu}}_n(t)$ denoting the instantaneous orientation of the velocity of each particle as

$$\rho(\mathbf{r}, t) = \sum_n \delta(\mathbf{r} - \mathbf{r}_n(t)), \tag{1a}$$

$$\mathbf{p}(\mathbf{r}, t) = \frac{1}{\rho(\mathbf{r}, t)} \sum_n \hat{\boldsymbol{\nu}}_n(t) \delta(\mathbf{r} - \mathbf{r}_n(t)). \tag{1b}$$

Although we are dealing with a nonequilibrium system, it is convenient and instructive to write the dynamical equations in a form in which terms that can be viewed as arising from a free-energy functional F_p (hence would also be present in an equilibrium system) are separated out from truly nonequilibrium ones:

$$\partial_t \rho + v_0 \boldsymbol{\nabla} \cdot (\rho \mathbf{p}) = -\boldsymbol{\nabla} \cdot \left(-\frac{1}{\gamma_\rho} \boldsymbol{\nabla} \frac{\delta F_p}{\delta \rho} + \mathbf{f}_\rho \right), \tag{2a}$$

$$\partial_t \mathbf{p} + \lambda_1 (\mathbf{p} \cdot \boldsymbol{\nabla}) \mathbf{p} = -\frac{1}{\gamma} \frac{\delta F_p}{\delta \mathbf{p}} + \mathbf{f}, \tag{2b}$$

where v_0 is the self-propulsion speed of the individual active particles, γ_ρ and γ kinetic coefficients. The first term inside the brackets on the right-hand side (rhs) of Eq. (2a) yields a familiar diffusive current, and $\mathbf{f}_\rho$ is the associated noise. For simplicity and consistency with Toner and Tu (1998) and with the derivation of Bertin, Droz, and Grégoire (2006) of the Toner-Tu equations from the model of Vicsek *et al.* (1995), both will be neglected in the following.[3] The parameter λ_1 controlling the strength of the advective term on the left-hand side of Eq. (2b) has dimensions of speed. This term resembles the familiar advective nonlinearity in the Navier-Stokes equation. Unlike the fluid, the nonequilibrium flocking model does not possess momentum conservation, as the particles are moving relative to a substrate, and is not constrained by Galilean invariance that would require $\lambda_1 = v_0$. As a result, λ_1 is a nonuniversal phenomenological parameter determined by microscopic properties. Derivations of the continuum equations from microscopic models, such as that of Bertin, Droz, and Grégoire (2009), yield a $(\mathbf{p} \cdot \boldsymbol{\nabla})\mathbf{p}$ term with coefficient different from that of the $\boldsymbol{\nabla} \cdot (\rho \mathbf{p})$ term in the density equation. In the Toner-Tu picture $\mathbf{p}$ is both a current and an orientational order parameter, and thus acts on itself by advection and flow alignment, both of which contribute to $(\mathbf{p} \cdot \boldsymbol{\nabla})\mathbf{p}$ in the $\mathbf{p}$ equation. In the density equation only the velocitylike character of $\mathbf{p}$ enters. The fact that $\lambda_1 \neq v_0$ allows for density and polarization fluctuations to be convected at different speeds. Finally, the last term on the right-hand side of Eq. (2b) captures the fluctuations and is taken to be white, Gaussian noise, with zero mean and correlations

$$\langle f_\alpha(\mathbf{r}, t) f_\beta(\mathbf{r}', t') \rangle = 2\Delta \delta_{\alpha\beta} \delta(\mathbf{r} - \mathbf{r}') \delta(t - t'). \tag{3}$$

In Eq. (2) and everywhere in the following we have taken the noise terms to be purely additive, ignoring dependence on the local values of ρ [see, e.g., Dean (1996)] or of the order parameter (here $\mathbf{p}$). This approximation is adequate for the present purposes of calculating two-point correlators in a linearized theory, but is actively under discussion (Mishra, 2009; Gowrishankar and Rao, 2012; Mishra *et al.*, 2012) for

[3]This approximation is justified in both the disordered and ordered phases of the flocking model because the thermal contribution to density diffusion is small compared to the effective diffusion constant $\sim v_0 v_1 / D_r$ that arises when fast variables are eliminated in favor of ρ in each phase.

situations of strong inhomogeneity such as the coarsening of active nematics.

Note that in the continuum flocking model $\mathbf{p}$ plays a dual role: on the one hand, $\mathbf{p}$ is the orientational order parameter of the system, and on the other hand, $v_0\mathbf{p}$ represents the particle velocity field. This duality is crucial in determining the large-scale behavior of this nonequilibrium system. The free-energy functional used in Eq. (2) is given by

$$F_p = \int_{\mathbf{r}} \left\{ \frac{\tilde{\alpha}(\rho)}{2}|\mathbf{p}|^2 + \frac{\tilde{\beta}}{4}|\mathbf{p}|^4 + \frac{\tilde{K}}{2}(\partial_\alpha p_\beta)(\partial_\alpha p_\beta) + \frac{w}{2}|\mathbf{p}|^2 \boldsymbol{\nabla}\cdot\mathbf{p} - w_1 \boldsymbol{\nabla}\cdot\mathbf{p}\frac{\delta\rho}{\rho_0} + \frac{A}{2}\left(\frac{\delta\rho}{\rho_0}\right)^2 \right\}, \tag{4}$$

where ρ_0 is the average density and $\delta\rho = \rho - \rho_0$ is the fluctuation in the density about its mean value ρ_0. Such fluctuations are penalized by the compression modulus A. The first two terms on the right-hand side of Eq. (4) control the mean-field continuous order-disorder transition that takes place as the parameter $\tilde{\alpha}$ goes through zero. In the derivation of Bertin, Droz, and Grégoire (2006), $\tilde{\alpha}$ depends on the local density ρ and the noise strength in the underlying microscopic model and turns negative at sufficiently large ρ. A reasonable phenomenological approach to describe the physics near the transition is to take $\tilde{\alpha}(\rho) = a_0(1 - \rho/\rho_c)$, changing sign at a characteristic density ρ_c. For stability reasons the coefficient $\tilde{\beta}$ is positive. The ratio $D_r = a_0/\gamma$ is a rotational diffusion rate with dimensions of frequency. In the following we use it to set our unit of time by letting $D_r = 1$. The third term in the free energy describes the energy cost for a spatially inhomogeneous deformation of the order parameter. The Frank constant $\tilde{K}$ is positive. For simplicity we employ a one-elastic constant approximation and use the same value for the stiffness associated with splay and bend deformations of the order parameter field, as also for gradients in its magnitude. Splay and bend anisotropy can, however, play an important role in active systems as demonstrated, for instance, by Voituriez, Joanny, and Prost (2006). The first two terms on the second line of Eq. (4) are allowed in equilibrium systems with polar symmetry [see, e.g., Kung, Marchetti, and Saunders (2006)]; they give the density and $|\mathbf{p}|^2$ contributions to the spontaneous splay. Upon integration by parts, they can be seen to enable gradients in ρ or in the magnitude $|\mathbf{p}|$ of the order parameter to provide a local aligning field for $\mathbf{p}$. Alternatively, the w term can be viewed as a splay-dependent correction to $\tilde{\alpha}(\rho)$: splay of one sign enhances and of the other sign reduces the local tendency to order.

By using Eq. (4) for the free energy, the equation for $\mathbf{p}$ takes the form

$$\partial_t\mathbf{p} + \lambda_1(\mathbf{p}\cdot\boldsymbol{\nabla})\mathbf{p} = -[\alpha(\rho) + \beta|\mathbf{p}|^2]\mathbf{p} + K\nabla^2\mathbf{p} - v_1\boldsymbol{\nabla}\frac{\rho}{\rho_0} + \frac{\lambda}{2}\boldsymbol{\nabla}|\mathbf{p}|^2 - \lambda\mathbf{p}(\boldsymbol{\nabla}\cdot\mathbf{p}) + \mathbf{f}, \tag{5}$$

where $v_1 = w_1/\gamma$ and $\lambda = w/\gamma$ have dimensions of velocity and all quantities without tilde are obtained from those with tilde by dividing by γ. The terms proportional to v_1 and λ would also be present in an equilibrium polar or ferroelectric liquid crystal and describe the coupling between density variation and local order. It is instructive to compare Eq. (5) with the Navier-Stokes equation for a simple fluid. If we think of $\mathbf{p}$ as proportional to a flow velocity, the second term on the right-hand side represents the effects of viscous forces. The third and fourth terms of Eq. (5) can be rewritten in an approximate pressure-gradient form as $-(1/\rho_0)\boldsymbol{\nabla}P$ with a pressure $P(\rho, |\mathbf{p}|) \simeq v_1\rho - (\lambda\rho_0/2)|\mathbf{p}|^2$. This highlights the parallel and the contrast with the Navier-Stokes equation: in the latter, an equation of state determines the thermodynamic pressure in terms of density and temperature and not the velocity field. The first term on the right-hand side of Eq. (5) arises from the role of $\mathbf{p}$ as an order parameter for a polarized state and does not have an analog in equilibrium fluid flow. There is, however, an equilibrium analog in the context of electrostriction, a property of all dielectric materials that causes them to change their shape under the application of an electric field, although in this case polarization does not correspond to velocity, but rather to reactive polarity. General symmetry arguments given by Toner, Tu, and Ramaswamy (2005) and Mishra, Baskaran, and Marchetti (2010) allow for more general polar terms in Eq. (5): $(\lambda_3/2)\boldsymbol{\nabla}|\mathbf{p}|^2 + \lambda_2\mathbf{p}(\boldsymbol{\nabla}\cdot\mathbf{p})$. The derivation based on the free energy (4) using Eq. (2b) yields $\lambda_3 = -\lambda_2 = \lambda$. For the out-of-equilibrium system considered here the coefficients of these two terms are not generally related, but the microscopic derivation of Bertin, Droz, and Grégoire (2006, 2009) also yields $\lambda_3 = -\lambda_2$ as well as $\lambda_i \sim v_0^2$ and $v_1 = v_0/2$.

Finally, we highlight the fact that a modified version of the Toner-Tu model that includes higher order spatial gradients in the local polarization-flow velocity has been used recently to describe quantitatively turbulent flows in dense bacterial suspensions in quasi-2D and 3D geometries (Wensink *et al.*, 2012). The fact that the observed statistical properties of turbulent flow can be fit by a dry model suggests that at high concentrations the collective motion of the bacteria is dominated by short-range repulsive interactions, while hydrodynamic couplings are negligible.

1. Homogeneous steady states

The dynamical model described by Eqs. (2a) and (2b) exhibits by construction, in a mean-field treatment of homogeneous configurations, a continuous transition from a disordered to an ordered state. For $\alpha > 0$, corresponding to an equilibrium density $\rho_0 < \rho_c$, the homogeneous steady state of the system is disordered or isotropic, with $\mathbf{p} = 0$ and a corresponding zero mean velocity. For $\alpha < 0$, corresponding to $\rho_0 > \rho_c$, the system orders in a state with uniform orientational order, with $|\mathbf{p}_0| = \sqrt{-\alpha_0/\beta}$, where $\alpha_0 = \alpha(\rho_0)$. In the ordered state, which is also a moving state, with $\mathbf{v} = v_0\mathbf{p}_0$, continuous rotational symmetry is spontaneously broken. This mean-field analysis survives fluctuation corrections even in two dimensions (Toner and Tu, 1995, 1998), evading the Mermin-Wagner theorem forbidding (at equilibrium) the spontaneous breaking of a continuous symmetry in two spatial dimensions (Mermin and Wagner, 1966; Hohenberg, 1967; Chaikin and Lubensky, 2000). In the present nonequilibrium system, however, the theorem does not apply.

The escape from the Mermin-Wagner theorem is primarily due to the advective nonlinearities in Eq. (2) which effectively generate long-range interactions in the system, even if density variations are ignored as shown recently by Toner (2012a).

The ordered phase itself, especially near the transition, is exceedingly complex as a result of coupling to the density. Although the mean density is an important control parameter for the transition to a flock, the local propensity to order depends, via $\alpha(\rho)$ in Eq. (4), on the local density $\rho(\mathbf{r}, t)$. This is analogous to the density-dependent exchange coupling in a compressible magnet in Milošević, Sasvári, and Tadić (1978). The analogy ends there: unlike in the magnet, the order parameter feeds back strongly into the density dynamics via the current on the right-hand side of Eq. (2b). See Sec. II.A.3 of Toner and Tu (1998), and the review by Toner, Tu, and Ramaswamy (2005) for a more complete discussion of this point.

2. Properties of the isotropic state

To study the linear stability of the homogeneous steady states we examine the dynamics of spatially inhomogeneous fluctuations $\delta\rho = \rho - \rho_0$ and $\delta\mathbf{p} = \mathbf{p} - \mathbf{p}_0$ from the values ρ_0 and $\mathbf{p}_0$ in each of the homogeneous states. The isotropic state is characterized by $\rho_0 < \rho_c$ and $\mathbf{p}_0 = 0$. The equations for the dynamics of linear fluctuations about these values are

$$\partial_t \delta\rho = -v_0\rho_0 \boldsymbol{\nabla}\cdot\mathbf{p}, \tag{6a}$$

$$\partial_t \mathbf{p} = -\alpha_0\mathbf{p} - \frac{v_1}{\rho_0}\boldsymbol{\nabla}\delta\rho + K\nabla^2\mathbf{p} + \mathbf{f}, \tag{6b}$$

where $\alpha_0 > 0$. Fourier transforming Eq. (6) in space and time to look at modes of the form $\exp(i\mathbf{q}\cdot\mathbf{r} - i\omega t)$ leads to dispersion relations between the frequency ω and wave vector $\mathbf{q}$ for small fluctuations about the uniform isotropic phase. Polarization fluctuations transverse to $\mathbf{q}$ decouple and decay at a rate $\alpha_0 + Kq^2$. The relaxation of coupled fluctuations of density and longitudinal polarization is controlled by coupled hydrodynamic modes with frequencies

$$\omega_{\pm}^{I}(q) = -\frac{i}{2}(\alpha_0 + Kq^2) \pm \frac{i}{2}\sqrt{(\alpha_0 + Kq^2)^2 - 4v_0v_1q^2}. \tag{7}$$

Linear stability requires that fluctuations decay at long times so that $\mathrm{Im}[\omega(q)] < 0$. The isotropic state is linearly stable for all parameter values, provided $v_0v_1 > 0$. The parameter v_1 enters Eq. (6b) like an effective compressional modulus. Microscopic derivations of the continuum model yielded $v_1 = v_0/2$ at low density (Bertin, Droz, and Grégoire, 2006, 2009; Baskaran and Marchetti, 2008b; Ihle, 2011). In this case $v_1 > 0$ and the isotropic state is always stable. At high density, however, caging effects can result in a density dependence of v_1, which can in turn lead to a density instability of the isotropic state as shown by Tailleur and Cates (2008) and Fily, Baskaran, and Marchetti (2012). Here we restrict our discussion to the situation where the isotropic state is linearly stable. Even in this case, it has unusual properties: approaching the mean-field ordering transition, i.e., decreasing α_0, is like decreasing friction. As argued by Ramaswamy and Mazenko (1982) for equilibrium fluids on a substrate, the dispersion relations can acquire a real part for $\alpha_0 \le v_0v_1/K$ and a range of wave vectors, $q_{c-} \le q \le q_{c+}$, with (Baskaran and Marchetti, 2008b)

$$q_{c\pm}^2 = \frac{2v_0v_1}{K^2}\left[1 - \frac{K\alpha_0}{2v_0v_1} \pm \sqrt{1 - \frac{K\alpha_0}{v_0v_1}}\right]. \tag{8}$$

Density fluctuations then propagate as waves rather than diffuse. Near the transition, where $\alpha_0 \to 0^+$, we find $q_{c-} \to 0$ and $q_{c+} \simeq 2\sqrt{v_0v_1}/K$ and the propagating waves resemble sound waves, with $\omega_{\pm}^{I} \simeq \pm q\sqrt{v_0v_1}$. These propagating soundlike density waves are ubiquitous in collections of self-propelled particles. We stress, however, that if the limit $q \to 0$ is taken first, density fluctuations always decay diffusively.

3. Properties of the ordered state

We now examine the linear stability of the ordered state by considering the linear dynamics of fluctuations about $\rho_0 > \rho_c$ and $\mathbf{p}_0 = p_0\hat{\mathbf{x}}$. The detailed analysis below is in two dimensions, but the general conclusions including the instability of the uniform ordered state just past threshold hold in all dimensions. It is useful to write the order parameter in terms of its magnitude and direction, by letting $\mathbf{p} = p\hat{\mathbf{n}}$, where $\hat{\mathbf{n}}$ is a unit vector pointing in the direction of local orientational order. Fluctuations in the polarization can then be written as $\delta\mathbf{p} = \hat{\mathbf{n}}_0\delta p + p_0\delta\mathbf{n}$. The condition $|\hat{\mathbf{n}}|^2 = 1$ requires that to linear order $\hat{\mathbf{n}}_0\cdot\delta\mathbf{n} = 0$. For the chosen coordinate system $\hat{\mathbf{n}}_0 = \hat{\mathbf{x}}$. Then in two dimensions $\delta\mathbf{n} = \delta n\hat{\mathbf{y}}$ and $\delta\mathbf{p} = \hat{\mathbf{x}}\delta p + \hat{\mathbf{y}}p_0\delta n$. The linearized equations are

$$(\partial_t + v_0p_0\partial_x)\delta\rho = -v_0\rho_0\boldsymbol{\nabla}\cdot\delta\mathbf{p}, \tag{9a}$$

$$\begin{aligned}(\partial_t + \lambda_1 p_0\partial_x)\delta\mathbf{p} = {}& -2|\alpha_0|\hat{\mathbf{x}}\delta p + a\mathbf{p}_0\delta\rho + \lambda_2\mathbf{p}_0(\boldsymbol{\nabla}\cdot\delta\mathbf{p}) \\ & - (v_1/\rho_0)\boldsymbol{\nabla}\delta\rho + \lambda_3 p_0\boldsymbol{\nabla}\delta p \\ & + K\nabla^2\delta\mathbf{p} + \mathbf{f},\end{aligned} \tag{9b}$$

where $a = -(\alpha' + \beta' p_0^2) = \alpha\beta'/\beta - \alpha' > 0$, and the primes denote derivatives with respect to density, e.g., $\alpha' = (\partial_\rho\alpha)_{\rho=\rho_0}$. For the analysis it is useful to explicitly display the three coupled equations for the fluctuations. For compactness, we introduce a vector with elements $\boldsymbol{\phi} = \{\delta\rho, \delta p, \delta n\}$ and write them in a matrix form as

$$\partial_t\boldsymbol{\phi}_{\mathbf{q}}(t) = \boldsymbol{M}(\mathbf{q})\cdot\boldsymbol{\phi}_{\mathbf{q}}(t) + \boldsymbol{F}_{\mathbf{q}}(t), \tag{10}$$

where the matrix $\boldsymbol{M}$ is given by

$$\boldsymbol{M}(\mathbf{q}) = \begin{pmatrix} -iq_xv_0p_0 & -iq_xv_0\rho_0 & -iq_yv_0\rho_0p_0 \\ ap_0 - iq_xv_1/\rho_0 & -2|\alpha_0| - iq_x\bar{\lambda}p_0 - Kq^2 & iq_y\lambda_2p_0^2 \\ -iq_yv_1/(\rho_0p_0) & iq_y\lambda_3p_0 & -iq_x\lambda_1p_0 - Kq^2 \end{pmatrix}. \tag{11}$$

The sign of the combination $\bar{\lambda} = \lambda_1 - \lambda_2 - \lambda_3$ is important in controlling the nature of the instabilities in the ordered phase. Notice that all microscopic derivations of the continuous equations for various systems of self-propelled particles (Bertin, Droz, and Grégoire, 2006, 2009; Baskaran and Marchetti, 2008b) yield $\bar{\lambda} > 0$. Finally, the noise vector $\boldsymbol{F}_{\mathbf{q}}(t)$ has components $\boldsymbol{F}_{\mathbf{q}}(t) = \{0, f_{\mathbf{q}}^{L}(t), \mathbf{f}_{\mathbf{q}}^{T}(t)\}$, with $f_{\mathbf{q}}^{L}(t) = \hat{\mathbf{q}}\cdot\mathbf{f}_{\mathbf{q}}(t)$,

$\mathbf{f}_{\mathbf{q}}^{T}(t) = \mathbf{f}_{\mathbf{q}}(t) - \hat{\mathbf{q}} f_{\mathbf{q}}^{L}(t)$, and $\hat{\mathbf{q}} = \mathbf{q}/q$. The dispersion relations of the hydrodynamic modes are the eigenvalues of the matrix $\boldsymbol{M}$. The solution of the full cubic eigenvalue problem is not, however, very instructive. It is more useful to discuss a few simplified cases (Bertin, Droz, and Grégoire, 2009; Mishra, Baskaran, and Marchetti, 2010).

a. Linear instability near the mean-field order-disorder transition

We first consider the behavior of fluctuations as the mean-field transition is approached from the ordered phase, i.e., for $\alpha_0 \to 0^-$ and $p_0 \to 0^+$. Fluctuations δp in the magnitude of polarization decay at rate $\sim|\alpha_0|$ and become long lived near the transition. In fact, in this limit one can neglect the coupling to director fluctuations and consider only the coupled dynamics of $\delta\rho$ and δp. This decoupling becomes exact for wave vectors $\mathbf{q}$ along the direction of broken symmetry $\mathbf{q} = q\hat{\mathbf{x}}$. The decay of director fluctuations is described by a stable, propagating mode $\omega_n = -q\lambda_1 p_0^2 - iKq^2$. For small q the imaginary part of the frequencies $\omega_{\pm}^{p}(\mathbf{q})$ of the modes describing the dynamics of density and order parameter magnitude takes the form

$$\mathrm{Im}[\omega_{+}^{p}] = -[s_2 q^2 + s_4 q^4 + \mathcal{O}(q^6)] \tag{12}$$

with

$$s_2 = \frac{v_0 v_1}{2|\alpha_0|}\left[1 - \frac{v_0 a^2 \rho_0^2}{4 v_1 |\alpha_0| \beta}\right],$$

implying an instability at small q when $s_2 < 0$, corresponding to $|\alpha_0| \le v_0 \rho_0^2 a^2/4 v_1 \beta$. Microscopic calculations yield $\alpha_0 \sim v_0$ and $v_1 \sim v_0$ (Bertin, Droz, and Grégoire, 2006, 2009), indicating that the instability exists for arbitrarily small v_0 and in a narrow region of densities above the mean-field order-disorder transition. The $\mathcal{O}(q^4)$ term in Eq. (12) stabilizes fluctuations at large wave vectors. In detail, near the mean-field transition ($\alpha_0 \to 0^-$) $s_2 \simeq -a^2/8\beta\alpha_0^2$ and $s_4 \simeq 5a^4/128\beta^2\alpha_0^5$ and the mode is unstable for $q < q_c \simeq 4\sqrt{\beta|\alpha_0|^3/5a^2} \sim (\rho_c - \rho_0)^{3/2}$. Numerical solutions of the nonlinear hydrodynamic equations with and without noise have shown that in this region the uniform polarized state is replaced by complex spatiotemporal structures. In the absence of noise, one finds propagating solitary waves in the form of ordered bands aligned transverse to the direction of broken symmetry and propagating along $\hat{\mathbf{x}}$ amidst a disordered background (Bertin, Droz, and Grégoire, 2009; Mishra, Baskaran, and Marchetti, 2010). As discussed below, these bands have been observed in numerical simulations of the Vicsek model (Grégoire and Chaté, 2004; Chaté, Ginelli, Grégoire, and Raynaud, 2008) and are shown in Fig. 9.

b. Sound waves

Deep in the ordered phase, i.e., for large negative α_0, fluctuations δp in the magnitude of the order parameter decay on nonhydrodynamic time scales. We assume δp has relaxed to zero on the time scales of interest and let for simplicity $p_0 \simeq 1$. In addition, we include a diffusive current and the associated noise that were neglected in the density equation (2a). The coupled equations for density and polar director fluctuations $\delta\rho$ and δn take the form

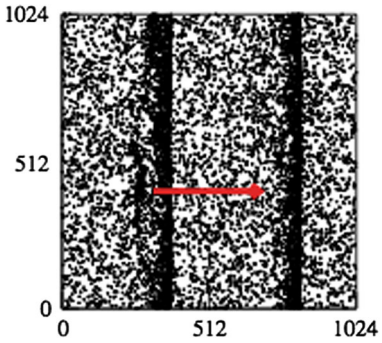

FIG. 9 (color online). Typical snapshots in the ordered phase of the Vicsek model. Points represent the position of individual particles and the arrow points along the global direction of motion. Note that in the simulations sharp bands can be observed only if the system size is larger than the typical width of the bands. Adapted from Chaté, Ginelli, Grégoire, Peruani, and Raynaud, 2008.

$$(\partial_t + v_0\partial_x)\delta\rho = -v_0\rho_0\partial_y\delta n + D\nabla^2\delta\rho + \boldsymbol{\nabla}\cdot\mathbf{f}_{\boldsymbol{\rho}}, \tag{13a}$$

$$(\partial_t + \lambda_1\partial_x)\delta n = -v_1\partial_y\left(\frac{\delta\rho}{\rho_0}\right) + K\nabla^2\delta n + f_y, \tag{13b}$$

where D is a diffusion constant and $\mathbf{f}_\rho$ and f_y describe white, Gaussian noise. The hydrodynamic modes, obtained from Eqs. (13a) and (13b), are stable propagating soundlike waves, with the dispersion relation

$$\omega_{\pm}^{s} = qc_{\pm}(\theta) - iq^2\mathcal{K}_{\pm}(\theta) + \mathcal{O}(q^3), \tag{14}$$

with speeds and dampings $c_{\pm}(\theta)$ and $\mathcal{K}_{\pm}(\theta)$, whose detailed forms are given in Toner, Tu, and Ramaswamy (2005) and depend on the angle θ between $\mathbf{q}$ and the direction $\hat{\mathbf{x}}$ of broken symmetry. For $\theta = \pi/2$, i.e., $\mathbf{q}$ along y, we find $c_{\pm} = \pm\sqrt{v_0 v_1}$ and $\mathcal{K}_{\pm} = (K + D)/2$, while for $\theta = 0$, corresponding to $\mathbf{q}$ along x, the two modes are decoupled and $\omega_{+}^{s} = qv_0 - iDq^2$ and $\omega_{-}^{s} = -q\lambda_1 - iKq^2$. The difference in the propagation speeds is due to the lack of Galilean invariance. In a normal fluid, sound waves propagate because of mass and momentum conservation and inertia. In contrast, the presence of propagating long-wavelength density disturbances here is a signature of the spontaneously broken orientational symmetry which renders δn "massless" (Ramaswamy, 2010).

Going back to the full form of the matrix $\boldsymbol{M}$ in Eq. (11), we notice that to leading order in q the relaxation of δp is governed by the

$$\partial_t \delta p_{\mathbf{q},\omega} = -2|\alpha_0|\delta p_{\mathbf{q},\omega} + a p_0 \delta\rho_{\mathbf{q},\omega} + \mathcal{O}(q). \tag{15}$$

This reminds us to be precise about what it means for a mode to be "fast": fluctuations in the magnitude of the order parameter cannot be neglected, but rather are slaved to density fluctuations on long time scales $\delta p_{\mathbf{q},\omega} \simeq (a p_0/2|\alpha_0|)\delta\rho_{\mathbf{q},\omega}$. Inserting this into Eq. (10) yields an effective dynamics for δn and ρ with an instability of splay fluctuations if $\lambda_3 > 2v_1\beta/\rho_0 p_0 a > 0$ (Mishra, Baskaran, and Marchetti, 2010). An analysis of the eigenvalues of the full matrix $\boldsymbol{M}$ confirms this result.

c. Giant density fluctuations

The linearized equations with noise can also be used to calculate correlation functions. Of particular interest is the static structure factor

$$S(\mathbf{q}) = \frac{1}{\rho_0 V}\langle \delta\rho_{\mathbf{q}}(t)\delta\rho_{-\mathbf{q}}(t)\rangle = \int_{-\infty}^{\infty}\frac{d\omega}{2\pi}S(\mathbf{q},\omega), \quad (16)$$

where

$$S(\mathbf{q},\omega) = \frac{1}{\rho_0 V}\int_0^{\infty} dt \exp(i\omega t)\langle \delta\rho_{\mathbf{q}}(0)\delta\rho_{-\mathbf{q}}(t)\rangle \quad (17)$$

is the dynamic structure factor. We are interested in calculating density fluctuations in the region away from the mean-field transition, where the ordered state is linearly stable. Equations (13a) and (13b) yield $S(\mathbf{q},\omega)$. For a reader wanting to work through the calculation, note that to leading order in the wave vector the noise $\mathbf{f}_\rho$ in the density equations can be neglected, except for $\mathbf{q}$ along the direction of broken symmetry ($\theta = 0$). Integrating over frequency as in Eq. (16), again to leading order in q, one obtains

$$S(\mathbf{q}) = \frac{v_0^2\rho_0\Delta\sin^2\theta}{(v_0+\lambda_1)^2\cos^2\theta + 4v_0v_1\sin^2\theta} \times\left[\frac{1}{\mathcal{K}_+(\theta)}+\frac{1}{\mathcal{K}_-(\theta)}\right]\frac{1}{q^2}. \quad (18)$$

For $\theta = 0$ the leading $1/q^2$ singularity displayed in Eq. (18) vanishes; to determine the finite value of $S(\mathbf{q})$ in that limit requires going to higher order in q which we will not do here. As we see below, the divergence of the static structure function at large wavelengths (as $1/q^2$ in the present linearized treatment) is a remarkable and robust property of uniaxially ordered active systems, whether polar or nematic, and follows generally from the orientational order that develops in a sufficiently dense collection of self-driven particles with anisotropic body shape (Toner and Tu, 1995, 1998; Simha and Ramaswamy, 2002a, 2002b; Ramaswamy, Simha, and Toner, 2003; Toner, Tu, and Ramaswamy, 2005). The $1/q^2$ term is also a dimension-independent property of our linearized theory; the numerical prefactors do, however, depend on the dimensionality d. The divergence of the static structure function for $q \to 0$ implies an important violation of the familiar scaling of number fluctuations in equilibrium. In the limit of vanishing wave vector the structure factor is simply a measure of number fluctuations, with

$$\lim_{q\to 0} S(q) = \frac{\Delta N^2}{\langle N\rangle}, \quad (19)$$

where N and $\langle N\rangle$ are the instantaneous and average number of particles in a region of size V, respectively, and $\Delta N^2 = \langle (N-\langle N\rangle)^2\rangle$ is the variance of number fluctuations. In an equilibrium system, $\Delta N \sim \sqrt{\langle N\rangle}$, so that $\Delta N/\langle N\rangle \sim 1/\sqrt{\langle N\rangle} \to 0$ as $\langle N\rangle \to \infty$. The $\sim 1/q^2$ divergence of $S(q)$ for $q \to 0$ predicted by Eq. (18) implies that in an active system ΔN grows faster than $\sqrt{\langle N\rangle}$. To understand this we rewrite Eq. (18) as $\Delta N \sim \sqrt{\langle N\rangle S(q\to 0)}$. Assuming that the smallest accessible wave vector is of the order of the inverse of the system size $V^{-1/d}$, with d the space dimension, we find $S(q\to 0) \sim V^{2/d} \sim \langle N\rangle^{2/d}$. This gives

$$\Delta N \sim \langle N\rangle^a, \qquad a = \frac{1}{2}+\frac{1}{d}. \quad (20)$$

The linear theory reviewed above predicts a strong enhancement of density fluctuations in the ordered state, with an exponent $a = 1$ in two dimensions (Toner and Tu, 1995; Toner, Tu, and Ramaswamy, 2005). We see in Sec. II.B that a similar linear theory also predicts the same scaling in the ordered state of active apolar nematic. In general, we expect the exponent to be substantially modified as compared to the theoretical value by fluctuation effects arising from the coupling of modes at different wave numbers as a result of nonlinear terms in the equations of motion. "Giant density fluctuations" have now been seen experimentally in both polar and apolar vibrated granular matter, with reported measured values of the exponent a of $2a_{\text{polar}} = 1.45 \pm 0.05$ (Deseigne, Dauchot, and Chaté, 2010) and $a_{\text{apolar}} \sim 1$ (Narayan, Ramaswamy, and Menon, 2007). See Sec. II.B.1 for a more detailed discussion of the apolar case. The scaling exponents, although measured over a limited dynamical range, are consistent, for the apolar case, with the linearized treatment presented here and in Ramaswamy, Simha, and Toner (2003), and with the renormalization-group treatment (Toner and Tu, 1995, 1998; Toner, Tu, and Ramaswamy, 2005) in $d = 2$ for polar flocks. Giant number fluctuations have also been seen in simulations of Vicsek-type models by Chaté and collaborators (Chaté, Ginelli, and Montagne, 2006; Chaté, Ginelli, Grégoire, Peruani, and Raynaud, 2008; Chaté, Ginelli, Grégoire, and Raynaud, 2008). Much remains to be understood about number fluctuations in flocks as revealed, for instance, by the experiments of Zhang *et al.* (2010) (see Fig. 10). Recent work also revealed mechanisms that can yield true phase separation (hence large number fluctuations) in active systems in the absence of an ordered state (Tailleur and Cates, 2008; Cates, 2012; Fily, Baskaran, and Marchetti, 2012). We refer the interested reader to Sec. II.C for further discussion of this point.

Recall that in thermal equilibrium the thermodynamic sum rule relates $S(q=0)$ to the isothermal compressibility $\chi_T = -(1/V)(\partial V/\partial p)_T$ according to $S(q\to 0) = \rho_0 k_B T \chi_T$, with

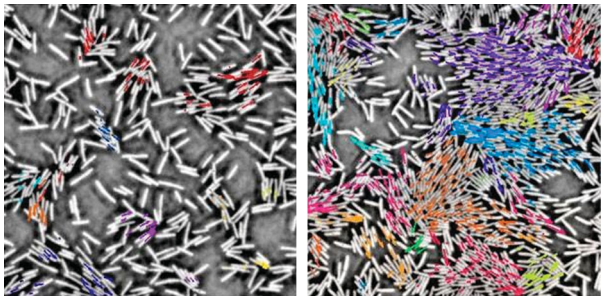

FIG. 10 (color). Swimming *bacillus subtilis* bacteria exhibit strong polar order and fluctuations that are smaller at low density (left frame) than at high density (right frame). Nearby bacteria with arrows of the same color belong to the same dynamic cluster; the arrows indicate a bacterium's speed and direction. At high density (right frame, corresponding to $N = 718$ bacteria in the imaging window of 60 μm $\times$ 60 μm) the measured number fluctuations scale with an exponent $a = 0.75 \pm 0.03$, smaller than predicted by theory in $d = 2$ [Eq. (20)], but substantially larger than the value obtained for a thermal system. Adapted from Zhang *et al.*, 2010.

$\rho_0 = \langle N \rangle / V$ the mean number density. One might then be tempted to say that orientationally ordered active systems are characterized by a diverging effective compressibility. This would in general be wrong. Augmenting the free-energy functional (4) with a linear coupling $\int U(\mathbf{r}, t)\delta\rho(\mathbf{r}, t)d^d r$ and calculating the response function $(\delta\langle\rho\rangle/\delta U)_{\mathbf{q},\omega}$ can readily be shown to yield a finite result for $\mathbf{q}$, $\omega \to 0$. The giant density fluctuations seen in the ordered state of active systems are an excess noise from the invasion of the density dynamics by the soft Goldstone mode of orientational order, not an enhanced response to perturbations. This invasion occurs in active systems and not in passive ones because orientational curvature in an active system leads to a local polarity and hence to a current. In an equilibrium system, such a distortion would simply relax via the interplay of elasticity and viscosity.

d. Long-range order of dry polar active matter in 2D

The ordered polar state is remarkable in that it exhibits long-range order of a continuous order parameter in two dimensions. This has been referred to as a violation of the Mermin-Wagner theorem, although it is important to keep in mind that the latter holds only for systems in thermal equilibrium. From Eqs. (13a) and (13b) one can immediately obtain the correlation function of fluctuations in the direction δn of polar order, with the result $\langle|\delta n_{\mathbf{q}}(t)|^2\rangle \sim 1/q^2$. Taken literally, this result implies quasi-long-range order in two dimensions in analogy with the equilibrium XY model. It has been shown, however, that nonlinearities in Eqs. (13a) and (13b) are strongly relevant in $d = 2$ and lead to a singular renormalization of the effective stiffness of the polar director at small wave numbers q, so that $\langle|\delta n_{\mathbf{q}}(t)|^2\rangle$ diverges more slowly than $1/q^2$ for most directions of $\mathbf{q}$, thus preserving long-range order (Toner and Tu, 1995, 1998; Toner, Tu, and Ramaswamy, 2005). A qualitative explanation of how this happens is given in Ramaswamy (2010), but a quantitative account can be found in Toner (2009). Exact arguments for scaling exponents in two dimensions are given by Toner (2012a) in the limit where the particle number is fast, i.e., not conserved locally.

e. Numerical simulation of Vicsek-type models

Although a review of numerical simulations of agent-based models is beyond the scope of this paper, for completeness we summarize the main findings. Quantitative agreement has been found between numerical experiments on microscopic models and the predictions of the coarse-grained theory, including long-range order in $d = 2$, the form of the propagating modes, anomalous density fluctuations, and superdiffusion of tagged particles (Grégoire and Chaté, 2004; Toner, Tu, and Ramaswamy, 2005). Early numerical studies (Vicsek *et al.*, 1995) and some later variants (Aldana *et al.*, 2007; Gönci, Nagy, and Vicsek, 2008; Baglietto and Albano, 2009) found a behavior consistent with a continuous onset of flocking, as a mean-field solution would predict. However, the currently agreed picture, in systems where particle number is conserved, is of a discontinuous transition (Grégoire and Chaté, 2004; Chaté, Ginelli, and Montagne, 2006; Chaté, Ginelli, and Grégoire, 2007; Chaté, Ginelli, Grégoire, and Raynaud, 2008). It was found in fact that in a large domain of parameter space, including the transition region, the dynamics is dominated by propagating solitary structures consisting of well-defined regions of high density and high polar order in a low-density, disordered background. The ordered regions consist of stripes or bands aligned transverse to the direction of mean order and traveling along the direction of mean motion with speed of order v_0 as shown in Fig. 9. Away from the transition, for weak noise strengths, a homogeneous ordered phase is found, although with anomalously large density fluctuations. Numerical solution and simplified analytical analysis of the nonlinear continuum model described by Eq. (2) has also yielded traveling wave structures (Bertin, Droz, and Grégoire, 2009; Mishra, Baskaran, and Marchetti, 2010; Gopinath *et al.*, 2012). Finally, traveling density waves have been observed in actin motility assays at very high actin density (Schaller *et al.*, 2010) as shown in Fig. 11. Although it is tempting to identify these actin density waves with the traveling bands seen in simulations of the Vicsek model, the connection is at best qualitative at the moment. In particular, it remains to be established whether these actin suspensions can indeed be modeled as dry systems, or hydrodynamic interactions are important, as suggested by Schaller, Weber, Frey, and Bausch, 2011.

B. Systems with nematic interactions on a substrate

Nematic order is the simplest kind of orientational order, with a spontaneously chosen axis which we designate as the $\hat{\mathbf{x}}$ direction, and no distinction between $\hat{\mathbf{x}}$ and $-\hat{\mathbf{x}}$. Lacking a permanent vectorial asymmetry, the system, although driven, has no opportunity to translate its lack of time-reversal symmetry into an average nonzero drift velocity. One would be forgiven for thinking that such a nonmoving state cannot possibly display any of the characteristics of a flock.

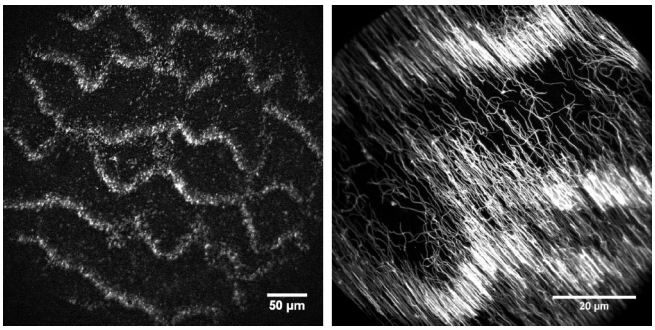

FIG. 11. Density waves in a dense actin motility assay. The left image is a snapshot of the traveling wave fronts of actin observed in motility assays for actin density above about 20 filaments/μm^2. Adapted from Schaller *et al.*, 2010. The right image (courtesy of V. Schaller) is obtained by overlaying maximal intensity projections of 20 consecutive images, corresponding to a total time of 2.5 s. The time overlay allows one to trace the trajectory of the filaments, showing that filaments in the high-density regions move collectively with high orientational persistence, while filaments lying outside the bands perform uncorrelated persistent random walks. The elongated density modulation travels in the direction of the filaments' long direction at a speed that remains approximately constant over the time scale of the experiment.

Remarkably, however, some of the most extreme fluctuation properties of ordered phases of active particles are predicted (Ramaswamy, Simha, and Toner, 2003) and observed in experiments (Narayan, Ramaswamy, and Menon, 2007) and earlier in simulations (Chaté, Ginelli, and Montagne, 2006; Mishra and Ramaswamy, 2006) on this flock that goes nowhere on average. As with polar active systems, several levels of description are possible for an active nematic–minimal agent-based stochastic model (Chaté, Ginelli, and Montagne, 2006) and Fokker-Planck treatments thereof (Shi and Ma, 2010), more detailed dynamical models that generalize rod-like-polymer dynamics to include the physics of motors walking on cytoskeletal filaments (Ahmadi, Marchetti, and Liverpool, 2005, 2006), or direct continuum approaches based on partial differential equations for the slow variables (Simha and Ramaswamy, 2002a). The microscopic models can in turn be coarse grained (Ahmadi, Marchetti, and Liverpool, 2006; Mishra, 2009; Shi and Ma, 2010; Mishra *et al.*, 2012; Bertin *et al.*, 2013) to yield the continuum equations in averaged (Ahmadi, Marchetti, and Liverpool, 2005; Shi and Ma, 2010) or stochastic (Mishra, 2009; Mishra *et al.*, 2012; Bertin *et al.*, 2013) form.

1. Active nematic

In this section we construct the equations of motion for active apolar nematics and discover their remarkable properties. We continue to work in a simplified description in which the medium through or over which the active particles move is merely a momentum sink, without its own dynamics. Effects associated with fluid flow are deferred to a later section. We consider again a collection of elongated active particles labeled by n, with positions $\mathbf{r}_n(t)$ and orientation described by unit vectors $\hat{\boldsymbol{\nu}}_n(t)$. As in the case of polar systems on a substrate, the only conservation law is that of a number. The slow variables of such a formulation are thus the number density $\rho(\mathbf{r}, t)$ at location $\mathbf{r}$ and time t, as defined in Eq. (1a), and the apolar nematic orientational order parameter, a traceless symmetric tensor $\mathbf{Q}$ with components

$$Q_{\alpha\beta}(\mathbf{r},t)=\frac{1}{\rho(\mathbf{r},t)}\sum_n\left(\hat{\nu}_{n\alpha}(t)\hat{\nu}_{n\beta}(t)-\frac{1}{d}\delta_{\alpha\beta}\right)\delta(\mathbf{r}-\mathbf{r}_n(t)) \tag{21}$$

measuring the local degree of mutual alignment of the axes of the constituent particles, without distinguishing head from tail. In constructing the equations of motion we keep track of which terms are permitted in a system at thermal equilibrium and which arise strictly from nonequilibrium activity. As we are ignoring inertia and fluid flow, the dynamics of the orientation is governed by

$$\partial_t\mathbf{Q}=-\frac{1}{\gamma_Q}\frac{\delta F_Q}{\delta\mathbf{Q}}+\mathbf{f}_Q \tag{22}$$

describing the balance between frictional torques governed by a rotational viscosity γ_Q and thermodynamic torques from a free-energy functional

$$F_Q=\int_{\mathbf{r}}\left[\frac{\alpha_Q(\rho)}{2}\mathbf{Q}\colon\mathbf{Q}+\frac{\beta_Q}{4}(\mathbf{Q}\colon\mathbf{Q})^2+\frac{K_Q}{2}(\boldsymbol{\nabla}\mathbf{Q})^2+C_Q\mathbf{Q}\colon\boldsymbol{\nabla}\boldsymbol{\nabla}\frac{\delta\rho}{\rho_0}+\frac{A}{2}\left(\frac{\delta\rho}{\rho_0}\right)^2\right] \tag{23}$$

that includes a tendency to nematic order for $\alpha_Q<0$ and $\beta_Q>0$, Frank elasticity as well as variations in the magnitude of $\mathbf{Q}$ via K_Q, bilinear couplings of $\mathbf{Q}$ and ρ, and a compression modulus A penalizing density fluctuations $\delta\rho$, as in Eq. (4). Note that all parameters in Eq. (23) can depend on ρ, as indicated explicitly for α_Q. We also stress that this form of the free energy applies only in two dimensions. For active nematic in three dimensions terms of order $\mathbf{Q}^3$ also need to be included. We included in Eq. (22) a spatiotemporally white statistically isotropic tensor noise $\mathbf{f}_Q$ to take into account fluctuations of thermal or active origin. It is implicit that all terms in Eq. (22) are traceless and symmetric. We ignored several possible terms in the equation of motion for $\mathbf{Q}$—additional couplings to ρ via off-diagonal kinetic coefficients, nonlinear terms not expressible as the variational derivative of a scalar functional, and terms of subleading order in gradients—none of which plays an important role in our analysis. The unique physics of the self-driven nematic state (Ramaswamy, Simha, and Toner, 2003) enters through active contributions to the current $\mathbf{J}$ in the conservation law

$$\partial_t\rho=-\boldsymbol{\nabla}\cdot\mathbf{J}, \tag{24}$$

where

$$\mathbf{J}=-\frac{1}{\gamma_\rho}\boldsymbol{\nabla}\frac{\delta F_Q}{\delta\rho}+\mathbf{J}_{\text{active}}, \tag{25}$$

with a mobility γ_ρ^{-1} controlling the passive contribution to the density current. There are several ways of generating the active current: one can write it down on the grounds that nothing rules them out in a nonequilibrium state (Simha and Ramaswamy, 2002a; Ramaswamy, Simha, and Toner, 2003), derive it from specific microscopic models involving motors and filaments (Ahmadi, Marchetti, and Liverpool, 2005, 2006) or apolar flocking agents (Chaté, Ginelli, and Montagne, 2006; Mishra, 2009; Mishra *et al.*, 2012; Bertin *et al.*, 2013), or frame it in the language of linear irreversible thermodynamics (de Groot and Mazur, 1984; Jülicher *et al.*, 2007). This last we will do later, in Sec. III. For now, Fig. 12 provides a pictorial argument. In a system with only an apolar order parameter, curvature $\boldsymbol{\nabla}\cdot\mathbf{Q}$ implies a local polarity and hence in a nonequilibrium situation maintained by a nonzero activity must in general give a current

$$\mathbf{J}_{\text{active}}=\zeta_Q\boldsymbol{\nabla}\cdot\mathbf{Q}, \tag{26}$$

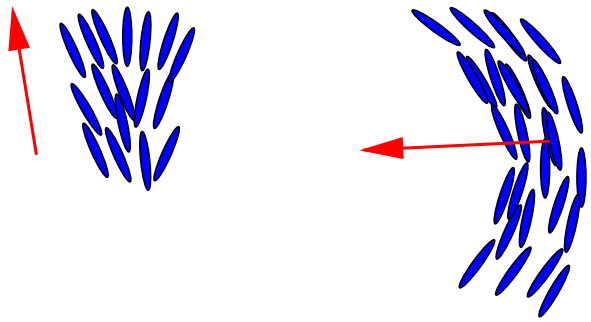

FIG. 12 (color online). Curvature generates temporary polarity in a nematic. Activity gives rise to a current in a direction determined by this polarity.

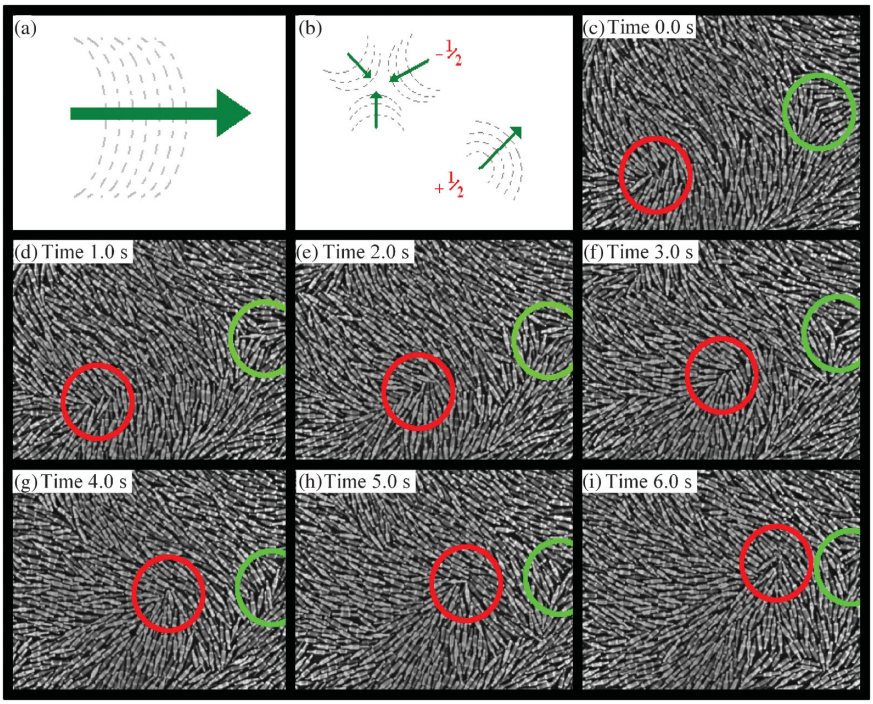

FIG. 13 (color). Curvature gives rise to self-propulsion in an apolar active medium, illustrating Eq. (26). A disclination of strength $+1/2$ (circled in red) in a nematic phase of a vibrated layer of rods. The locally polar director structure, together with the absence of time-reversal symmetry in a driven state, leads to directed motion. The curvatures around a nearby defect of strength $-1/2$ (circled in green) lack a preferred direction; that defect does not move. Adapted from Narayan, Ramaswamy, and Menon, 2007.

where ζ_Q is a phenomenological active parameter. Graphic experimental evidence of curvature-induced current can be found in Fig. 13; for details see Narayan, Ramaswamy, and Menon (2007). As shown by Ramaswamy, Simha, and Toner (2003) and reiterated below, this ζ_Q term leads to giant number fluctuations in active nematics. This is despite the fact that Eq. (26) has one more gradient than the current in the polar case in Eq. (2). We comment below on this subtlety after we summarize the calculation and the relevant experiments and simulations.

Using Eq. (23) in Eq. (22), and including both active and passive contributions to the current $\mathbf{J}$ given in Eqs. (25) and (26), leads to

$$\partial_t \rho = D\nabla^2\rho + B\nabla^2\boldsymbol{\nabla\nabla}\colon\mathbf{Q} + \zeta_Q\boldsymbol{\nabla\nabla}\colon\mathbf{Q} + \boldsymbol{\nabla}\cdot\mathbf{f}_\rho, \quad (27)$$

with $D = A/\rho_0^2\gamma_\rho$, $B = C_Q/\rho_0\gamma_\rho$. We have treated ζ_Q as constant, and we have introduced number-conserving fluctuations through the random current $\mathbf{f}_\rho$ which, again, we take to be statistically isotropic and delta correlated in space and time.

Despite its apparent structural simplicity the apolar active nematic state has been explored less than its polar counterpart. The ordering transition appears numerically (Chaté, Ginelli, and Montagne, 2006) to be of the Kosterlitz-Thouless type, but analytical approaches must confront the difficulties of the coupling of order parameter and density and have not been attempted so far, beyond mean field (Ahmadi, Marchetti, and Liverpool, 2005, 2006) which predicts a continuous transition in two dimensions. Working with equations similar to Eqs. (22) and (27), Shi and Ma (2010) obtained in a Boltzmann-equation approach from the model of Chaté, Ginelli, and Montagne (2006), with a finite-wave number instability of the uniform nematic state just past onset, and a "perpetually evolving state." Note that similar behavior has been obtained by Giomi and collaborators for wet nematic fluids (Giomi *et al.*, 2011, 2012) and has been observed in recent experiments on *in vitro* suspensions of microtubule-kinesin bundles (Marchetti, 2012; Sanchez *et al.*, 2012). Finally, there are preliminary numerical indications (Mishra, 2009; Mishra *et al.*, 2012; Bertin *et al.*, 2013) of anomalous growth kinetics of active nematic order following a quench from the isotropic phase, with a strong clumping of the density. We will not pursue these issues further in this review. In the remainder of this section we restrict ourselves to a simple understanding of the statistics of linearized density fluctuations deep in a well-ordered active nematic. Tests of the resulting predictions, through experiments and numerical studies, will be discussed thereafter.

For the purposes of this section it is enough to work in two dimensions denoted (x, y), so that $\mathbf{Q}$ has components $Q_{xx} = -Q_{yy} = Q = S\cos 2\theta$, $Q_{xy} = Q_{yx} = P = S\sin 2\theta$. We take $\alpha_Q < 0$, $\beta_Q > 0$ in Eq. (23), yielding a phase with uniform nematic order and density ρ_0 in mean-field theory, and choose our basis so that this reference state has $\theta = 0$. Expressing Eqs. (22) and (27) to linear order in perturbations about the reference state, $\rho = \rho_0 + \delta\rho(\mathbf{r}, t)$, $\mathbf{Q} = \mathrm{diag}(S, -S) + \delta\mathbf{Q}$, where $\delta Q_{xy} = \delta Q_{yx} \simeq 2S\theta$ and $\delta Q_{xx} = -\delta Q_{yy} = O(\theta^2)$, and working in terms of the space-time Fourier transforms $\delta\rho_{\mathbf{q}\omega}$, $\theta_{\mathbf{q}\omega}$, it is straightforward to calculate the correlation functions $S^\rho_{\mathbf{q}\omega} = (1/\rho_0 V)\langle|\delta\rho_{\mathbf{q}\omega}|^2\rangle$, $S^\theta_{\mathbf{q}\omega} = (1/V)\langle|\theta_{\mathbf{q}\omega}|^2\rangle$, and $S^{\rho\theta}_{\mathbf{q}\omega} = (1/V)\langle\delta\rho_{\mathbf{q}\omega}\theta^*_{\mathbf{q}\omega}\rangle$. Rather than dwelling on the details of this calculation

(Ramaswamy, Simha, and Toner, 2003), we suggest that one can verify for themselves a few essential facts. (a) Parameter ranges of nonzero measure can be found such that the real parts of the eigenvalues of the dynamical matrix for this coupled problem are negative, i.e., active nematics are not generically unstable. (b) Terms involving C_Q from Eq. (23) are irrelevant—subdominant in wave number in Eq. (27) and leading only to a finite renormalization of parameters in Eq. (22). (c) Ignoring C_Q, the dynamics of $\mathbf{Q}$ through Eq. (22) becomes autonomous, independent of ρ. In the nematic phase it is straightforward to show that $\theta_{\mathbf{q}}$ has equal-time correlations $S^{\theta}_{\mathbf{q}} = \int (d\omega/2\pi) S^{\theta}_{\mathbf{q}\omega} \propto 1/q^2$, and a lifetime $\propto 1/q^2$. The term $\boldsymbol{\nabla\nabla}$: $\mathbf{Q}$ through which $\theta_{\mathbf{q}\omega}$ appears in the density equation (27) can be reexpressed as $\partial_x \partial_y \theta$. This autonomy of θ means that this term can be viewed as colored noise with variance $\propto q_x^2 q_y^2/q^2$, and relaxation time $\sim 1/q^2$. The zero-frequency weight of this noise is thus $\sim q_x^2 q_y^2/q^4$, i.e., of order q^0 but anisotropic. By contrast, the conserving noise $\boldsymbol{\nabla} \cdot \mathbf{f}^{\rho}$ has zero-frequency weight that vanishes as q^2 and is thus irrelevant in the face of the active contribution $\boldsymbol{\nabla\nabla}$: $\mathbf{Q}$, whose long-time, long-distance effects are now revealed to be analogous to those of a number-non-conserving noise. The deterministic part of the dynamics of ρ, on the other hand, is diffusive and hence number conserving. This combination implies immediately that the equal-time correlator $S^{\rho}_{\mathbf{q}} \sim$ (noise strength) $\times$ (relaxation time) $\sim q_x^2 q_y^2/q^6$, i.e., direction dependent but of order $1/q^2$, as argued in greater detail in Sec. II.A.3.c for a linearized description of density fluctuations in a *polar* flock.

There is a puzzle here at first sight. We remarked that the apolar contribution to the active current (26) is 1 order higher in gradients than the polar term. Why then do density fluctuations in the linearized theory for polar and apolar flocks show equally singular behavior? The reason is that in polar flocks density gradients act back substantially on the polarization $\mathbf{p}$ through the pressurelike term $v_1 \boldsymbol{\nabla}\rho/\rho_0$ in Eq. (5), reducing the orientational fluctuations that engendered them. The effect of density gradients on θ in the apolar case is far weaker, a quadrupolar aligning torque $\sim \partial_x \partial_z \rho$ which does not substantially iron out the orientational curvature that engendered the density fluctuations.

It should be possible to check, on a living system, the rather startling prediction that flocks that go nowhere have enormous density fluctuations. Melanocyte suspensions at high concentration show well-ordered nematic phases when spread on a substrate as seen by Gruler, Dewald, and Eberhardt (1999). However, we know of no attempts to measure density fluctuations in these systems. The prediction of giant number fluctuations has been tested and confirmed first in a computer simulation of an apolar flocking model by Chaté, Ginelli, and Montagne (2006) and then in an experiment on a vertically vibrated monolayer of head-tail symmetric millimeter-sized bits of copper wire by Narayan, Ramaswamy, and Menon (2007). Of particular interest is the fact that the experiment observed a logarithmic time decay of the autocorrelation of the local density, a stronger test of the theory than the mere occurrence of giant fluctuations. Issues regarding the origin of the fluctuations in the experiment were nonetheless raised by Aranson *et al.* (2008), with a response by Narayan, Ramaswamy, and Menon (2008). Faced with such large density fluctuations, it is natural to ask whether the active nematic state is phase separated in the sense of Das and Barma (2000). This idea was tested by Mishra and Ramaswamy (2006) in a simulation model in which particles were advected by the nematic curvature (Lebwohl and Lasher, 1973), and indeed the steady state showed the characteristics of Das and Barma (2000)'s fluctuation-dominated phase separation.

2. Self-propelled hard rods: A system of "mixed" symmetry?

The Vicsek model contains an explicit alignment rule that yields an ordered polar, moving state. The alignment interaction is in this case explicitly polar, in the sense that it aligns particles head to head and tail to tail. A different model of elongated self-propelled particles where the alignment interaction has nematic, rather than polar, symmetry has been studied by Baskaran and Marchetti (2008a, 2008b, 2010). They considered the dynamics of a collection of hard rods self-propelled at speed v_0 along their long axis, moving on a frictional substrate and interacting via hard core collisions. Numerical simulations of self-propelled hard rods have also been carried out by Kraikivski, Lipowsky, and Kierfeld (2006), Peruani, Deutsch, and Bär (2006, 2008), and Yang, Marceau, and Gompper (2010) and have revealed a rich behavior. Related models of self-propelled particles with nematic aligning rules have also been considered (Ginelli *et al.*, 2010). The analysis by Baskaran and Marchetti (2010) of the collisions of two self-propelled hard rods (see Fig. 14) shows that, although self-propulsion enhances longitudinal momentum transfer and effectively tends to align two colliding rods, the alignment is in this case "apolar," in the sense that it tends to align particles without distinguishing head from tail. Baskaran and Marchetti (2010) derived an Onsager-type theory of self-propelled hard rods, obtaining a Smoluchowski equation modified in several ways by self-propulsion. They then obtained hydrodynamic equations by explicit coarse graining of the kinetic theory. One result of this work is that self-propelled hard rods do not order into a polar moving state in bulk. In spite of the polarity of the individual particles, provided by the self-propulsion, the symmetry of the system remains nematic at large scales. Self-propulsion does, however, enhance nematic order, as shown earlier by Kraikivski, Lipowsky, and Kierfeld (2006) in a model of actin motility assays, where the propulsion is provided by myosin motors tethered to the plane. It is well known (in a mean-field approximation neglecting

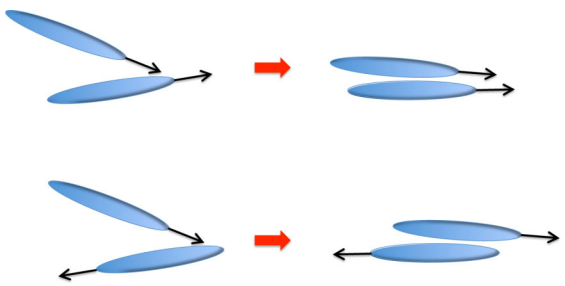

FIG. 14 (color online). The cartoon shows that the binary collision of self-propelled hard rods provides an *apolar* aligning interaction in the sense that it aligns rods regardless of their polarity.

fluctuations) that thermal hard rods of length ℓ undergo a continuous isotropic-nematic transition in two dimension at a density $\rho_{\mathrm{Ons}} = 3/(2\pi\ell^2)$ (Doi and Edwards, 1986), as first shown by Onsager (1949). Self-propelled rods perform a persistent random walk (Kareiva and Shigesada, 1983; ten Hagen, van Teeffelen, and Löwen, 2009; Kudrolli, 2010) consisting of ballistic flights randomized by rotational diffusion. At long time the dynamics is diffusive and isotropic, with effective diffusion constant $D_e = D + v_0^2/2D_r$, where D is the longitudinal thermal diffusion coefficient and D_r is the rotational diffusion rate. Self-propelled rods of length ℓ then behave as rods with an effective length $\ell_{\mathrm{eff}} \simeq \sqrt{D_e/D_r} = \ell\sqrt{1 + v_0^2/[2(DD_r)]^{1/2}}$ (Kraikivski, Lipowsky, and Kierfeld, 2006) and undergo an isotropic-nematic transition at a density

$$\rho_{IN} = \rho_{\mathrm{Ons}} \Big/ \left(1 + \frac{v_0^2}{2\ell^2 D_r^2}\right),$$

where we used $D \sim \ell^2 D_r$. The microscopic derivation carried out by Baskaran and Marchetti (2008a) supports this estimate. The suppression of ρ_{IN} from self-propulsion was verified recently via large-scale simulations of self-propelled hard rods (Yang, Marceau, and Gompper, 2010) and particles with nematic aligning rules (Ginelli *et al.*, 2010).

The statistical mechanics of self-propelled hard rods and the derivation of the modified Smoluchowski equations is described by Baskaran and Marchetti (2010) and will not be repeated here. Instead the hydrodynamic equations for this system are introduced phenomenologically and their consequences are discussed. Once again, the only conserved field is the density $\rho(\mathbf{r}, t)$ of self-propelled rods. Theory and simulations indicated that although self-propelled particles with apolar interactions do not order in polar states, their dynamics is qualitatively different from that of active nematic and requires consideration of both the vector order parameter $\mathbf{p}$ defined in Eq. (1b) and the alignment tensor Q_{ij} of Eq. (21). In other words, although the polarization $\mathbf{p}$ does not describe a broken symmetry, it is necessary to incorporate its dynamics to capture the rich physics of the system into a continuum description. We then consider coupled equations for the conserved particle density ρ and the two coupled orientational order parameters $\mathbf{p}$ and $\mathbf{Q}$. Once again, the equations can be written in terms of a "free energy" as[4]

$$\partial_t \rho = -\boldsymbol{\nabla}\cdot(v_0\rho\mathbf{p}) + D\nabla^2\rho + \frac{1}{\gamma_\rho}\boldsymbol{\nabla}\boldsymbol{\nabla}:\frac{\delta F_{pQ}}{\delta \mathbf{Q}} + \boldsymbol{\nabla}\cdot\mathbf{f}^{\rho}, \tag{28a}$$

$$\partial_t \mathbf{p} + \lambda_1(\mathbf{p}\cdot\boldsymbol{\nabla})\mathbf{p} - \delta_1 \mathbf{p}\cdot\mathbf{Q} + \delta_2 \mathbf{Q}{:}\mathbf{Q}\mathbf{p} = -\frac{1}{\gamma_p}\frac{\delta F_{pQ}}{\delta \mathbf{p}} + \mathbf{f}, \tag{28b}$$

$$\partial_t \mathbf{Q} + \lambda_1'(\mathbf{p}\cdot\boldsymbol{\nabla})\mathbf{Q} = -\frac{1}{\gamma_Q}\left[\frac{\delta F_{pQ}}{\delta \mathbf{Q}}\right]_{ST} + \mathbf{f}^{Q}, \tag{28c}$$

where the subscript ST denotes the symmetric, traceless part of any second order tensor $\mathbf{T}$, i.e., $[\mathbf{T}]_{ST}$ has components $T_{ij}^{ST} = \frac{1}{2}(T_{ij} + T_{ji}) - \frac{1}{2}\delta_{ij}T_{kk}$, and

$$F_{pQ} = F_Q + \int_{\mathbf{r}}\left\{\frac{\alpha_{pQ}}{2}|\mathbf{p}|^2 + \frac{K}{2}(\partial_\alpha p_\beta)(\partial_\alpha p_\beta) + P(\rho, p, S)(\boldsymbol{\nabla}\cdot\mathbf{p}) - v_2 Q_{\alpha\beta}(\partial_\alpha p_\beta)\right\}. \tag{29}$$

We grouped several terms [including some that were made explicit, for instance, in Eq. (4)] by writing a local spontaneous splay in terms of a "pressure" $P(\rho, p, S)$. Note that it is essential to retain the general dependence of this pressure on ρ, p, and S to generate all terms obtained from the microscopic theory. Here $p = |\mathbf{p}|$ and the magnitude S of the alignment tensor has been defined by noting that in uniaxial systems in two dimensions we can write $Q_{\alpha\beta} = 2S(n_\alpha n_\beta - \frac{1}{2}\delta_{\alpha\beta})$, with $\mathbf{n}$ as a unit vector. Then $Q_{\alpha\gamma}Q_{\gamma\beta} = S^2\delta_{\alpha\beta}$. The kinetic theory of Baskaran and Marchetti yields $\alpha_{pQ} > 0$ at all densities, indicating that no isotropic-polar transition occurs in the system. In contrast, $\alpha_Q(\rho)$ is found to change sign at a characteristic density ρ_{IN}, signaling the onset of nematic order. The closure of the moments equations used in Baskaran and Marchetti (2008a, 2008b) to derive hydrodynamics gives terms only up to quadratic in the fields in the continuum equations, but is sufficient to establish the absence of a polar state and to evaluate the renormalization of the isotropic-nematic transition density due to self-propulsion. Cubic terms such as $\sim\beta_Q\mathbf{Q}^3$ needed to evaluate the value of the nematic order parameter in the ordered state and the active $\sim\delta_2\mathbf{Q}{:}\,\mathbf{Q}\mathbf{p}$ can be obtained from a higher order closure and are included here for completeness. A higher order closure also confirms the absence of a term proportional to $\mathbf{p}^3$ in the polarization equation, which could, if present, yield a bulk polar state. We note that a $\mathbf{p}\cdot\mathbf{Q}\cdot\mathbf{p}$ term in the free energy is permitted and would yield both the $\mathbf{p}\cdot\mathbf{Q}$ term on the left-hand side of the $\mathbf{p}$ equation and a $\mathbf{pp}$ term in the Q equation, with related coefficients.

[4]We note that there are some differences between the equations derived in the literature for long, thin self-propelled rods (Baskaran and Marchetti, 2008a, 2010) and those for point particles with nematic aligning rules (Peshkov *et al.*, 2012). The differences arise because (i) the thin rod approximation yields only terms with nematic symmetry in the collision integral, and (ii) advective-type terms arising from the finite size of the rods are neglected in the point particle model. The continuum description of self-propelled entities with nematic interactions is still evolving.

The joint presence of these terms can lead to the existence of a polar ordered state. The hard-rod kinetic theory of Baskaran and Marchetti produces only the $\mathbf{p}\cdot\mathbf{Q}$ term. The fact that the theory does not generate the **pp** term, which would be obligatory had the dynamics been governed entirely by a free-energy functional, underlines the nonequilibrium nature of the dynamics we are constructing. It would be of great interest to find the minimal extension of self-propelled hard-rod kinetic theory that could produce a phase with polar order.

a. Homogeneous steady states and their stability

The only homogeneous steady states of the system are an isotropic state with $\rho=\rho_0$ and $\mathbf{p}=\mathbf{Q}=0$ and a nematic state where $\mathbf{p}=0$, but $\mathbf{Q}$ is finite. The transition occurs at ρ_{IN} where $\alpha_{pQ}\sim\rho_{IN}-\rho$ changes sign. As in the case of the active nematic, we work in two dimensions denoted x and y, so that $\mathbf{Q}$ has components $Q_{xx}=-Q_{yy}=S\cos2\theta$ and $Q_{xy}=Q_{yx}=S\sin2\theta$. In the nematic state $\alpha_Q<0$, $\beta_Q>0$ in Eq. (28c), yielding a phase with uniform nematic order and $S=\sqrt{-\alpha_Q/(2\beta_Q)}$. We choose our coordinates so that this reference state has $\theta=0$. The phase transition line is shown in Fig. 15 as a function of density ρ_0 and self-propulsion speed v_0 for the microscopic hard-rod model discussed in Baskaran and Marchetti (2008a, 2008b).

As in the case of polar and nematic active systems, the isotropic state is stable. It can also support finite-wave-vector propagating soundlike waves (Baskaran and Marchetti, 2008b). The properties of the ordered state, on the other hand, are more subtle and not yet fully explored (Baskaran and Marchetti, 2012; Peshkov *et al.*, 2012).

Numerical simulations of collections of self-propelled rods with steric repulsion recently revealed a rich behavior, quite distinct from that of polar Vicsek-type models. As predicted by theory, self-propelled rods with only excluded volume interactions do not order in a macroscopically polarized state, but exhibit only nematic order, which appears to be long ranged in two dimensions. Again, simulations also confirmed that selfpropulsion enhances the tendency for nematic ordering as well as aggregation and clustering, in both self-propelled rods (Ginelli *et al.*, 2010) and particles

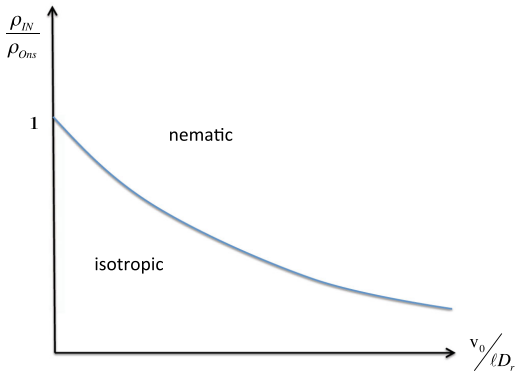

FIG. 15 (color online). The mean-field isotropic-nematic transition line for self-propelled hard rods. Adapted from Baskaran and Marchetti, 2008a.

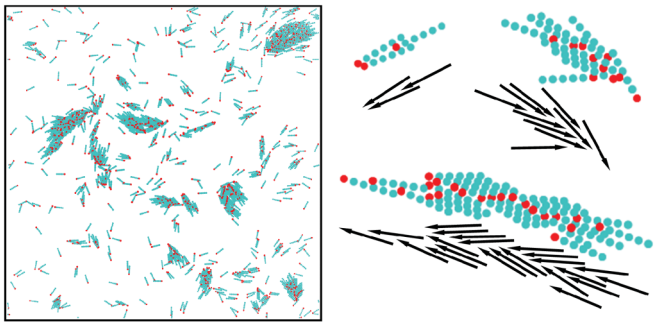

FIG. 16 (color). Snapshots from simulations of self-propelled hard rods. The red dots mark the front end of the rods, i.e., the direction of self-propulsion. The rods are otherwise head-tail symmetric. The left image is for a density $\rho_{\rm rod}L_{\rm rods}^2=0.7744$, where $L_{\rm rod}$ is the length of the rod, and $1/\mathrm{Pe}=0.005$, where $\mathrm{Pe}=L_{\rm rod}v_0/D_\parallel$ is the Peclet number, with v_0 the self-propulsion speed of each rod and $D_\parallel$ the diffusion coefficient for motion along the long direction of the rod. The right image shows a close-up of clusters of sizes $n=3$, 10, and 22, highlighting the partially blocked structure and the "smecticlike" ordering of rods within a cluster. The clusters are chosen from a simulation with parameters $1/\mathrm{Pe}=0.000\,95$ and the same density as in the left image. Adapted from Yang, Marceau, and Gompper, 2010.

with nematic aligning rules (Peruani, Deutsch, and Bär, 2006; Yang, Marceau, and Gompper, 2010). After an initial transient, the particles form polar clusters that travel in a directed fashion, as shown in Fig. 16. Large clusters can form by collisions of smaller ones and break up due to collisions with other clusters or due to noise. Eventually the system reaches a stationary state, in which the formation rate of any cluster size equals its breakup rate, and the rods and particles aggregate in large stationary clusters. Above the order-disorder transition, phase separation manifests itself with the formation of nematic bands, consisting of high-density regions where the particles are on average aligned with the long direction of the band, but move in both directions, exhibiting no polar order, as shown in Fig. 17, although deeper in the ordered nematic phase, the bands seem to give way to a stable homogeneous nematic state (Ginelli *et al.*, 2010). Self-propulsion has also been shown to increase the segregation tendency in a mixture of self-propelled rods with distinctly different motilities

FIG. 17. Typical snapshots of nematic bands above the order-disorder transition in the ordered phase. Arrows indicate the polar orientation of particles; only a fraction of the particles are shown for clarity reasons. Adapted from Ginelli *et al.*, 2010.

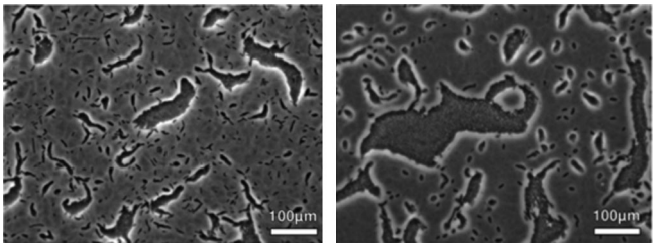

FIG. 18. Cluster formation in myxobacteria mutants (SA2407) that cannot reverse their gliding direction. At long times the dynamical clustering process reaches a steady state that depends on cell density. The images show the clusters obtained at two different packing fractions $\eta = \rho a$, with ρ the two-dimensional cell density and $a = 4.4\ \mu m^2$ the average area covered by a bacterium, with $\eta = 0.16$ (left) and $\eta = 0.24$ (right). Adapted from Peruani *et al.*, 2012.

(McCandlish, Baskaran, and Hagan, 2012). In closing this section, we remark that mixed-symmetry models of the sort just presented may well be the best description of the collective crawling of rodlike bacteria such as those studied by Wu *et al.* (2011). Cluster formation qualitatively similar to that observed in simulations of self-propelled (SP) rods has been observed in recent experiments in myxobacteria (Peruani *et al.*, 2012, Fig. 18). Finally nematic aligning interactions have also been suggested to control the rich collective behavior of microtubules propelled by dynein motor proteins grafted to a glass surface in recent *in vitro* motility assays (Sumino *et al.*, 2012).

C. Current status of dry active matter

Although much progress has been made in the understanding and classification of dry active matter, a number of open questions remain.

Clustering and phase separation, with associated giant number fluctuations, are ubiquitous in active systems. It was first suggested that giant number fluctuations may be a distinct property of the ordered state (nematic and polar) of active systems, intimately related to the existence of a spontaneously broken orientational symmetry (Toner and Tu, 1998; Simha and Ramaswamy, 2002a; Ramaswamy, Simha, and Toner, 2003). In ordered states such large fluctuations can indeed be understood as arising from curvature-driven active currents unique to the ordered state of active systems (Narayan, Ramaswamy, and Menon, 2007). More recently giant pretransitional fluctuations in the number density, associated with the approach to a nonequilibrium critical point, consistent with a standard deviation growing linearly with the mean number N of particles, rather than the $\sqrt{N}$ expected in situations where the central limit theorem applies, have been reported in active systems of symmetric disks with no alignment rule that do not exhibit any orientational broken symmetry (Fily, Baskaran, and Marchetti, 2012). In this case strong clustering (with unavoidable large density fluctuations) and phase separation seem to arise from the general mechanism proposed by Tailleur and Cates (2008) and Cates *et al.* (2010) and reviewed recently by Cates (2012) associated with the breaking down of detailed balance in systems that are driven out of equilibrium by a local input of energy on each constituent, as in self-propelled systems or bacterial suspensions. Strong density inhomogeneities leading to persistent clustering have also been seen in layers of vibrated granular spheres (Prevost *et al.*, 2004; Aranson *et al.*, 2008), as well as in collections of living (Schwarz-Linek *et al.*, 2012) and artificial (Theurkauff *et al.*, 2012) swimmers, where, however, attractive interactions may also be important. Again, although in this case other mechanisms such as the inelasticity of collisions may play a role, more work is needed to elucidate the generic aspect of this ubiquitous phenomenon.

Although some controversy still remains (Vicsek *et al.*, 1995; Aldana *et al.*, 2007; Gönci, Nagy, and Vicsek, 2008), there is now strong numerical evidence (Chaté, Ginelli, and Grégoire, 2007) that the order-disorder transition in dry active systems is discontinuous, with an associated wealth of coexistence phenomena. One unusual aspect of the transition is that density fluctuations destabilize the ordered state right at the mean-field order transition. This behavior seems to be associated with a phenomenon that has been referred to as "dynamical self-regulation" (Baskaran and Marchetti, 2012; Gopinath *et al.*, 2012) associated with the fact that in this class of active systems the parameter that controls the transition, namely, the density of active particles, is not tuned from the outside, as in familiar equilibrium phase transitions, but rather it is dynamically convected or diffused by nonequilibrium active currents controlled by the order parameter itself. It would of course be interesting to attempt to use formal field theory and renormalization-group methods to shed some light on this unusual nonequilibrium transition.

The behavior of collections of self-propelled or active particles is strongly affected by the presence of boundaries and obstacles (Wensink and Löwen, 2008; Elgeti and Gompper, 2009). Ratchet effects have been demonstrated experimentally and theoretically for active particles interacting with asymmetric obstacles or on asymmetric substrates, without any external forcing (Angelani, DiLeonardo, and Giancarlo, 2009; DiLeonardo *et al.*, 2010). For bacteria undergoing run-and-tumble dynamics or self-propelled particles performing persistent random walks, the guiding effect of asymmetric boundaries can yield a variety of rectification effects (Galajda *et al.*, 2007; Wan *et al.*, 2008), that can even power submillimiter gears, as demonstrated in recent experiments (DiLeonardo *et al.*, 2010; Sokolov *et al.*, 2010). Understanding the interaction of bacteria with obstacles and with passive particles is crucial for harnessing the collective power of these living systems and developing micron-scale mechanical machines powered by microorganisms. Whether these phenomena can be described in the dry limit discussed in this section or require a proper treatment of flow as introduced in the next section and even hydrodynamic interactions is still an open question.

Finally there has been a surge of recent interest in the properties of dense active matter and the living crystalline or glassy states that may be formed in these systems. The nonequilibrium freezing of active particles may be directly relevant to the behavior of suspensions of self-propelled Janus colloids or other artificial microswimmers (Palacci *et al.*, 2010; Enculescu and Stark, 2011). Recent work demonstrated that active particles form crystalline states,

but the freezing and melting is in this case a true nonequilibrium phenomenon that cannot be described simply in terms of an effective temperature for the system (Bialké, Speck, and Löwen, 2012). *In vitro* experiments on confluent monolayers of epithelial cells suggest that the displacement field and stress distribution in these living systems strongly resemble both the dynamical heterogeneities of glasses and the soft modes of jammed packings (Poujade *et al.*, 2007; Trepat *et al.*, 2009; Angelini *et al.*, 2010, 2011; Petitjean *et al.*, 2010). This observation has led to new interest in the study of active jammed and glassy states (Henkes, Fily, and Marchetti, 2011) obtained by packing self-propelled particles at high density in confined regions or by adding attractive interactions. In these models the interaction with the substrate has so far been described simply as frictional damping. Although a rich and novel dynamical behavior has emerged, it has become clear that a more realistic description of stress transfer with the substrate will be needed to reproduce the active stress distribution observed experimentally (Trepat *et al.*, 2009) in living cellular material.

III. ACTIVE GELS: SELF-DRIVEN POLAR AND APOLAR FILAMENTS IN A FLUID

In this section we describe an alternative method for constructing hydrodynamic theories for a class of active materials. This approach involves a systematic derivation of the hydrodynamic equations based on a generalized hydrodynamic approach close to equilibrium closely following the work of Martin, Parodi, and Pershan for nemato hydrodynamics (Martin, Parodi, and Pershan, 1972; de Gennes and Prost, 1993). As in the previous sections, the theory is mostly based on symmetries and does not involve significant microscopic considerations; it is thus applicable to a whole range of systems, which share the appropriate polar or nematic symmetries and which are liquid at long times. We focus here on an "active gel," defined as a fluid or suspension of orientable objects endowed with active stresses, with momentum damping coming from the viscosity of the bulk fluid medium, rather than from friction with a substrate or a porous medium (Simha and Ramaswamy, 2002a, 2002b; Kruse *et al.*, 2004; Jülicher *et al.*, 2007). The equations that emerge are those proposed by Simha and Ramaswamy (2002a) for self-propelling organisms, but the development by Kruse *et al.* (2004) and Jülicher *et al.* (2007) was carried out in the context of the cytoskeleton of living cells, a network of polar actin filaments, made active by molecular motors that consume ATP.

In Sec. III.B we consider an active system with a polarization field $\mathbf{p}$. It turns out that, for the linear Onsager theory that we propose, the final equations are invariant under the change of $\mathbf{p}$ to $-\mathbf{p}$. At this linear order, the dynamical equations are therefore the same for a polar active gel and a nonpolar active nematic gel where $\mathbf{p}$ is the director. An alternative approach for a nematic gel is to describe the ordering not by a director field but by a nematic alignment tensor $\mathbf{Q}$. This approach, also part of the phenomenological treatment in Simha and Ramaswamy (2002a), is presented by Salbreux, Prost, and Joanny (2009). A brief discussion of polar active gels and of the effects of polarity on the dynamics beyond the linear theory is given in Sec. III.C.

A. Hydrodynamic equations of active gels

For simplicity, in this section we discuss only a one-component active polar gel considering therefore that the complex composition of active materials such as the cytoskeleton can be described by an effective single component. The original formulation of Simha and Ramaswamy (2002a) for the hydrodynamics of self-propelled orientable suspensions was already an explicitly multicomponent formulation of active liquid-crystal hydrodynamics, but without a formal link to the nonequilibrium thermodynamic approach to active systems of Jülicher *et al.* (2007). Generalizations of the latter approach to multicomponent systems are possible and have been recently proposed by Joanny *et al.* (2007) and Callan-Jones and Jülicher (2011). The multicomponent theory properly takes into account the relative permeation between the various components which is neglected in the simpler one-component description. As in the previous sections, we retain as slow variables the number density ρ, the polarization $\mathbf{p}$, and the momentum density $\mathbf{g} = \rho m \mathbf{v}$, where $\mathbf{v}$ is the local velocity of the gel and m is the (effective) mass of the molecules.

1. Entropy production

The derivation of generalized hydrodynamic equations is based on the identification of fluxes and forces from the entropy production rate $\dot{\mathcal{S}}$ as in de Groot and Mazur (1984). We do not consider heat exchange here; we assume that the active gel has a constant temperature, meaning that it is in contact with a reservoir at a finite temperature T. In this case, the entropy production rate is related to the rate of change in the free energy of the active gel $T\dot{\mathcal{S}} = -dF/dt$.

For a passive gel at rest, the free-energy density f is a function of the two intensive variables, the density ρ and the polarization $\mathbf{p}$, and its differential is $df = \mu d\rho - h_\alpha dp_\alpha$. The field conjugate to the density is the chemical potential μ and the field conjugate to the polarization is the orientational field $\mathbf{h}$. For a passive system moving at a velocity $\mathbf{v}$, the density of kinetic energy $\frac{1}{2}\rho m \mathbf{v}^2$ must be added to the free energy.

For an active gel one must also take into account the fact that energy is constantly locally injected into the gel. A simple intuitive way to introduce the energy injection is to assume that as in the case of the cytoskeleton, this is due to a nonequilibrium chemical reaction such as the consumption of ATP. If the energy gain per ATP molecule is denoted by $\Delta\mu$, and the rate of advancement of the reaction (the number of ATP molecules consumed per unit time and unit volume) is denoted by r, then the associated rate of change of the free energy per unit volume is $-r\Delta\mu$. Taking into account all contributions, we find the entropy production rate of an active gel at a constant temperature T (Kruse *et al.*, 2004, 2005):

$$T\dot{\mathcal{S}} = \int d\mathbf{r}\left\{-\frac{\partial}{\partial t}\left(\frac{1}{2}\rho m \mathbf{v}^2\right) - \mu\frac{\partial \rho}{\partial t} + h_\alpha \dot{p}_\alpha + r\Delta\mu\right\}. \tag{30}$$

2. Conservation laws

The two conserved quantities in an active gel are the density and the momentum. The density conservation law reads

$$\frac{\partial \rho}{\partial t} + \boldsymbol{\nabla} \cdot (\rho \mathbf{v}) = 0. \tag{31}$$

The momentum conservation law can be written as

$$\frac{\partial g_\alpha}{\partial t} + \partial_\beta \Pi_{\alpha\beta} = 0, \tag{32}$$

where the momentum flux in the system is $\Pi_{\alpha\beta} = \rho m v_\alpha v_\beta - \sigma^t_{\alpha\beta}$, where the first term is associated with the so-called Reynolds stress and $\sigma^t_{\alpha\beta}$ is the total stress in the system. For most active gels, in particular, for biological systems, the Reynolds number is very small and we ignore the Reynolds stress contribution in the following.

3. Thermodynamics of polar systems

For generality, in this section we consider active gels in three dimensions. The polarization free energy of an active polar material is a functional of the three components of the polarization vector $\mathbf{p}$. However, if the system is not in the vicinity of a critical point, there are only two soft modes associated with rotations of the polarization. The modulus of the polarization is not a hydrodynamic variable and is taken to be constant. Without any loss of generality, we assume that the polarization is a unit vector, and that the effect of its modulus is integrated in the phenomenological transport coefficients. The polarization free energy of the active gel is then the classical Frank free energy of a nematic liquid crystal (de Gennes and Prost, 1993)

$$F_p = \int_{\mathbf{r}} \Big[\frac{K_1}{2} (\boldsymbol{\nabla} \cdot \mathbf{p})^2 + \frac{K_2}{2} [\mathbf{p} \cdot (\boldsymbol{\nabla} \times \mathbf{p})]^2 + \frac{K_3}{2} [\mathbf{p} \times (\boldsymbol{\nabla} \times \mathbf{p})]^2 + v \boldsymbol{\nabla} \cdot \mathbf{p} - \frac{1}{2} h^0_{\|} \mathbf{p}^2 \Big]. \tag{33}$$

The first three terms correspond to the free energies of splay, twist, and bend deformations. The three Frank constants K_i are positive. We have also added in this free energy a Lagrange multiplier $h^0_{\|}$ to insure that the polarization is a unit vector. This free energy is very similar to the free energy of Eq. (4), although in Eq. (4) we made the additional approximation that the Frank constants are equal. In the case where the polarization is a critical variable, one would also need to add to Eq. (33) a Landau expansion in powers of the polarization modulus as done in Eq. (4).

The orientational field is obtained by differentiation of the free energy (33). It is useful to decompose it into a component parallel to the polarization $h_{\|}$ and a component perpendicular to the polarization $h_\perp$

In the simple case where the system is two dimensional, the polarization can be characterized by its polar angle θ. In the approximation where the Frank constants are equal the perpendicular molecular field is $h_\perp = K \nabla^2 \theta$.

In a nonisotropic medium the stress is not symmetric. There is an antisymmetric component of the stress associated with torques in the medium. As for nematic liquid crystals, this antisymmetric component can be calculated from the conservation of momentum in the fluid (de Gennes and Prost, 1993) and is given by $\sigma^A_{\alpha\beta} = \frac{1}{2}(h_\alpha p_\beta - p_\alpha h_\beta) \sim h_\perp$.

TABLE II. Fluxes and associated forces controlling the entropy production in a one-component nematic active gel.

Flux	Force
$\sigma_{\alpha\beta}$	$v_{\alpha\beta}$
P_α	h_α
r	$\Delta\mu$

4. Fluxes, forces, and time reversal

Using the conservation laws and performing integrations by parts, the entropy production can be written as

$$T\dot{\mathcal{S}} = \int d\mathbf{r} \{ \sigma_{\alpha\beta} v_{\alpha\beta} + P_\alpha h_\alpha + r \Delta\mu \}, \tag{34}$$

where $\sigma_{\alpha\beta}$ is the symmetric deviatoric stress tensor defined by

$$\sigma^t_{\alpha\beta} = \sigma_{\alpha\beta} + \sigma^A_{\alpha\beta} - \delta_{\alpha\beta} P, \tag{35}$$

with $\sigma^t_{\alpha\beta}$ and $\sigma^A_{\alpha\beta}$ the total and the antisymmetric part of the stress tensor, respectively, and P the pressure. We also introduced the strain-rate tensor $v_{\alpha\beta}$ and the antisymmetric part of the velocity gradients associated with the vorticity $\omega_{\alpha\beta}$ defined as

$$v_{\alpha\beta} = \tfrac{1}{2}(\partial_\alpha v_\beta + \partial_\beta v_\alpha), \tag{36a}$$

$$\omega_{\alpha\beta} = \tfrac{1}{2}(\partial_\alpha v_\beta - \partial_\beta v_\alpha). \tag{36b}$$

Finally, $P_\alpha = D p_\alpha / Dt$, with

$$\frac{D p_\alpha}{Dt} = \frac{\partial p_\alpha}{\partial t} + v_\beta \partial_\beta p_\alpha + \omega_{\alpha\beta} p_\beta \tag{37}$$

the comoving and corotational derivative of the polarization. Note that if the system is chiral, kinetic momentum conservation must be properly taken into account and the local rotation is no longer given by $\omega_{\alpha\beta}$ (Furthauer *et al.*, 2012).

This form of the entropy production allows for the identification of three forces: $v_{\alpha\beta}$, which has a signature -1 under time reversal, h_α, which has a signature $+1$ under time reversal, and $\Delta\mu$, which also has a signature $+1$ under time reversal. The conjugated fluxes are $\sigma_{\alpha\beta}$, P_α, and r, respectively. The fluxes and associated driving forces that control the hydrodynamics of active gels are summarized in Table II.

In a linear generalized hydrodynamic theory, the constitutive equations of the active gel are obtained by writing the most general linear relation between fluxes and forces respecting the symmetries of the problem, such as translational and rotational symmetries with one vector p_α and one tensor $q_{\alpha\beta} = p_\alpha p_\beta - \frac{1}{3}\delta_{\alpha\beta}$ in 3D. Particular care must be taken in considering the time-reversal symmetry. The fluxes must all be separated into a reactive component with a signature opposite to that of the conjugate force and a dissipative component with the same signature as the conjugate force. As an example, the reactive component of the stress is the elastic stress and the dissipative component is the viscous stress. Only the dissipative component of each flux contributes to the entropy production.

B. Linear theory of active polar and nematic gels

1. Constitutive equations

We first consider an active polar liquid for which the relationship between fluxes and forces is local in time.

It is convenient to split all tensors into diagonal and traceless parts: $\sigma_{\alpha\beta} = \sigma\delta_{\alpha\beta} + \tilde{\sigma}_{\alpha\beta}$, with $\sigma = (1/3)\sigma_{\alpha\alpha}$, $\tilde{\sigma}_{\alpha\alpha} = 0$, and d the dimensionality. Similarly, we let $v_{\alpha\beta} = (u/3)\delta_{\alpha\beta} + \tilde{v}_{\alpha\beta}$, where $u = \partial_\gamma v_\gamma$ is the divergence of the velocity field. Finally all fluxes are written as the sums of reactive and dissipative parts,

$$\sigma_{\alpha\beta} = \sigma^r_{\alpha\beta} + \sigma^d_{\alpha\beta}, \tag{38a}$$

$$P_\alpha = P^r_\alpha + P^d_\alpha, \tag{38b}$$

$$r = r^r + r^d. \tag{38c}$$

a. Dissipative fluxes

Only fluxes and forces with the same time signature are coupled and $\sigma_{\alpha\beta}$ is coupled only to $v_{\alpha\beta}$. This leads to the constitutive equations

$$\sigma^d = \bar{\eta}u, \tag{39a}$$

$$\tilde{\sigma}^d_{\alpha\beta} = 2\eta\tilde{v}_{\alpha\beta}. \tag{39b}$$

We ignore here the tensorial character of the viscosity and assume only two viscosities as for an isotropic fluid: the shear viscosity η and the longitudinal viscosity $\bar{\eta}$. The two other fluxes are coupled and the corresponding constitutive equations read (Kruse *et al.*, 2004, 2005)

$$P^d_\alpha = \frac{h_\alpha}{\gamma_1} + \epsilon p_\alpha \Delta\mu, \tag{40}$$

$$r^d = \Lambda\Delta\mu + \epsilon p_\alpha h_\alpha. \tag{41}$$

γ_1 is the rotational viscosity and we use here the Onsager symmetry relation which imposes that the "dissipative" Onsager matrix is symmetric.

b. Reactive fluxes

The reactive Onsager matrix is antisymmetric and couples fluxes and forces of opposite time-reversal signatures,

$$\sigma^r = -\bar{\zeta}\Delta\mu + \bar{\nu}_1 p_\alpha h_\alpha, \tag{42a}$$

$$\tilde{\sigma}^r_{\alpha\beta} = -\zeta\Delta\mu q_{\alpha\beta} + \frac{\nu_1}{2}\left(p_\alpha h_\beta + p_\beta h_\alpha - \frac{2}{3}p_\gamma h_\gamma \delta_{\alpha\beta}\right), \tag{42b}$$

$$P^r_\alpha = -\bar{\nu}_1 p_\alpha \frac{u}{3} - \nu_1 p_\beta \tilde{v}_{\alpha\beta}, \tag{42c}$$

$$r^r = \bar{\zeta}\frac{u}{3} + \zeta q_{\alpha\beta}\tilde{v}_{\alpha\beta}. \tag{42d}$$

In most of the following we consider incompressible fluids so that $u = \nabla\cdot\mathbf{v} = 0$. In this case the diagonal component of the stress can be included in the pressure which is a Lagrange multiplier ensuring incompressibility and one can set $\bar{\zeta} = \bar{\nu}_1 = \bar{\eta} = 0$.

To summarize, the hydrodynamic equations for an incompressible one-component active fluid of nematic symmetry are given by

$$m\rho(\partial_t + \mathbf{v}\cdot\nabla)\mathbf{v} = -\nabla P + \nabla\cdot\boldsymbol{\sigma}, \tag{43a}$$

$$(\partial_t + \mathbf{v}\cdot\nabla)p_\alpha + \omega_{\alpha\beta}p_\beta = -\nu_1 v_{\alpha\beta}p_\beta + \frac{1}{\gamma_1}h_\alpha + \epsilon\Delta\mu p_\alpha, \tag{43b}$$

to be supplemented with the incompressibility condition $\nabla\cdot\mathbf{v} = 0$. Assuming the Frank constants are all equal to K, the molecular field h_α is given by

$$h_\alpha = K\nabla^2 p_\alpha + h^0_\parallel p_\alpha, \tag{44}$$

with $h^0_\parallel$ a Lagrange multiplier to be determined by the condition $|\mathbf{p}| = 1$. Finally it is convenient for the following to write the deviatoric stress tensor given by the sum of trace and deviatoric parts of the dissipative and reactive components by separating out passive and active parts as

$$\sigma_{\alpha\beta} = \sigma^p_{\alpha\beta} + \sigma^a_{\alpha\beta}, \tag{45}$$

with passive and active contributions given by

$$\sigma^p_{\alpha\beta} = 2\eta\tilde{v}_{\alpha\beta} + \frac{\nu_1}{2}\left(p_\alpha h_\beta + p_\beta h_\alpha - \frac{2}{3}p_\gamma h_\gamma\delta_{\alpha\beta}\right), \tag{46a}$$

$$\sigma^a_{\alpha\beta} = -\zeta\Delta\mu q_{\alpha\beta}. \tag{46b}$$

In many biological applications inertial effects are negligible and the Navier-Stokes equation (43a) can be replaced by the Stokes equation obtained by simply neglecting all inertial terms on the left-hand side of Eq. (43a) and corresponding to a force balance equation, given by

$$-\nabla P + \nabla\cdot\boldsymbol{\sigma} = 0. \tag{47}$$

2. Microscopic interpretation of the transport coefficients

The Onsager approach that we outlined introduces several transport coefficients. Some of these coefficients exist for passive nematic liquid crystals such as the viscosities, the rotational viscosity γ_1, or the flow-coupling coefficient ν_1. The two important new coefficients are the transport coefficients associated with the activity of the system, ϵ and ζ. The active stress in the system is $\sigma^{\text{active}}_{\alpha\beta} = -\zeta\Delta\mu q_{\alpha\beta}$. In the case of the cytoskeleton this can be viewed as the stress due to the molecular motors, which tend to contract the gel. The sign of the activity coefficient ζ is not imposed by theory. A negative value corresponds to a contractile stress as in the actin cytoskeleton. A positive value of ζ corresponds to an extensile stress as observed in certain bacterial suspensions. Conceptually, active stresses in living matter were first discussed by Finlayson and Scriven (1969). They, however, specifically steered clear of uniaxial stresses arising from motor-protein contractility. The first incorporation of self-propelling stresses into the generalized hydrodynamics of orientable fluids was by Simha and Ramaswamy (2002a), although it has long been understood that the minimal description of a single force-free swimmer is a force dipole (Brennen and Winet, 1977; Pedley and Kessler, 1992).

The other active coefficient ϵ is an active orientational field that tends to align the polarization when it is positive. In the limit where the modulus of the polarization is $p = 1$ one can always consider that $\epsilon = 0$ and introduce an effective activity

coefficient $\zeta + \epsilon\gamma_1\nu_1$. In the following we therefore choose $\epsilon = 0$ and use this effective value of the activity coefficient ζ.

3. Viscoelastic active gel

An active gel is not in general a simple liquid but rather a viscoelastic medium with a finite viscoelastic relaxation time, which is liquid only at long time scales. In a passive viscoelastic medium the constitutive relation between stress and strain is nonlocal in time. The simplest description of a viscoelastic medium is the so-called Maxwell model where the system has only one relaxation time (Larson, 1988). Within this model the constitutive equation is

$$\frac{D\tilde{\sigma}_{\alpha\beta}}{Dt} + \frac{1}{\tau}\tilde{\sigma}_{\alpha\beta} = 2E\tilde{v}_{\alpha\beta}. \tag{48}$$

The Maxwell model involves two material constants, the viscoelastic relaxation time τ and the shear modulus E. The long time viscosity of the medium is then $\eta = E\tau$. In order to respect rotational and translational invariance, we use a convected Maxwell model with a convected time derivative of the stress tensor

$$\frac{D\tilde{\sigma}_{\alpha\beta}}{Dt} = \frac{\partial\tilde{\sigma}_{\alpha\beta}}{\partial t} + v_\gamma\partial_\gamma\tilde{\sigma}_{\alpha\beta} + \omega_{\alpha\gamma}\tilde{\sigma}_{\gamma\beta} + \tilde{\sigma}_{\gamma\alpha}\omega_{\beta\gamma}.$$

Note that there are several ways of defining the convective derivative of tensors. For simplicity we use the same notation D/Dt to denote convected derivatives of vectors and tensors.

The generalization of the Onsager hydrodynamic approach of the previous section to a viscous elastic polar passive medium leads to the constitutive equations for an active gel (Jülicher *et al.*, 2007):

$$2\eta v_{\alpha\beta} = \left(1 + \tau\frac{D}{Dt}\right)\left(\tilde{\sigma}_{\alpha\beta} + \zeta\Delta\mu q_{\alpha\beta} - \frac{\nu_1}{2}(p_\alpha h_\beta + p_\beta h_\alpha)\right), \tag{49a}$$

$$\frac{Dp_\alpha}{Dt} = \frac{1}{\gamma_1}\left(1 + \tau\frac{D}{Dt}\right)h_\alpha - \nu_1 v_{\alpha\beta}p_\beta, \tag{49b}$$

where for simplicity we have considered only an incompressible active gel where the modulus of the polarization is unity. Note that the memory of the system not only plays a role for the stress but also for the dynamics of the orientation and that we have supposed that the two corresponding relaxation times are equal.

It is important to note that the dynamical equation for the polarization is very similar to Eq. (2b), which has been obtained using the same symmetry arguments; Eq. (2b) ignores memory effects and therefore the viscoelasticity of the polarization response; all the extra terms in Eq. (2b) do not appear here because the Onsager approach that we use derives only the linear hydrodynamic theory.

C. Active polar gels

1. Polarity effects

For simplicity, we presented here only the derivation of the hydrodynamic theory of active gels in the simplest case where the system is a single component fluid and has nematic symmetry, $\mathbf{p}$ being the director, and ignore any type of noise. Several extensions of this theory have been proposed.

For a polar system, there is an extra polar term in the free energy (33), $F_p = \int d\mathbf{r}v(\rho)(\boldsymbol{\nabla}\cdot\mathbf{p})$. This spontaneous splay term is a surface term if the coefficient v is a constant. If v depends on the local density, this term, that was included in Eq. (4), yields a "pressure-gradient" proportional to $\boldsymbol{\nabla}\rho$ in the equation for the polarization. Other nonlinear polar terms that can be added on the right-hand side of the dynamical equation for the polarization (49) are proportional to $\mathbf{p}\cdot\nabla\mathbf{p}$, $\nabla\mathbf{p}^2$, and $\mathbf{p}\nabla\cdot\mathbf{p}$. These terms have already been considered in Eq. (2b). The first of these terms cannot be derived from a free energy and is therefore an active term proportional to $\Delta\mu$. Its effect in a dynamics linearized about an ordered state was considered for active liquid-crystalline suspensions by Simha and Ramaswamy (2002a). The other two terms can be derived from a free energy and have both active and passive contributions. Within the Onsager linear hydrodynamics scheme, other polar terms in the equations show up only at nonlinear order or at subleading order in a gradient expansion. Active stresses proportional to $\Delta\mu(\partial_i p_j + \partial_j p_i)$ unique to polar fluids are obtained from the microscopic theory (Marchetti and Liverpool, 2007), but are considered nonlinear in the driving forces in the context of the Onsager approach. The effect of these polar terms was studied in detail by Giomi, Marchetti, and Liverpool (2008). In general these polar terms are important when describing an active suspension as opposed to the one-component system considered here. In this case these terms yield spatial inhomogeneities in the concentration of active particles (Tjhung, Cates, and Marenduzzo, 2011; Giomi and Marchetti, 2012) that are not obtained in active suspensions with nematic symmetry (Giomi *et al.*, 2011, 2012).

2. Noise in active gels

The effect of noise in active polar gels can be studied by introducing random Langevin forces in the constitutive equations. For treatments including thermal and active nonthermal noise sources in a systematic way, see Lau *et al.* (2003), Hatwalne *et al.* (2004), Chen *et al.* (2007), Basu *et al.* (2008), Lau and Lubensky (2009), and Sarkar and Basu (2011). The precise description of the statistics of active noise requires a microscopic description of the gel which is not generic and goes beyond the scope of this review (Basu *et al.*, 2008). Hatwalne *et al.* (2004) introduced the active noise in the isotropic phase of an active gel through the fluctuating active stress in the Navier-Stokes equation and used scaling arguments to estimate the apparent temperature it would generate in a tracer diffusion measurement.

3. Multicomponent active gels

Most active systems described in the earlier sections are multicomponent systems containing a solvent and active objects. In many instances these systems can be described by an effective one-component theory as described here. However, in particular, when considering viscoelastic effects the one-component theory ignores the permeation of the solvent through the active gel. A detailed two-component theory of active gels that properly takes into account permeation effects is given by Callan-Jones and Jülicher (2011).

The new main feature in a multicomponent gel is the existence of currents of the various components. We show here how the active currents in nematic (Sec. II.B) and polar (Sec. II.A) systems follow naturally from the forces-and-fluxes framework. In this short treatment we ignore fluid flow. Consider a mesoscopic region in our active medium, in a chemical potential gradient $\nabla\Phi$ corresponding to the concentration ρ, and subjected to a nonzero chemical potential difference $\Delta\mu$ between a fuel (ATP) and its reaction products [adenosine diphosphate (ADP) and inorganic phosphate]. For small departures from equilibrium, the fluxes r (the rate of consumption of ATP molecules) and $\mathbf{J}$ must be linearly related to $\Delta\mu$ and $\nabla\Phi$. The presence of local orientational order in the form of $\mathbf{p}$ and $\mathbf{Q}$ allows one to construct scalars $\mathbf{p}\cdot\nabla\Phi$ and $\nabla\cdot\mathbf{Q}\cdot\nabla\Phi$; thus r in general gets a contribution $(\zeta_p\mathbf{p}+\bar{\zeta}_Q\nabla\cdot\mathbf{Q})\cdot\nabla\Phi$, where ζ_p and $\bar{\zeta}_Q$ are kinetic coefficients depending in general on ρ and other scalar quantities. The symmetry of dissipative Onsager coefficients then implies a contribution

$$\mathbf{J}_{\text{active}}=(\zeta_p\mathbf{p}+\bar{\zeta}_Q\nabla\cdot\mathbf{Q})\Delta\mu \tag{50}$$

to the current. In the presence of a maintained constant value of $\Delta\mu$ the current (50) rationalizes, through the ζ_p and $\bar{\zeta}_Q$ terms, the form of Eq. (2a) (with $\zeta_p\Delta\mu\rightarrow v_0\rho$) and Eq. (26) (with $\bar{\zeta}_Q\Delta\mu\rightarrow\zeta_Q$). In particular, it underlines the fact that active currents do not require an explicit polar order parameter. Even without $\mathbf{p}$, the term in $\bar{\zeta}_Q$ in Eq. (50) tells us that curvature in the spatial arrangement of active filaments gives rise to particle motion. In retrospect this is not shocking: a splayed or bent configuration of a nematic phase has a vectorial asymmetry, as argued through Fig. 12. In a system out of equilibrium this asymmetry should reflect itself in a current. As shown by Ramaswamy, Simha, and Toner (2003) and discussed in Sec. II.B, $\bar{\zeta}_Q$ leads to giant number fluctuations in active nematics.

D. Active defects

Ordered phases of active matter, like their counterparts at thermal equilibrium, should exhibit topological defect configurations, generated through either specific boundary conditions or spontaneously in the bulk. As in equilibrium systems, the nature of these defects depends on whether the system has polar or apolar symmetry (Palffy-Muhoray, Lee, and Petschek, 1988; de Gennes and Prost, 1993; Kung, Marchetti, and Saunders, 2006). The selection criterion for the defect strength in active systems is not obvious, as one cannot *a priori* invoke free-energy minimization as in equilibrium systems. However, it does appear that experiments see strength $+1$ and strength $+1/2$ defects, respectively, in polar (Nédélec *et al.*, 1997) and apolar (Narayan, Ramaswamy, and Menon, 2007) active systems. Activity confers a particularly interesting property on defects, namely, rotational (Nédélec *et al.*, 1997; Kruse *et al.*, 2005) or translational (Narayan, Ramaswamy, and Menon, 2007; Marchetti, 2012; Sanchez *et al.*, 2012) movement, with sense or direction determined by the chirality or polarity associated with the defect.

The first quantitative experiments which explicitly demonstrated how active mixtures of long rods (microtubules) and motors (kinesin) could spontaneously form defects such as asters and spirals were reported by Nédélec *et al.* (1997) and Surrey *et al.* (2001); see Fig. 2. These patterns showed a remarkable resemblance to the microtubule-based spindle patterns in the cell, thus suggesting that the gross features of spindle patterning could be understood as arising from a self-organization of simple elements. Several qualitative features of these experiments including the defect patterns could be simply understood using continuum models describing the polar orientation of the rigid filaments and the density of processive motors (Lee and Kardar, 2001; Sankararaman, Menon, and Kumar, 2004).

A detailed study of the nature of defects and their phase transitions within the framework of the active gel theory was done by Kruse *et al.* (2004, 2005) who showed that flows arising from active stresses lead to systematic rotation of chiral defects. We summarize here the calculation, working as in Kruse *et al.* (2004) with the ordered state described by a vectorial order parameter $\mathbf{p}$ in two dimensions. Polarity enters nowhere in the analysis, except as justification for working with a strength $+1$ defect. We parametrize a two-dimensional defect configuration of the polarization field $\mathbf{p}$ (of unit magnitude) with topological charge ±1 using polar coordinates (r,θ). Thus charge $+1$ defects such as *asters*, *vortices*, and *spirals* may be represented by an angle ψ, with $p_r=\cos\psi$ and $p_\theta=\sin\psi$, such that $\psi=0$ (or π) is an aster, $\psi=\pm\pi/2$ a vortex, and $\psi=\psi_0$ (any other constant) a spiral. At equilibrium, a situation corresponding to defect configurations in a ferroelectric nematic liquid crystal, the optimal value of ψ is obtained by minimizing the Frank free-energy functional F, Eq. (33), with $K_2=0$ (no twist as we are working in two dimensions). With appropriate boundary conditions, it is easy to see that the stable defect configurations are (i) asters when $K_1<K_3$, so that splay is favored, (ii) vortices when $K_1>K_3$, i.e., bend is favored, and (iii) spirals when $K_1=K_3$. In the special case when $K_1=K_3$, the energy is degenerate and asters, vortices, and spiral defects have the same energy. In an active system, however, the stability of defect configurations is obtained by solving the dynamical equations for the polarization $\mathbf{p}$ together with the conditions of force balance and overall incompressibility, as in Sec. III.B

Suppose $K_1<K_3$, so that the aster is stable in the absence of activity $\Delta\mu=0$. Now introduce activity. Linear stability analysis shows that at sufficiently large contractile active stresses $\zeta\Delta\mu<0$ the aster gets destabilized giving rise to a spiral with an angle ψ_0 set by the flow-alignment parameter ν_1 (assuming stable flow alignment). An entirely similar analysis, starting from a stable vortex for $K_1>K_3$, with $\Delta\mu=0$, shows again an instability for large enough $\Delta\mu$. The reason this happens here and does not happen for systems without activity is that the active stresses associated with the perturbed director configuration give rise to flows whose effect on the director is to reinforce the perturbation. Figures 19 and 20 illustrate the flow associated with the spiral instability and the stability domains of the defects, respectively. The active spiral has a sense of direction and will therefore rotate. The angular speed can be obtained by solving the steady-state equations for ψ and v_θ, leading to

$$v_\theta(r)=\omega_0 r\log\left(\frac{r}{r_0}\right), \tag{51}$$

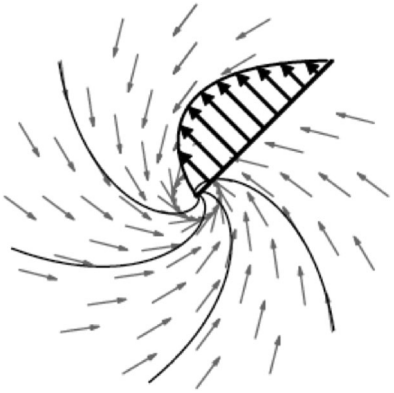

FIG. 19. Sketch of a rotating spiral defect in an active nematic fluid with vanishing elastic anisotropy $\delta K = 0$. The gray arrows mark the director, and the solid lines show its spiral structure. The hydrodynamic velocity field is in the azimuthal direction, and its profile is indicated by the dark arrows. Adapted from Kruse *et al.*, 2004.

where, as is inevitable on dimensional grounds, ω_0 scales as the ratio of the active stress to a viscosity, with a detailed form that includes a dependence on the director kinetic coefficient and the flow-alignment parameter. In a finite system of size R, imposing a vanishing velocity at the outer boundary due to the presence of a wall, we can set the length scale $r_0 = R$.

In the above analysis we ignored the dynamics of the concentration field ρ. This is probably acceptable when the active units are long and rigid or when their concentration is so high that excluded volume considerations do not permit significant density inhomogeneities. We can include ρ (Gowrishankar and Rao, 2012) through an extra term $w_1 \int d^3r(\delta\rho/\rho_0)\nabla\cdot\mathbf{p}$ in the free energy (33) [see also Eq. (4)], with the form of a spontaneous splay that depends on the local concentration, and restore the concentration equation $\partial_t\rho = -\nabla\cdot\mathbf{J}$, where the filament current $\mathbf{J} = v_0\rho\mathbf{p} - D\nabla\rho$ has an active advective and a diffusive contribution. Now for large enough w_1, the defect configurations are generated by the internal dynamics (and insensitive to the boundary for large systems) and so have finite size. When advection is negligible, the defect size is set by the ratio of the spontaneous splay coupling strength w_1 to a Frank modulus K as it would be in an equilibrium polar liquid crystal. On the other hand, when advection is appreciable

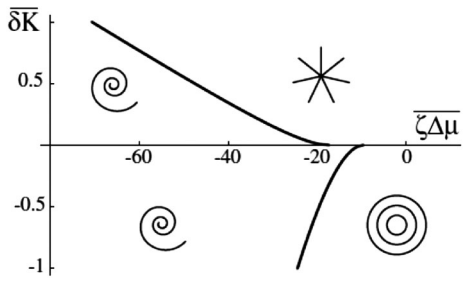

FIG. 20. Stability diagram of topological defects in an active nematic fluid. For small values of the activity $\zeta\Delta\mu$ one gets asters and vortices, respectively, for $\overline{\delta K} = K_1 - K_3 < 0$ and >0. When $\zeta\Delta\mu$ is of sufficiently large magnitude both asters and spirals are unstable to the formation of a rotating spiral. Adapted from Ben-Jacob, Cohen, and Levine, 2000.

so as to have density clumping in regions where $\mathbf{p}$ points inward toward a common center, the defect size is set by the ratio of diffusion to active advection D/v_0. We note that since the advection current $\mathbf{J} \propto \rho\mathbf{p}$, a small perturbation of the vortex configuration renders it unstable and the only stable defects are inward pointing asters and spirals (Gowrishankar and Rao, 2012).

Since defects now have a finite size, it is possible to have an array of defects which interact with each other. Such studies have shown that, under certain conditions, one obtains a stable lattice of asters accompanied by a variety of phase transitions (Ziebert and Zimmermann, 2005; Voituriez, Joanny, and Prost, 2006; Gowrishankar and Rao, 2012). A detailed study of defect-defect interactions and the dynamics of defects and their merger in this active context are open problems for the future.

So far we have discussed charge 1 defects generated in polar active media. Apolar active media, described by a local orientational tensor $\mathbf{Q}$, exhibit $\pm 1/2$ strength disclinations, topologically identical to those obtained in equilibrium nematic liquid crystals (see Fig. 7). The orientation field around a defect of strength $+1/2$ has a polarity, whereas that around a $-1/2$ has a threefold symmetric appearance. On general grounds, the $+1/2$ defect should move spontaneously, whereas the $-1/2$ defect should show no such tendency. Precisely this behavior seems to be observed in the active nematic phase in a vibrated granular-rod monolayer (Narayan, Ramaswamy, and Menon, 2007).

E. Current status on active gels

The nonequilibrium thermodynamic description of active systems is a systematic approach based on symmetries and, in particular, on invariance against time inversion. It is, however, based on a linear expansion of fluxes in terms of forces and can in principle describe only systems close to equilibrium where $\Delta\mu$ tends to zero. One of the main applications though is to biological systems that are mostly far from equilibrium systems. There is no systematic extension of the theory to systems far from equilibrium. One must rely either on a microscopic description that generates nonlinear contributions by coarse graining to large length scales and long-time scales or on experimental results that emphasize specific nonlinear aspects, which can then be introduced in theory. Microscopic or mesoscopic descriptions of molecular motors are a good example of the first case and lead to motor forces or velocities that are not linear in $\Delta\mu$ (Jülicher and Prost, 1997; Liverpool *et al.*, 2009). Several experiments suggest that the treadmilling associated with the polymerization and depolymerization of actin in a cell depends on the force applied on the filaments or the local stress in a nonlinear way (Mogilner and Oster, 1999; Prost *et al.*, 2007).[5] The force-dependent treadmilling is essential for many cellular processes such as cell migration or cell adhesion and a full description including these effects in the active gel theory has not yet been proposed (Keren *et al.*, 2008).

[5]In a cell actin filaments polymerize at the so-called barbed end and depolymerize at the so-called pointed end. This constant turnover of active filaments is called treadmilling.

Another intrinsic limitation of the current active gel theory is the assumption of linear rheology and the use of the Maxwell model with a single relaxation time. A large body of experimental work shows that for many types of cells as well as for actomyosin gels there is a broad distribution of relaxation times leading to a complex modulus decreasing as a power law of frequency with a small exponent between 0.1 and 0.25 (Fabry *et al.*, 2001). An *ad hoc* power-law distribution of relaxation times could be introduced in the active gel hydrodynamic theory but despite some efforts, this type of law is not understood on general grounds (Balland *et al.*, 2006). The nonlinear rheology of actin networks has also been studied in detail, and actin networks in the absence of molecular motors have been found to strain thicken (Gardel *et al.*, 2004). This behavior can at least in part be explained by the inextensibility of the actin filaments. In the presence of myosin motors, the active stress induced by the molecular motors itself stiffens the active gel (Koenderink *et al.*, 2009).

The hydrodynamic description of active polar or nematic gels is very close to that of nematic liquid crystals. Nevertheless the existence of an active stress leads to several nonintuitive and spectacular phenomena. The most spectacular is the flow instability described below that leads to spontaneously flowing states. Other spectacular effects are associated with active noise in these systems. In all active systems the noise has a thermal component and a nonthermal active component. The properties of the active noise cannot be inferred from the macroscopic hydrodynamic theory and must be derived in each case from a specific microscopic theory. The study of tracer diffusion in a thin active film, for example (Basu *et al.*, 2012), leads to an anomalous form of the diffusion constant that does not depend on the size of the particle but only on the thickness of the film. We believe that there are still many unusual properties of active gels to be discovered and that in many cases, this will require detailed numerical studies of the active gel hydrodynamic equations such as the one performed by Marenduzzo, Orlandini, and Yeomans (2007).

Active gel models have also been used to describe cross-linked motor-filament systems that behave as soft solids at large scales (MacKintosh and Levine, 2008; Levine and MacKintosh, 2009; Yoshinaga *et al.*, 2010; Banerjee and Marchetti, 2011) and also to understand the origin of sarcomeric oscillations, both from a microscopic and from a continuum viewpoint (Günther and Kruse, 2007; Banerjee and Marchetti, 2011). Further, active gel models have been shown to successfully account for the experimentally observed traction stresses exerted by cells and cell sheets on compliant substrates (Banerjee and Marchetti, 2011; Edwards and Schwarz, 2011; Mertz *et al.*, 2012).

Finally a large part of the theoretical activity on active gels aims at a quantitative description of biological phenomena at the scale of the cell and of cellular processes involving the cytoskeleton. Some success has already been obtained in discussing lamellipodium motion (Kruse *et al.*, 2006) or the formation of contractile rings during cell division (Salbreux, Prost, and Joanny, 2009). An important step is the connection of the parameters of the hydrodynamic theory with the more microscopic parameters that can be monitored experimentally which requires an explicit coarse-graining of the microscopic theories as discussed in Sec. IV.D. At larger scales one can build a hydrodynamic theory of tissues that shares many features with the active gel theory described here (Ranft *et al.*, 2010).

IV. HYDRODYNAMIC CONSEQUENCES OF ACTIVITY

In this section we describe a number of remarkable hydrodynamic phenomena induced by activity. Most of the section is devoted to the description of material properties of active gels, such as thin film instabilities and rheology. In Sec. IV.D we also highlight some of the remarkable successes of the hydrodynamic theory of active gels in describing phenomena observed in living cells. A more complete review of this latter class of phenomena can be found in Joanny and Prost (2009b).

A. Instabilities of thin liquid active films

1. Spontaneous flow of active liquid films

One generic property of active orientable liquids, whether polar or apolar, is the instability of any homogeneous nonflowing steady state toward an inhomogeneous spontaneously flowing state as shown by Simha and Ramaswamy (2002a). We illustrate this instability in the simple geometry of a thin active nematic liquid film (Voituriez, Joanny, and Prost, 2005).

We study a thin film of thickness h supported by a solid substrate. For simplicity we consider only the two-dimensional geometry sketched in Fig. 21 where the substrate is along x and the normal of the film is along y. We choose anchoring conditions parallel to the film surface so that for $y = 0, h$ the polarization is along x, $p_x = 1$, and $p_y = 0$. An obvious solution for the equations of motion of an active liquid is a nonflowing state $\mathbf{v} = \mathbf{0}$ with a constant polarization parallel to x. We now discuss the stability of this steady state. We look for a state of the system which is invariant by translation along x so that all derivatives with respect to x vanish and with a polarization that is not parallel to the film surfaces $p_x = \cos\theta(y)$, $p_y = \sin\theta(y)$. The velocity is along the x direction and the shear rate tensor has only one nonvanishing component $v_{xy} \equiv w = \frac{1}{2}\partial_y v_x$.

The total stress can be written as $\sigma^t_{\alpha\beta} = -P\delta_{\alpha\beta} + \sigma^A_{\alpha\beta} + \sigma_{\alpha\beta}$ where the last term is the deviatoric stress given by the constitutive equations (49) and the previous term is the antisymmetric component of the stress. Force balance in the film

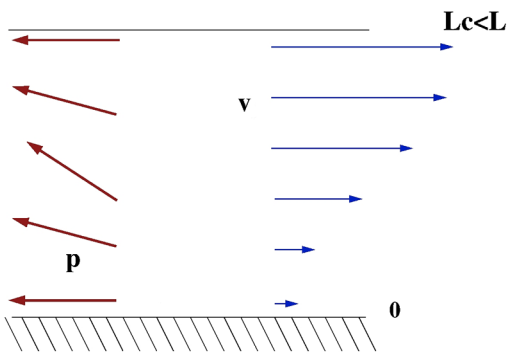

FIG. 21 (color online). Spontaneously flowing film of active liquid.

is written as $\partial_y \sigma^t_{yx} = 0$. Taking into account the fact that on the free surface the shear stress vanishes, we obtain $\sigma^t_{yx} = 0$. Using the constitutive equation, this leads to

$$-h_\perp = 4\eta w - \zeta\Delta\mu \sin 2\theta + \nu_1(h_\parallel \sin 2\theta + h_\perp \cos 2\theta), \tag{52}$$

where we introduced the parallel and perpendicular components of the orientational field $h_\parallel = h_x \cos\theta + h_y \sin\theta$ and $h_\perp = h_y \cos\theta - h_x \sin\theta$.

The constitutive equations for the polarization of Eq. (49) give

$$\begin{aligned} -w \sin\theta &= \frac{h_x}{\gamma_1} - \nu_1 w \sin\theta, \\ w \cos\theta &= \frac{h_y}{\gamma_1} - \nu_1 w \cos\theta. \end{aligned} \tag{53}$$

Combining Eqs. (52) and (53), we obtain the perpendicular field and the velocity gradient

$$\begin{aligned} h_\perp &= \frac{\zeta\Delta\mu \sin 2\theta(1 + \nu_1 \cos 2\theta)}{4\eta/\gamma_1 + 1 + \nu_1^2 + 2\nu_1 \cos 2\theta}, \\ w &= \frac{\zeta\Delta\mu \sin 2\theta}{4\eta/\gamma_1 + 1 + \nu_1^2 + 2\nu_1 \cos 2\theta}. \end{aligned} \tag{54}$$

In the approximation where the Frank constants are equal, the perpendicular molecular field is

$$h_\perp = -\frac{\delta F}{\delta\theta} = K\frac{\partial^2\theta}{\partial y}.$$

If the angle θ is small, an expansion of Eq. (54) for the perpendicular field to lowest order in θ gives $\nabla^2\theta + \theta/L^2 = 0$ where the characteristic length L is defined by

$$\frac{1}{L^2} = \frac{-2\zeta\Delta\mu(1 + \nu_1)}{K[4\eta/\gamma_1 + (1 + \nu_1)^2]}. \tag{55}$$

Assuming $1 + \nu_1 > 0$, if the activity coefficient ζ is negative corresponding to a contractile stress, $L^2 > 0$ and the length L is indeed real. The polarization angle varies then as $\theta = \theta_0 \sin(y/L)$. This satisfies the anchoring condition on the solid surface $y = 0$, but the anchoring condition on the free surface $y = h$ can be satisfied only if $h = \pi L$. If the film is thin $h \leq \pi L = L_c$, there is no solution with a finite θ and the nonflowing steady state is stable. For a film thicker than the critical value $h = \pi L$ the nonflowing steady state is unstable and a stable solution with a finite value of the polarization angle θ exists. If $h > L_c$ there is spontaneous symmetry breaking and two possible solutions with amplitudes $\pm\theta_0$. The amplitude θ_0 can be obtained by expansion at higher order of Eq. (54) and vanishes if $h = \pi L$. In this case the second equation of Eq. (54) gives a finite velocity gradient and the film spontaneously flows with a finite flux. Note that in general the onset of spontaneous flow is controlled by the sign of the combination $\zeta(1 + \nu_1)$. The flow coupling coefficient (also known as the flow-alignment parameter) ν_1 can in general have both positive and negative values (de Gennes and Prost, 1993). It is controlled by the shape of the active units and the degree of nematic order. Deep in the nematic state, $\nu_1 < -1$ corresponds to elongated rodlike particles, while $\nu_1 > 1$ corresponds to disklike particles. The onset of spontaneous flow is therefore controlled by the interplay of the contractile-tensile nature of the active forces and the shape of the active particles. A detailed description of this can be found in Giomi, Marchetti, and Liverpool (2008) and Edwards and Yeomans (2009).

This transition is very similar to the Frederiks transition of nematic liquid crystals in an external electric or magnetic field (de Gennes and Prost, 1993). The active stress $\zeta\Delta\mu$ plays the role of the external field. If the thickness is larger than the critical value L_c, a distortion of the polarization appears. Any distortion of the polarization creates a gradient of active stress that must be balanced by a viscous stress which implies the appearance of a finite flow.

The Frederiks transition could also be considered at a constant film thickness varying the active stress $\zeta\Delta\mu$. The film spontaneously flows if the active stress is large enough (in absolute value).

Finally, to properly describe the spontaneous-flow transition for polar active films one needs to consider a two-fluid model that allows for variations in the concentration of active particles. In this case spontaneous flow is accompanied by spatial inhomogeneities in the concentration or "banding" not seen in active nematics (Giomi, Marchetti, and Liverpool, 2008). In addition, for stronger values of activity in polar films steady spontaneous flow is replaced by oscillatory flow that becomes increasingly complicated and even chaotic for strong polarity.

2. Instabilities of thin films

The Fredericks active film instability discussed in Sec. IV.A.1 occurs in situations where the geometry of the film is fixed and its surface cannot deform, whereas many phenomena in thin film flow (Oron, Davis, and Bankoff, 1997; Sarkar and Sharma, 2010) involve distortions of the free surface, as does the dynamics of the lamellipodium (Verkhovsky, Svitkina, and Borisy, 1999; Small *et al.*, 2002) (see Sec. IV.D), and the spreading of bacterial suspensions (Bees *et al.*, 2000, 2002). However, we discuss here simpler situations where mechanisms such as cell division in the bacterial case and actin treadmilling in the lamellipodium case are not included and that in a first step could be compared only to model experiments on reconstituted systems (Marchetti, 2012; Sanchez *et al.*, 2012). Despite these limitations, the problems of an active drop or film are interesting as novel variants of classic fluid mechanics problems and as settings for phenomena of relevance to biology.

We review in this section the hydrodynamics of thin films of fluid containing orientable degrees of freedom and endowed with locally uniaxial active stresses, spread on a solid surface, with the upper surface free to undulate. We present in detail the case of a laterally unbounded film (Sankararaman and Ramaswamy, 2009). Our system is a fluid with suspended active particles, i.e., in the language of the previous section, a multicomponent active fluid. We assume that the polar material velocity with respect to the background fluid (related to the relative current between the two components) is strictly slaved to the polar order and equals $v_0\mathbf{p}$. This assumption is meaningful in the case of bacterial colonies but would have to be reconsidered in the discussion of a cell lamellipodium. We

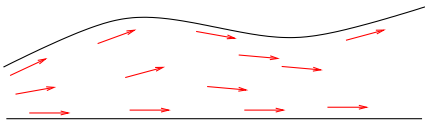

FIG. 22 (color online). A film of ordered polar active suspension, illustrating the anchoring boundary condition on the filaments, parallel to the free surface and the base.

also sketch results for the case of a finite, partially wetting drop with small equilibrium contact angle and *apolar* orientational order (Joanny and Ramaswamy, 2012), where topological defects play a role. In both cases, we consider only planar alignment (de Gennes and Prost, 1993), where the local orientation field is anchored parallel to the free surface and the rigid base, and free to point in any direction in the plane of anchoring. Our focus is of course on the effects specifically due to the active stresses and currents.

Following Sankararaman and Ramaswamy (2009), we considered a fluid film (see Fig. 22) containing active particles with number density $\rho(\mathbf{r}, t)$ and orientation field $\mathbf{p}(\mathbf{r}, t)$ as a function of time t and three-dimensional position $\mathbf{r} = (\mathbf{r}_\perp, z)$, where z denotes the coordinate normal to the horizontal coordinates $\mathbf{r}_\perp = (x, y)$, and the solid surface lies at $z = 0$. In the case of the drop, where we consider only apolar order, we identify the vector $\mathbf{p}$ with the nematic director field, with $\mathbf{p} \to -\mathbf{p}$ symmetry. The free surface is located at $z = h(\mathbf{r}_\perp, t)$. The flow of the film is characterized by the three-dimensional incompressible velocity field $\mathbf{v}(\mathbf{r}, t)$. We focus on the case where the film or drop has macroscopic order, i.e., the mean $\langle \mathbf{p} \rangle$ is nonzero, which means that variations in the direction, not the magnitude, of $\mathbf{p}$ play the central role. Our aim is to obtain an effective equation of motion for the thickness h and the z-averaged density and polarization. This requires solving the Stokes equation in the presence of stresses generated by the active particles. At the end of the section, we offer a qualitative physical explanation as well.

The dynamics of the height h is related to the velocity through the kinematic condition $\dot{h} = v_z - \mathbf{v}_\perp \cdot \boldsymbol{\nabla}_\perp h$ (Stone, 2005). The incompressibility of the suspension implies volume conservation, so that the height dynamics becomes a local conservation law (Stone, 2005)

$$\partial_t h + \boldsymbol{\nabla}_\perp \cdot (h \bar{\mathbf{v}}_\perp) = 0 \tag{56}$$

in the $\perp$ plane, where $\bar{\mathbf{v}}_\perp$ is the in-plane velocity field averaged over the thickness of the film. With our assumptions, the flux of active particles in the laboratory reference frame is $\mathbf{j} = \rho(\mathbf{v} + v_0 \mathbf{p})$ so that the concentration ρ obeys the continuity equation

$$\partial_t \rho = -\boldsymbol{\nabla} \cdot [\rho(\mathbf{v} + v_0 \mathbf{p})], \tag{57}$$

which simply generalizes Eq. (2a) to the case where the particles are moving not through an inert background but through a suspension with velocity field $\mathbf{v}$. The velocity field $\mathbf{v}$ obeys the Stokes equation

$$\eta \nabla^2 \mathbf{v} = \boldsymbol{\nabla} P - \boldsymbol{\nabla} \cdot (\boldsymbol{\sigma}^a + \boldsymbol{\sigma}^p), \tag{58}$$

with viscosity η and pressure P. The stresses $\boldsymbol{\sigma}^a = -\zeta \Delta\mu \rho \mathbf{p} \cdot \mathbf{p}$ and $\boldsymbol{\sigma}^p$ arise, respectively, from the activity of strength $\zeta \Delta\mu$ and from the nematic elasticity (de Gennes and Prost, 1993), as given in Eqs. (46a) and (46b). Note that we imposed an explicit linear dependence of the active stress $\boldsymbol{\sigma}^a$ on the local concentration ρ of active particles as expected in a bacterial suspension, whereas for filament-motor systems the active stress increases faster than linear with the filament density. The polar order parameter $\mathbf{p}$ obeys

$$\frac{D p_\alpha}{D t} + \nu_1 v_{\alpha\beta} p_\beta + \lambda_1 (\mathbf{p} \cdot \boldsymbol{\nabla}) p_\alpha = -\frac{\delta F_p}{\delta p_\alpha} + \frac{C}{h} \nabla_\alpha^\perp h + f_\alpha, \tag{59}$$

where D/Dt is defined in Eq. (37), ν_1 is the flow-alignment parameter introduced in Eq. (42b) and familiar from liquid-crystal hydrodynamics (de Gennes and Prost, 1993), λ_1 is the coefficient of the advective nonlinearity in Eq. (2b), and $v_{\alpha\beta}$ is the strain-rate tensor defined in Eq. (36a). This is the liquid limit ($\tau = 0$) of Eq. (49) where the polar active term proportional to λ_1 has been included. Finally, F_p is the free-energy functional for $\mathbf{p}$ and ρ given in Eq. (4), whose content will be discussed further. Equation (59) generalizes Eq. (5) to include a fluid medium (Simha and Ramaswamy, 2002a) and a free surface.

In a geometry of finite z thickness with a free surface, symmetry cannot rule out a term of the form $(C/h)\boldsymbol{\nabla}_\perp h$, in the z-averaged equation of motion for $\mathbf{p}$ (Sankararaman and Ramaswamy, 2009). The coefficient C encodes the preference of $\mathbf{p}$ to point uphill or downhill with respect to the tilt $\nabla_\perp h$. From the discussion of possible microscopic mechanisms and estimates for C in Sankararaman and Ramaswamy (2009) we see, crucially, that such an effect, while allowed by symmetry, must explicitly involve properties of the free surface and the base and cannot emerge simply from a z averaging of bulk 3D hydrodynamics. We therefore add such a term to Eq. (59).

We now proceed to solve Eq. (58) for the velocity in terms of ρ, $\mathbf{p}$, and h.

We study perturbations about a reference configuration of the film with uniform concentration ρ_0 and height h_0, spontaneously ordered into a state with nonzero mean polarization $\langle \mathbf{p} \rangle = p_0 \hat{\mathbf{x}}$. As we have chosen the active-particle current relative to the medium in Eq. (57) to be entirely along $\mathbf{p}$, with no explicit diffusive contribution, and as the particles cannot escape the fluid film, the normal components of $\mathbf{p}$ must vanish at the bounding surfaces at $z = 0$ and $z = h$ in agreement with the planar alignment boundary condition. In a perturbed state with a nonuniform film thickness, this means that $p_z(z = h) \simeq \partial_x h$ to linear order in $\boldsymbol{\nabla} h$. The z direction being the smallest dimension in the problem, it is consistent to assume that the variation of $\mathbf{p}$ with respect to z is at instantaneous mechanical equilibrium via nematic elasticity, implying $p_z = (z/h)\partial_x h$ or, in a z-averaged description, $p_z = (1/2)\partial_x h$ and $\partial_z p_z \simeq h^{-1} \partial_x h$.

We represent the perturbed state as $\mathbf{p}_\perp = \hat{\mathbf{x}} + \theta \hat{\mathbf{y}}$, $\theta \ll 1$ and linearize the active stress in θ.

In the lubrication approximation (Oron, Davis, and Bankoff, 1997; Batchelor, 2000; Stone, 2005) $v_z = 0$, $|\partial_z \mathbf{v}| \gg |\nabla_\perp \mathbf{v}|$, we obtain the pressure and then the linearized expression for the in-plane velocity

$$\mathbf{v}_\perp(z) = \frac{hz - z^2/2}{\eta}\left(\gamma \boldsymbol{\nabla}_\perp \nabla_\perp^2 h - \frac{1}{2}\zeta \Delta\mu h \partial_x^2 \boldsymbol{\nabla}_\perp h - \mathbf{f}_\perp\right), \tag{60}$$

where $\mathbf{f}_\perp = \zeta\Delta\mu[(\partial_y\theta + \partial_x\rho/\rho_0 + h^{-1}\partial_x h)\hat{\mathbf{x}} + \partial_x\theta\hat{\mathbf{y}}]$ contains the dominant contributions of activity. Inserting this result into the incompressibility condition (56) and linearizing $h = h_0 + \delta h$, $\rho = \rho_0 + \delta\rho$, leads to the dynamical equations

$$\partial_t \delta h_{\mathbf{q}} = -\frac{\zeta\Delta\mu h_0^2}{3\eta}\left[2h_0 q_x q_y \theta_{\mathbf{q}} + h_0 q_x^2 \frac{\delta\rho_{\mathbf{q}}}{\rho_0} + \left(1 - \frac{1}{2}h_0^2 q^2\right) q_x^2 \delta h_{\mathbf{q}}\right] - \frac{\gamma h_0^3}{3\mu} q^4 \delta h_{\mathbf{q}} \tag{61}$$

for the in-plane spatial Fourier transforms $\delta h_{\mathbf{q}}(t)$, $\delta\rho_{\mathbf{q}}(t)$, and $\theta_{\mathbf{q}}(t)$ of the perturbations in height, concentration, and orientation. The group of terms multiplied by $\zeta\Delta\mu$ on the right-hand side of Eq. (61) displays four consequences of activity, from right to left: (i) pumping by curvature (see Fig. 23), (ii) anisotropic osmotic flow, (iii) splay-induced flow from tilting the free surface, and (iv) an anisotropic active tension. One can see that (iii) and (iv) are, respectively, destabilizing and stabilizing for contractile stresses, and the other way around for extensile stresses. From Eq. (49), the linearized, z-averaged, long-wavelength equation of motion for the orientation θ reads

$$\partial_t \theta_{\mathbf{q}} = +\frac{iC}{h_0} q_y \delta h_{\mathbf{q}} - (D_+ q_x^2 + D_- q_y^2 + i\lambda_1 q_x)\theta_{\mathbf{q}} - (i\zeta q_y - \Phi q_x q_y)\delta\rho_{\mathbf{q}}, \tag{62}$$

where $D_\pm = D - (\lambda_1 \pm 1)h_0^2\zeta\Delta\mu/4\eta$, $D \sim K/\eta$ being a director diffusivity with K a Frank constant and $\Phi = (\nu_1 - 1)h_0^2\zeta\Delta\mu/4\rho_0\eta$.

Linearizing the active-particle conservation law (57) about the ordered uniform state gives to leading order in wave number:

$$\partial_t \delta\rho_{\mathbf{q}} = -i\rho_0 v_0 q_y \theta_{\mathbf{q}} - i v_0 q_x \delta\rho_{\mathbf{q}} + O(q_x^2\delta\rho_{\mathbf{q}}, q_x^2\delta h_{\mathbf{q}}). \tag{63}$$

The most accessible and interesting instability, arising from the combination of activity and the tilt coupling C, can be understood by ignoring the concentration and motility

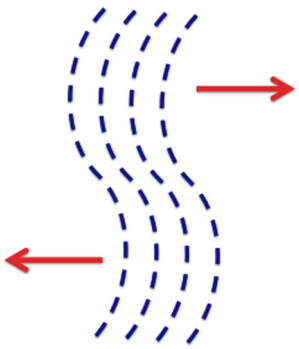

FIG. 23 (color online). Curvature of the director of an active liquid-crystalline phase gives rise to flows. The arrows indicate direction of flow if the active stresses are contractile.

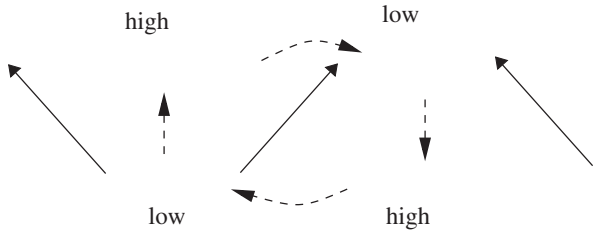

FIG. 24. Tilt of the free surface leads to active flow; the arrow's directions are for the contractile case.

($v_0 = 0$), but retaining contractile or extensile active stresses ($\zeta\Delta\mu \neq 0$). The dispersion relation has the following complex form:

$$\omega = \pm\frac{1 + i\,\mathrm{sgn}(q_x C\zeta\Delta\mu)}{\sqrt{2}}\left(\frac{h_0^2}{3\eta}\right)^{1/2}|C\zeta\Delta\mu q_x|^{1/2}|q_y|. \tag{64}$$

The relative signs of $\zeta\Delta\mu$ and C determine the direction ($\pm\hat{\mathbf{x}}$) of propagation of the unstable mode. Figure 24 attempts to explain the mechanism of this intriguing instability. The effects of concentration fluctuations, and the suppression of the instability as the motility v_0 is increased, are discussed in Sankararaman and Ramaswamy (2009).

So far we have assumed an unbounded film. We now briefly consider the spreading kinetics of a finite drop, as discussed by Joanny and Ramaswamy (2012), containing apolar active filaments in a state of nematic order. We choose a planar anchoring condition as in the case of the unbounded film, i.e., no component normal to the free surface or base. The geometry of the drop forces a topological defect in the interior that itself induces a deformation of the drop. Two possible defect structures are two "boojums" with orientation pattern as in Fig. 25 (left) and an aster as in Fig. 25 (right). The simplest case to consider is the two-boojums pattern of Fig. 25 (left), with the assumption that the drops spread uniaxially in the x direction. The active stress amounts to a peculiar kind of disjoining pressure $P_{\mathrm{act}} = \zeta\Delta\mu\ln(h/h_0)$, which can be rationalized on dimensional grounds by noting that the activity strength itself has units of stress so that the dependence on thickness has to be logarithmic. The resulting static shape of a drop depends on the sign of the active stress: the drop is flat if the active stress is extensile, and elevated, if it is contractile. For a linear structure like Fig. 25 (left), if we assume spreading only along

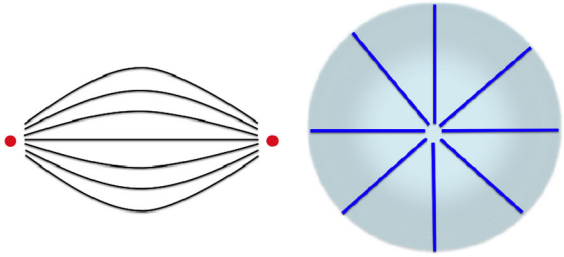

FIG. 25 (color online). Left: Two half-strength defects (boojums) at the ends of a drop. Right: A radial strength-1 aster defect. Both defects are viewed from above the plane in which the drop lies. The lines are the director orientation.

the long axis at fixed width w the result, for a fixed volume Ω and viscosity η, is a drop of linear dimension

$$R(t) \sim \left(\frac{\zeta \Delta \mu \Omega^2 t}{w^2 \eta}\right)^{1/4}. \tag{65}$$

A drop of volume Ω with an aster defect as in Fig. 25 (right) spreads isotropically with

$$R(t) \sim \left(\frac{\zeta \Delta \mu \Omega^2 t}{\eta}\right)^{1/6}. \tag{66}$$

Further details including the behavior of other defect configurations are discussed by Joanny and Ramaswamy (2012).

B. Polar active suspensions with inertia

In Sec. III we summarized the continuum flocking model of Toner and Tu (1995, 1998) for polar self-propelling particles moving on a frictional substrate. Deep in the ordered phase, the theory predicted novel propagating soundlike waves, coupling orientation and density fluctuations, with direction-dependent wave speeds and giant density fluctuations. The discussion thereafter, when the ambient fluid medium was introduced, focused on *destabilizing* effects arising from the interplay of activity and the hydrodynamic interaction for bulk suspensions in the Stokesian regime where viscosity dominates. However, we claimed in Sec. I that our hydrodynamic approach applied to flocks from subcellular to oceanic scales. Bacterial suspensions, cell aggregates, and the cytoskeleton or its extracts (see Sec. III) are well approximated in the Stokesian limit where inertia is altogether ignored. For collections of large swimmers, such as fish, where inertial effects are important and the role of viscosity can be ignored an alternative emphasis is appropriate. Simha and Ramaswamy (2002a) originally formulated their general theory of ordered states and fluctuations for active particles suspended in a fluid with a view to describing both viscosity- and inertia-dominated flows. We briefly review the discussion of Simha and Ramaswamy (2002a) in the case where inertia is taken into account through the *acceleration* term in the momentum equation. We ignore the advective nonlinearity $\mathbf{v}\cdot\nabla\mathbf{v}$, so the treatment amounts to the unsteady Stokes equation, but this is precisely the level of description in which the propagating modes of translationally ordered crystalline or liquid-crystalline phases are discussed by Martin, Parodi, and Pershan (1972).

The slow variables in a polar active suspension are the number density, the broken-symmetry variable $\mathbf{p}$ for polar order (defined in Sec. II.A), and the momentum density of the suspension $\mathbf{g}$. We proceed initially as in Sec. III.A.2, through the momentum equation (32) $\partial_t g_\alpha = -\partial_\beta \Pi_{\alpha\beta}$, with the stress tensor $\Pi_{\alpha\beta} = -\sigma^t_{\alpha\beta} + m\rho v_\alpha v_\beta$, where $\sigma^t_{\alpha\beta}$ contains the various contributions listed in Eqs. (39), (42a), (42b), and (45), including the crucial active stress. In systems where inertia is important, it is essential to retain the acceleration $\partial_t \mathbf{g}$ even while ignoring the inertial contributions $m\rho v_\alpha v_\beta$ to the stress which are nonlinear in $\mathbf{g}$. The equation for the vector order parameter $\mathbf{p}$ is as in Sec. III. The number density is governed by Eq. (57).

The hydrodynamic modes implied by these equations of motion are obtained by linearizing and Fourier transforming in space and time (Simha and Ramaswamy, 2002a). Imposing overall incompressibilty with the condition $\nabla\cdot\mathbf{g} = 0$, the number of modes is five. We briefly state here the main results of this analysis (Simha and Ramaswamy, 2002a). First, when viscosity is ignored and acceleration is included, polar ordered suspensions are not in general linearly unstable; that is, a parameter range of nonzero measure exists for which stable behavior is found. The dynamic response displays a whole new range of propagating waves as a result of the interplay of hydrodynamic flow with fluctuations in orientation and concentration: a pair of bend-twist waves and three waves, generalizations of those in Toner and Tu (1998), coupling splay, concentration, and drift each with exceedingly complicated direction-speed wave relations (Simha and Ramaswamy, 2002a). The bend and twist waves result from the interplay of $\nabla\times\mathbf{p}_\perp$ and $\nabla\times\mathbf{v}_\perp$, which provides a qualitative difference with respect to dry flocks. These propagating modes can be observed on length scales where it is reasonable to ignore their damping—due to viscosity for the total momentum and velocity fluctuations, and diffusion for concentration fluctuations. This gives a large range of length scales for large fast swimmers like fish. Possibly experiments like those of Makris *et al.* (2006), which speak of fish density waves, could test the existence of these modes in detail. Second, within this linearized treatment, equal-time density correlations of the density show the same features in the ordered phase as already seen for dry systems in Sec. II.A.3.c, with the number variance, scaled by the mean N, predicted to diverge as $N^{1/2+1/d}$ in d dimensions as in Eq. (20). Presumably nonlinearities, which powercounting readily shows to be relevant below four dimensions, but which are even more painful to analyze than in dry flocks, will change the exponents but not the essential fact of supernormal fluctuations. It is not clear whether the power-law static structure factor seen by Makris *et al.* (2006) in shoals[6] is evidence for these giant fluctuations; a fair test of flocking theories requires a school rather than a shoal.

C. Rheology

The active hydrodynamic framework of Sec. III not only allows us to predict spontaneous-flow instabilities as in Secs. IV.A.1 and IV.A.2 but also the response of an active fluid to an *imposed* flow, i.e., the *rheology* of active soft matter (Hatwalne *et al.*, 2004; Liverpool and Marchetti, 2006; Haines *et al.*, 2009; Giomi, Liverpool, and Marchetti, 2010; Saintillan, 2010).

For concreteness, we associate the purely coarse-grained description of Sec. III with a microscopic picture of a suspension containing active particles of linear size ℓ, at concentration ρ, each particle carrying a force dipole of strength $f\ell$, where f is the propulsive thrust, with the activity of an individual particle correlated over a time τ_0, and collective fluctuations in the activity correlated over length scales ξ and time scales τ.

[6]In biology, a shoal is any group of fish that stays together, for instance, for social reasons. If the group swims in the same direction in a coordinated manner, it is called a school.

We apply this approach to the isotropic phase of active particles in a fluid to extract linear rheological properties (Hatwalne *et al.*, 2004; Liverpool and Marchetti, 2006) and the autocorrelation of spontaneous stress fluctuations (Hatwalne *et al.*, 2004; Chen *et al.*, 2007) when noise is included.

We consider an apolar system described by orientation order in terms of the tensor $\mathbf{Q}$, defined in Eq. (21). We obtain predictions for the rheology of active suspensions through the coupled dynamics of $\mathbf{Q}$ and the hydrodynamic velocity field $\mathbf{v} = \mathbf{g}/\rho_{\mathrm{tot}}$, where $\mathbf{g}$ and ρ_{tot} are the total densities of momentum and mass of the suspension. Neglecting inertial contribution to the stress tensor, conservation of total momentum of particles and fluid is expressed by $\partial_t \mathbf{g} = \boldsymbol{\nabla} \cdot \boldsymbol{\sigma}^t$, where the stress tensor $\boldsymbol{\sigma}^t$ is as in Sec. III.B.1. In addition, we must allow for noise sources of thermal and nonthermal origin. The former, although mandated in the equilibrium limit by the fluctuation-dissipation relation connecting them to the solvent viscosity in Eq. (39), are quantitatively negligible in comparison to effects arising from activity. Such active fluctuating stresses can further arise in two ways: directly, as additive white-noise contributions to the stress in Eqs. (39)–(45), which we ignore as they add no new physics to the macroscopic rheology discussed below, or indirectly, via the stochastic dynamics of the orientation field, which is the case of interest.

Consistent with Sec. III, we write the active stress in terms of the alignment tensor in the form

$$\sigma^a_{\alpha\beta} = -\zeta \Delta\mu Q_{\alpha\beta}. \tag{67}$$

We note for later reference that we eventually consider the concentration dependence of active stresses $\zeta \propto \rho$, which is physically reasonable and also follows from an explicit realization in terms of dipolar force densities associated with the active particles (Simha and Ramaswamy, 2002a; Hatwalne *et al.*, 2004; Baskaran and Marchetti, 2009). Note that we are dealing with force-free, neutrally buoyant, self-propelling particles. Thus there are no *external* forces on the system, so that the simplest active particle, on long time scales, is a permanent force dipole (Brennen and Winet, 1977; Pedley and Kessler, 1992). Although we already discussed the magnitude and sign of $\zeta\Delta\mu$ in Sec. III, it is useful to note here that for a system with concentration ρ the quantity $\zeta\Delta\mu/\rho \sim \ell f$ characterizes the strength of the elementary force dipoles associated with, for example, individual swimming organisms. Negative and positive $\zeta\Delta\mu$ refer, respectively, to contractile swimmers, or "pullers," and extensile swimmers, or "pushers," whose distinct rheological behavior we outline below.

The rheology is obtained from the momentum equation together with the equations of motion for the order parameter field and particle concentration. We begin with a description of the linear rheology of active matter in the isotropic and orientationally ordered phases and follow it up with a brief survey of the nonlinear rheology of active matter.

1. Linear rheology of active isotropic matter

To appreciate what is unique about active-matter rheology, it is useful to recall the linear rheology of passive nematogens. The stresses arising from distortions of the orientational order parameter $\mathbf{Q}$ and concentration ρ are derived from a free-energy functional $F_Q[\mathbf{Q}, \rho]$ [Eq. (23)], giving rise to a passive deviatoric order parameter stress (Forster, 1974),

$$\boldsymbol{\sigma}^{op} = 3\mathbf{H} - \mathbf{H}\cdot\mathbf{Q} - \mathbf{Q}\cdot\mathbf{H}, \tag{68}$$

where $\mathbf{H} \equiv -\delta F_Q/\delta\mathbf{Q} + (1/3)\mathbf{I}\,\mathrm{Tr}\delta F_Q/\delta\mathbf{Q}$ is the nematic molecular field. The mean deviatoric passive stress (68) is zero in the isotropic phase at equilibrium (and in the nematic phase as well). In addition, fluctuations of the deviatoric stress are small as one nears the transition to the nematic phase, as can be seen by making small perturbations $\delta\mathbf{Q}$ in the isotropic phase, leading to a change in the free energy $F_Q \propto (\alpha_Q/2)\int \mathrm{Tr}(\delta\mathbf{Q})^2$, which in turn gives rise to stress fluctuations $\sim\alpha_Q\delta\mathbf{Q}$ with a coefficient α_Q that decreases on approaching the isotropic-nematic (IN) transition to the ordered phase. Thus even though fluctuations of $\mathbf{Q}$ are large as one approaches the IN transition, their contribution to rheology is small, resulting simply in a renormalization of τ, the order parameter relaxation time. As shown, this pretransitional feature is fundamentally different in active isotropic systems. In the following we take a purely coarse-grained approach and closely follow the work of Hatwalne *et al.* (2004), Liverpool and Marchetti (2006), and Giomi, Liverpool, and Marchetti (2010); for a more microscopic treatment see Haines *et al.* (2009) and Saintillan (2010).

For the active system, the deviatoric reactive stress has to be obtained from the equations of motion for the order parameter and concentration, rather than simply from the free-energy functional. The linearized equations for $\mathbf{Q}$ in the isotropic phase are of the form

$$\frac{\partial Q_{\alpha\beta}}{\partial t} = -\frac{1}{\tau}Q_{\alpha\beta} + D\nabla^2 Q_{\alpha\beta} + \nu_1 v_{\alpha\beta} + \cdots + f_{\alpha\beta}, \tag{69}$$

where Eq. (69) can be regarded as the modification of Eq. (22) to include the effect of shear flow to linear order. Here τ is the orientational relaxation time, which could, for example, be the run time in a collection of run-and-tumble bacteria, or the rotational diffusion time, perhaps modified by collective and/or active effects in an actomyosin extract, D is a diffusivity ($\sim \ell^2/\tau_0$) related to the ratio of a Frank constant to a viscosity, ν_1 is a "reversible" kinetic coefficient or flow coupling parameter, taken for simplicity to be of the same order as the one entering the equation for polarization $\mathbf{p}$ (Forster, 1974), $f_{\alpha\beta}$ is a traceless, symmetric, spatiotemporally white tensor noise representing active fluctuations, and the dots include the coupling of orientation to flow. Note that this form of the linearized equation is valid for the passive system too, with the time scale τ_Q given by the order parameter relaxation time proportional to $1/\alpha_Q$, which gets larger as one approaches the IN transition.

One can now proceed to calculate the linear viscoelastic properties of the active suspension. In addition to the active deviatoric stress (67), we include the contribution from the viscous dissipative stress $\sigma^d_{\alpha\beta}$ given in Eqs. (39). For simplicity we neglect the tensorial nature of the viscosity of fluids with orientational order. Using Eqs. (67)–(69), and applying them to spatially uniform ($q = 0$) oscillatory shear flow at frequency ω in the x-y plane one obtains, to linear order in the fields,

$$\sigma_{xy}(\omega) = \left[\eta + \frac{(\alpha_Q - \zeta\Delta\mu)\nu_1}{-i\omega + \tau_Q^{-1}}\right] v_{xy}. \tag{70}$$

The rheological response is defined by the complex modulus $G(\omega) = \sigma_{xy}(\omega)/\epsilon_{xy}(\omega)$, with $\epsilon_{xy}(\omega) = v_{xy}(\omega)/(-i\omega)$ the strain. The corresponding storage (in-phase) and loss (out-of-phase) moduli $G'(\omega)$ and $G''(\omega)$, defined by $G(\omega) = G'(\omega) + iG''(\omega)$, characterize the elastic and viscous responses of the system to an oscillatory shear flow. These moduli can be readout from Eq. (70).

The active isotropic system is rheologically a Maxwell fluid to linear order. This is best highlighted by the behavior of the apparent shear viscosity $\eta_{\rm app} = \lim_{\omega\to 0} G(\omega)/(-i\omega)$, which shows an active excess viscosity $\eta_{\rm act} \propto -\zeta\Delta\mu\tau_Q\nu_1$, corresponding to either an enhancement or reduction, depending on the sign of ζ. This active thickening (thinning) can be understood as follows (see Fig. 26): in an imposed flow, in the absence of activity, disks (rods) tend to align their symmetry axis along the compression (extension) axis of the flow (Forster, 1974). When activity is switched on, the flow induced by the intrinsic force dipoles clearly opposes the imposed flow in Figs. 26(a) and 26(b), and enhances it in Figs. 26(c) and 26(d). Activity thus enhances viscosity in Figs. 26(a) and 26(b), since $\zeta\Delta\mu < 0$, and reduces it in Figs. 26(c) and 26(d) ($\zeta\Delta\mu > 0$). For $\zeta\Delta\mu < 0$, Eq. (70) shows that the viscosity grows substantially as the system approaches a transition to orientational order as τ_Q is increased, and in fact should diverge if τ_Q could grow without bound. Even more strikingly, a system of pushers, i.e., extensile swimmers, should show a prodigious reduction in viscosity as τ_Q grows; indeed, nothing rules out a negative viscosity (although this is actually unstable in one dimension) or even a negative yield stress (Cates *et al.*, 2008; Fielding, Marenduzzo, and Cates, 2011). Experiments by Sokolov and Aranson (2009) have indeed shown that the extensile activity of *Bacillus subtilis*, a pusher swimmer, can substantially lower the viscosity of a suspension. By contrast, in a passive, i.e., thermal equilibrium, system approaching a continuous or weak first-order transition to a nematic phase, the excess viscosity $\sim\alpha_Q\tau_Q$ is roughly constant since $\tau_Q \propto 1/\alpha_Q$ as required by the constraints of thermal equilibrium.

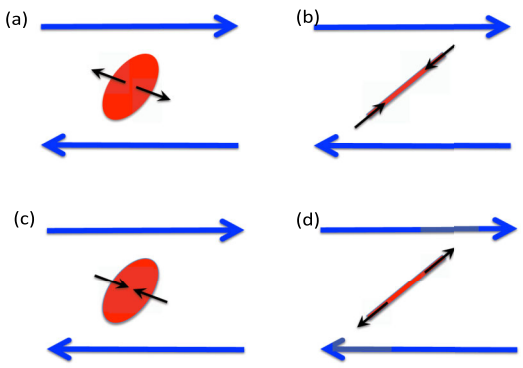

FIG. 26 (color online). Disks (a) and (c), and rods (b) and (d) with active force densities attached along their symmetry axes, under shear (horizontal arrows). The parameter $\zeta\Delta\mu < 0$ in (a) and (b) and >0 in (c) and (d).

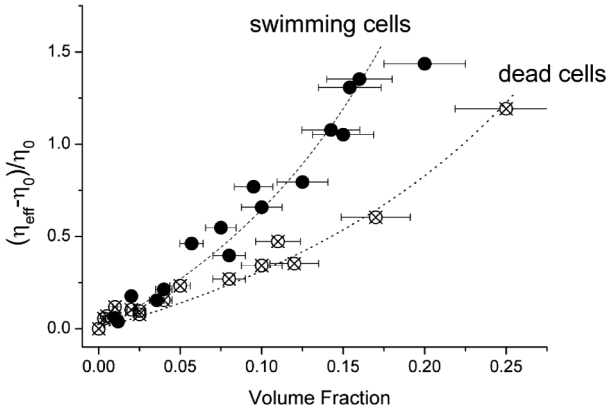

FIG. 27. The contractile activity of "puller" swimmers can increase the viscosity of a suspension. The data represent the effective viscosity of chlamydomonas suspensions relative to the viscosity η_0 of the culture medium as a function of the volume fraction of bacteria. Solid symbols represent live cell data and crossed symbols represent dead cell data. The mechanism producing flow orientation, however, remains unclear. Adapted from Rafaï, Jibuti, and Peyla, 2010.

The active excess viscosity obtained within the linear theory should be compared to the well-known result of Einstein (1906, 1911) that the fractional excess viscosity due to the addition of passive particles to a fluid is proportional to the particle volume fraction $\phi = \pi\rho\ell^3/6$, to lowest order in ϕ, with a coefficient $5/2$ for spheres. For this purpose it is convenient to take the active coupling proportional to the concentration ρ and define an active stress per particle W as

$$\zeta\Delta\mu = f\ell\rho \equiv W\phi, \tag{71}$$

where $W = f/\ell^2$. Then

$$\eta_{\rm act} = -W\tau_Q\phi. \tag{72}$$

Equation (72) can be viewed as an additive correction to the $5/2$, proportional to $W\tau_Q$, which of course can be of either sign. Behavior consistent with these predictions is seen in recent experiments measuring the activity-induced thickening in a system of *Chlamydomonas* algae (pullers, $W < 0$), as shown in Fig. 27 (Rafaï, Jibuti, and Peyla, 2010), and extreme thinning in a system of *Bacillus subtilis* bacteria (pushers, $W > 0$) (Sokolov and Aranson, 2009). In the case of chlamydomonas, there is some question as to the direct applicability of the mechanism discussed above, as recent experiments have shown that the flow field generated by these microorganisms, although contractile, is more complex than dipolar (Drescher *et al.*, 2010; Guasto, Johnson, and Gollub, 2010). In general the linear rheology is controlled by the interplay of the nature of the active stresses, determined by ζ, and the flow-alignment coefficient ν_1. A remarkable duality has been identified that shows that extensile ($\zeta > 0$) rod-shaped flow-aligning particles ($|\nu_1| > 1$) are rheologically equivalent (to linear order in the strain rate) to contractile ($\zeta < 0$) discotic flow-tumbling particles ($|\nu_1| > 1$) (Giomi, Liverpool, and Marchetti, 2010).

Equation (70) also predicts strong viscoelasticity as τ_Q increases. For *passive* systems, $\zeta\Delta\mu = 0$ and $\alpha_Q \propto \tau_Q^{-1}$, and so $G'(\omega\tau_Q \gg 1)$ decreases as $\nu_1\eta/\tau_Q$, suggesting as earlier that there is little viscoelasticity near an equilibrium IN transition. For *active* contractile ($\zeta\Delta\mu < 0$) systems, by contrast, the active contribution is of $O(1)$ and independent of τ_Q even close to the IN transition. Thus, as τ_Q grows,

$$G'(\omega\tau_Q \gg 1) \simeq -\zeta\Delta\mu\nu_1 \tag{73}$$

independent of τ_Q. In addition to this enhanced elasticity, the dynamic range over which elastic behavior is seen increases. This is quite a dramatic rheological manifestation of activity, since at equilibrium one would expect such strong viscoelastic behavior from a fluid or suspension near *translational* freezing, as at a glass transition, not near *orientational* ordering. Put more radically, the orientationally ordered phase of contractile active particles is a peculiar yield-stress material, with nonzero shear and normal stresses in the limit of zero shear rate (Hatwalne *et al.*, 2004; Liverpool and Marchetti, 2006; Marenduzzo, Orlandini, and Yeomans, 2007; Giomi, Liverpool, and Marchetti, 2010) as discussed in Sec. IV.C.3.

Another observable manifestation of activity is an enhanced noise temperature as inferred, for example, from tracer diffusion measurements in bacterial suspensions (Wu and Libchaber, 2000), and frequency-dependent shear viscosity arising from fluctuations in stress and concentration (Hatwalne *et al.*, 2004; Chen *et al.*, 2007). Activity is the transduction of chemical energy, say in the form of ATP hydrolysis equal to about $20k_BT$ per ATP molecule. This suggests that fluctuations from this athermal noise are significant. Following Hatwalne *et al.* (2004), we estimate the strength of nonequilibrium stress fluctuations that result from fluctuations of the force generation of active particles, through the variance of the active stress at zero wave number and frequency. The divergence of the active stress $\boldsymbol{\sigma}^a = -\zeta\Delta\mu\mathbf{Q}$ appears as a forcing term in the momentum equation. Assuming the active objects, whether biofilaments or bacteria, are collectively in a spatially isotropic state, this forcing can be viewed as a noise on scales large compared to the correlation length and time ξ and τ_Q defined at the start of this section. Recall that in fluctuating hydrodynamics (Landau and Lifshitz, 1998), for a thermal equilibrium fluid with shear viscosity η and temperature T, the variance of the random stresses at zero frequency is ηT. For an active fluid, then, the *apparent* temperature as probed by the motion of a tracer particle can be estimated by the zero-frequency, zero-wave-number variance of the active stress $\eta T_{\text{eff}} \sim (\zeta\Delta\mu)^2\times \int d^3r dt\langle\mathbf{Q}(\mathbf{0},0):\mathbf{Q}(\mathbf{r},t)\rangle$. The simplest dimensional argument then gives $T_{\text{eff}} \sim (\zeta\Delta\mu)^2\xi^3\tau_Q/\eta$. An Ornstein-Zernike form $(\ell/r)\exp(-r/\xi)$ for the equal-time correlations of $\mathbf{Q}$, which requires the introduction of a microscopic length which we take to be the active-particle size ℓ, gives instead $T_{\text{eff}} \sim (\zeta\Delta\mu)^2\xi^2\ell\tau_Q/\eta$. From Eq. (71), using rough estimates for the bacterial system of Wu and Libchaber (2000) $f \sim v/\eta\ell$ with $\eta \simeq 10^{-2}$ Poise, $\ell \sim 1$ μm, $\phi \sim 0.1$ $\xi \simeq 20$ μm corresponding to a "run" for a time $\tau_Q = 1$ s and speed $v \simeq 20$ μm/s yields T_{eff} about 400 times room temperature, consistent with the measurements of Wu and Libchaber (2000). Note that this enhancement is independent of the sign of $\zeta\Delta\mu$, i.e., the diffusivity increases regardless of whether the viscosity decreases or increases, a telltale sign of the nonequilibrium nature of the system. A further interesting consequence (Hatwalne *et al.*, 2004) of this excess noise is a large enhancement of the amplitude of the well-known $t^{-d/2}$ long-time tails in the autocorrelation of tagged-particle velocities. We know of no experiment that has probed this last feature.

More extended analyses of fluctuations in active systems, demarcating the dynamical regimes lying within and beyond the conventional fluctuation-dissipation theorem, include work by Mizuno *et al.* (2007) and Kikuchi *et al.* (2009).

We now turn to nonlinear fluctuation effects (Hatwalne *et al.*, 2004; Chen *et al.*, 2007). From Eq. (67), the fluctuations in the deviatoric stress get contributions from fluctuations bilinear in the orientation $\mathbf{Q}$ and the concentration ρ. The stress autocorrelation is therefore a convolution of $\mathbf{Q}$ and ρ correlations. The former is evaluated from Eq. (69), while the latter can be calculated from the linearized equations for the concentration $\partial_t\delta\rho = -\nabla\cdot\mathbf{J}$, where the current $J_\alpha = -D\partial_\alpha\delta\rho - W'\rho_0\partial_\beta Q_{\alpha\beta} + f^\rho_\alpha$, with D the diffusion constant, ρ_0 the mean concentration, f^ρ_α a random noise, and W' an activity parameter. The resulting key findings of Chen *et al.* (2007) and Lau and Lubensky (2009) are an excess fluctuation $\phi\omega^{-1/2}$ in the stress *fluctuations*, and no excess *response*, i.e., viscosity, in the range studied, again a sign of nonequilibrium behavior. Hatwalne *et al.* (2004) considered stress contributions nonlinear in $\mathbf{Q}$ and showed they should lead to excess viscosity as well as of a similar form, but the effect is presumably below detectable levels in the Chen *et al.* (2007) experiment.

2. Linear rheology of active oriented matter

In extending the study of rheology to active oriented matter, we immediately encounter a problem. As remarked in Sec. IV.A.1, long-range uniaxial orientational order, whether polar or apolar, in active Stokesian suspensions of polar particles is always hydrodynamically unstable to the growth of long-wavelength splay or bend fluctuations, depending on the sign of $\zeta\Delta\mu$. This instability has no threshold in a spatially unbounded system (Simha and Ramaswamy, 2002a), and the growth rate is highest at wave number $q = 0$. Frank elasticity with stiffness K stabilizes modes with q greater than

$$q_0 \propto \sqrt{|\zeta\Delta\mu|/K}, \tag{74}$$

so that there is a band of unstable modes from 0 to q_0. Note that q_0 is simply an approximate form of the length scale defined by Eq. (55). In any case, in the limit of infinite system size there is no stable reference state, no ideal active nematic or polar liquid crystal whose rheology one can study as a geometry-independent material property. We must therefore ask what suppresses this generic instability (Ramaswamy and Rao, 2007). A mechanism for suppression of the instability is confinement by boundary walls. The existence of a crossover wave number (74) implies that the instability exists only if

the sample's narrowest dimension $h > \sqrt{K/|\zeta \Delta \mu|}$; equivalently, for fixed h the activity must cross a threshold $\sim K/h^2$. This is the essential content of the treatment of Voituriez, Joanny, and Prost (2005) discussed in Sec. IV.A.1. Confinement along y, with the director spontaneously aligned along x and free to turn in an unbounded x-z plane, shows (Ramaswamy and Rao, 2007) a similar threshold but with a q^2 dependence of the growth rate at small in-plane q. In either case, it is clear that confinement can produce a stable active liquid crystal whose linear rheology one can study. Alternatively, the instability can be suppressed by imposing an external shear flow or by the presence of partial translational order, either columnar or lamellar. Orientational stabilization can also be achieved in flow-aligning systems ($|\nu_1| > 1$) by imposing a uniform shear flow with shear rate $\dot{\gamma}$. This stabilizes those wave vectors whose growth rate is smaller than the shear rate $\dot{\gamma}$. As $\dot{\gamma}$ is increased more and more modes are stabilized, until at a threshold $\dot{\gamma}_c$, the oriented phase is completely stabilized by the shear flow, yielding a stability diagram controlled by two variables, the flow-alignment parameter ν_1 and the ratio of the shear to active stress (Muhuri, Rao, and Ramaswamy, 2007; Giomi, Liverpool, and Marchetti, 2010). Translational order, either partial as in smectic or columnar liquid crystal or full as in three-dimensional crystalline systems, can also yield a stable active system, whose properties have been the subject of recent studies (Adhyapak, Ramaswamy, and Toner, 2013).

Stabilizing the orientationally ordered phase of active matter now sets the stage for a study of its unusual rheology (Hatwalne *et al.*, 2004; Liverpool and Marchetti, 2006; Giomi, Liverpool, and Marchetti, 2010). We have already seen that, on approaching the orientationally ordered state from the isotropic fluid, a suspension of active *contractile* elements ($W < 0$) exhibits solidlike behavior without translational arrest. In the orientationally ordered phase, the orientational order parameter $\langle \mathbf{Q} \rangle \neq 0$, which by Eq. (67) immediately leads to a nonzero steady-state average of the deviatoric stress, in the absence of any external deformation. This *prestress* is a truly nonequilibrium effect, and has no analog in a passive equilibrium nematic fluid which has a purely isotropic mean stress, i.e., a pressure, despite its orientational order. This prestress implies that in a flow experiment, the shear stress will not vanish at zero deformation rate. The same features of being first order in shear rate and having a nonzero value at zero shear rate are exhibited by the normal stresses $\sigma_{yy} - \sigma_{xx}$. We emphasize that this strange kind of yield stress is a manifestation of the rheology of an active oriented fluid without any form of translational arrest.

We conclude this section on the rheological properties of active oriented matter by drawing attention to an interesting analogy between active stress of contractile filaments with macroscopic orientational order and fragile jammed granular matter, as discussed by Ramaswamy and Rao (2007).

3. Nonlinear rheology of active nematics

We now turn to the rheological properties of orientationally ordered active fluids beyond the linear regime. As detailed in Sec. IV.C.2, the generic instability of orientationally ordered active suspensions (Simha and Ramaswamy, 2002a) can be suppressed by confinement or by imposing an external shear (Marenduzzo, Orlandini, and Yeomans, 2007; Muhuri, Rao, and Ramaswamy, 2007). It is therefore meaningful to explore the dynamics and rheology of these phases in confined geometries. Extensive numerical studies of active nematic and polar films (Marenduzzo, Orlandini, and Yeomans, 2007; Cates *et al.*, 2008; Giomi, Liverpool, and Marchetti, 2010; Fielding, Marenduzzo, and Cates, 2011) under shear reveal a rich variety of phenomena influenced by boundary conditions and geometry. This complex behavior results again from the interplay between local stresses generated by activity (quantified by the parameter ζ), the flow-aligning property of these particles (characterized by the parameter ν_1), and the typical self-propulsion velocity v_0 in polar active fluids. A complete understanding of their response to shear necessitates exploring the space spanned by these parameters under various boundary conditions.

We present a summary only of the main results obtained in the literature. While detailed theoretical and numerical studies of linear active rheology including the effect of polarity can be found in Giomi, Marchetti, and Liverpool (2008) and Giomi, Liverpool, and Marchetti (2010), the nonlinear rheology has so far been studied mainly for apolar systems. For contractile active fluids in an orientationally ordered state, numerical studies of the hydrodynamic equations (Cates *et al.*, 2008) when only one-dimensional variation is allowed show the onset of solidlike behavior of Hatwalne *et al.* (2004) and the existence of a yield shear stress as in Liverpool and Marchetti (2006) and Ramaswamy and Rao (2007). Studies of *extensile* fluids, allowing variation in one (Cates *et al.*, 2008) and two (Fielding, Marenduzzo, and Cates, 2011) spatial directions display the onset of spontaneous flowing states, with complex flow states including bands in 1D and rolls and turbulence in 2D. Related experimental findings include large-scale chaotic flows in bacterial systems (Dombrowski *et al.*, 2004; Aranson *et al.*, 2007), as remarked earlier. An important general feature (Cates *et al.*, 2008; Fielding, Marenduzzo, and Cates, 2011) is that dimensionality matters: imposed restrictions to 1D spatial variation lead to significantly different rheology from that seen when 2D variation is allowed, for example. Active stresses generally appear to stabilize shear bands, but have the opposite effect close to the isotropic-nematic transition. In systems with free boundary conditions, the approach to the isotropic-nematic contractile transition shows (Cates *et al.*, 2008) an active enhancement of viscosity. As claimed by Hatwalne *et al.* (2004), orientational ordering in active systems indeed resembles translational arrest in equilibrium systems.

The relation between the rheology of active fluids in external shear and the onset of spontaneous flow in the absence of shear is discussed by Giomi, Liverpool, and Marchetti (2010). This work also analyzed in detail the nonlinear rheology of active fluids, revealing strongly nonmonotonic stress versus strain-rate curves beyond a threshold value of activity, as suggested by Hatwalne *et al.* (2004), with macroscopic yield-stress behavior and hysteresis. Finally, at

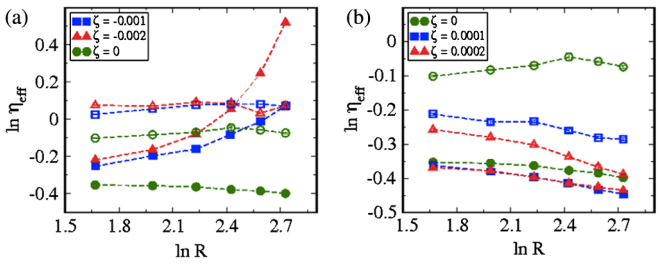

FIG. 28 (color online). Dependence of the apparent viscosity η_{eff} that would be obtained in a microrheology experiment on the size R of the probe for (a) an active contractile and (b) an active extensile fluid. Different symbols refer to different values of the activity parameter ζ (see legend). Filled and open symbols correspond to probes pulled along and perpendicular to the direction of the far field director, respectively, and dashed lines are to guide the eye. Adapted from Foffano *et al.*, 2012.

even higher activity, the theoretical stress-strain curve has a discontinuous jump at zero strain rate, corresponding to a finite "spontaneous stress" in the absence of applied shear. In recent work, Foffano *et al.* (2012) compared microrheology and macrorheology in a numerical study of the continuum hydrodynamics equations of active fluids. Among their key results is that the rheological properties are a strong function of the anchoring condition of the orientation at the surfaces of probe particles and container walls, and of the sizes of the system and the probe particle. An example of their results is seen in Fig. 28. Given the complexity and richness of the nonlinear rheology of active fluids, see the literature for further details.

D. Applying the hydrodynamic theory to phenomena in living cells

To demonstrate that the hydrodynamic theory of active gels described in the previous sections indeed provides generic tools for addressing questions relevant to living cells, we briefly summarize a few examples of concrete successes of the theory. A more complete review can be found in Grill (2011).

The first example is directly relevant to cell motility, in particular, to the migration of fish keratocytes, eukaryotic cells extracted from fish scales that are among the fastest moving cells, migrating on a substrate at a steady speed of about 10 μm/min. These cells have a characteristic fan shape, with a large flat region extending in front of their nucleus, toward the direction of forward motion, known as the lamellipodium. This region is filled with a cross-linked actin gel, where myosin motor complexes use the energy from ATP hydrolysis to grab on neighboring actin filaments and exert stress. Actin polymerization takes place at the leading edge of the lamellipodium, while the filaments disassemble in the rear region, in a process that plays a crucial role in driving the motility. Kruse *et al.* (2006) used active gel theory in two dimensions (the thickness and one spatial dimension) to calculate the shape of the lamellipodium, the actin velocity field inside the lamellipodium, and the cell velocity. In agreement with experiments, at the front edge of the cell, the actin flow is found to be retrograde in

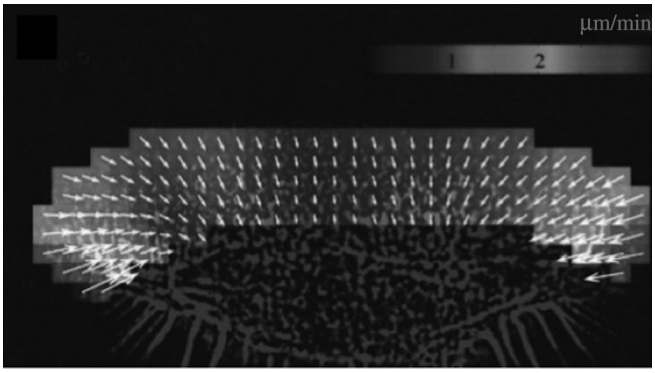

FIG. 29. Velocity field determined by speckle microscopy in a keratocyte lamellipodium. Adapted from Vallotton *et al.*, 2005.

the direction opposite to the motion. The important result is that the cell velocity is mostly determined by the actin depolymerization velocity, and the retrograde flow by the active contractile stress $\zeta\Delta\mu$. A direct comparison with the experiments of Vallotton *et al.* (2005) shown in Fig. 29 allows for an estimate of the active stress $\zeta\Delta\mu \sim -1000$ Pa.

A second example is that of shape oscillations, observed ubiquitously in many cells when they do not adhere to the substrate. An example is shown in Fig. 30. Salbreux *et al.* (2007) interpreted these oscillations as an instability of the cortical actin layer, which is itself an active actomyosin gel. The cortical layer is indeed unstable at large enough values of the active stress but does not show any oscillatory instability. Experimentally, the existence of oscillations depends crucially on the presence of calcium ions in the external medium and is inhibited upon addition of molecules blocking calcium channels. Salbreux *et al.* (2007) augmented the active gel theory by assuming a coupling of the active stress to calcium channels in the cell membrane that in turn are gated by the deformations in the actin cortical layer. Calcium concentration couples to local myosin activity that in turn controls the stretching and compression of the actin layer, in a feedback loop that results in sustained oscillations. They calculated a stability diagram of the cortical actin layer which shows oscillatory instabilities in a large region of parameter space when the active stress is large enough. Assuming an active stress $|\zeta\Delta\mu| \sim 1000$ Pa, the period of the oscillation is of the same order as the experimental period (30 s) and decreases with $|\zeta\Delta\mu|$ as observed in the experiments. Although of course the active gel theory is a phenomenological model and contains several unknown parameters, the fact that the same value of activity $\zeta\Delta\mu$ is consistent with the experimentally measured oscillation period of the cortical actin layer and the retrograde flow of the lamellipodium is an important validation of the model.

The active gel theory has also been used recently to model cortical flow during the first division of the *C. elegans* zygote (Mayer *et al.*, 2010), as shown in Fig. 31. The experiments are based on laser ablation to measure the anisotropy of the local tension of the actin cortex. They used a simplified version of the active gel theory in one dimension to relate the cortical tension to the actin flow. This allows them to identify two prerequisites for the existence of the large-scale cortical flow

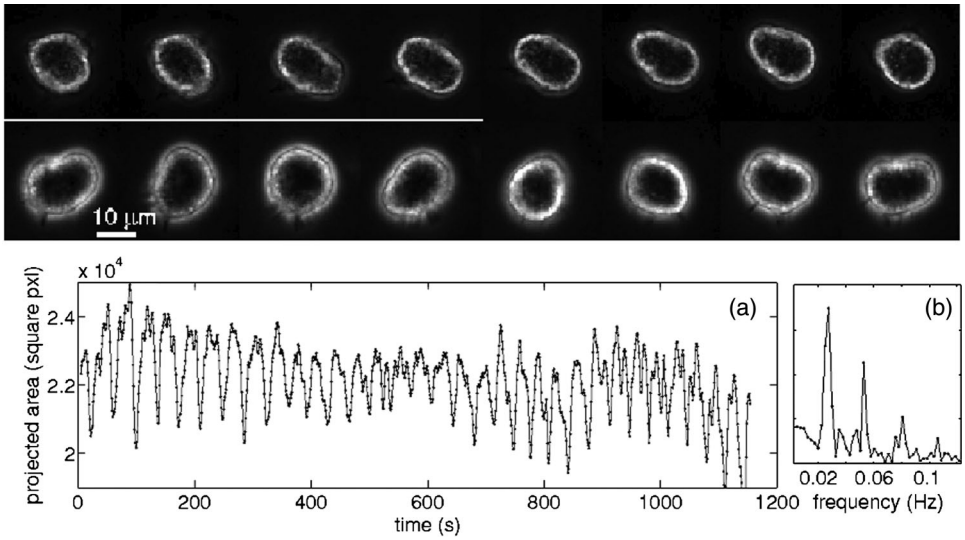

FIG. 30. Shape oscillations of nonadhering fibroblasts. The second frame shows the periodic oscillation of the projected area of the cell and the associated Fourier spectrum. The period of the oscillation of these cells is very well defined and of the order of 30 s. The oscillation period is found to decrease when myosin activity increases. The latter can in turn be modulated by the addition of various drugs. Adapted from Salbreux *et al.*, 2007.

necessary to initiate the anteroposterior cell polarization which directs the asymmetry of the first mitotic division: a gradient in actomyosin contractility to drive the flow, and a sufficiently large viscosity of the cortex to allow flow to be long ranged.

Another recent success of active hydrodynamics has come from its application to the organization and dynamics of molecules on the *surface* of living metazoan cells (Gowrishankar *et al.*, 2012). The lateral compositional heterogeneity of the plasma membrane at submicron scales, termed "lipid rafts," has been the subject of intense research (Lingwood and Simons, 2010). Most attempts to understand this heterogeneity are based on equilibrium thermodynamics. Using a variety of fluorescence microscopy techniques, and confirmed by other methods, it has been shown that the dynamics, spatial distribution, and statistics of clustering of a key raft component are regulated by the active dynamics of cortical actin filaments (Goswami *et al.*, 2008). Following this, Gowrishankar *et al.* (2012) developed a model for an active composite cell membrane based on active hydrodynamics, which shows how the dynamics of transient asterlike regions formed by active polar filaments (actin) can drive passive advective scalars (molecules such as GPI-anchored proteins) to form dynamic clusters. In addition to successfully explaining the many striking features of the dynamics and statistics of clustering of GPI-anchored proteins on the cell surface, this model makes several predictions, including the existence of giant number fluctuations which have been verified using fluorescence microscopy (Gowrishankar *et al.*, 2012). These studies suggest that rafts are actively constructed and that the active mechanics of the cortical cytoskeleton regulates local composition at the cell surface via active currents and stresses.

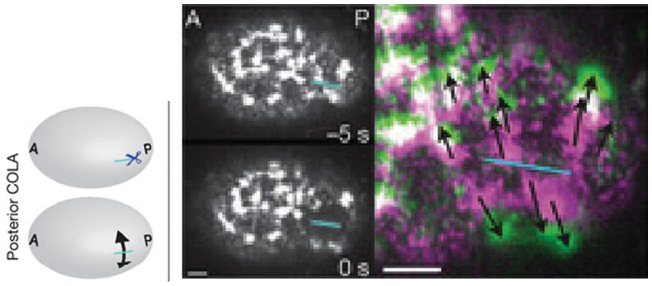

FIG. 31 (color). A display of the imaging of tension in the cortex of a *C. elegans* zygote obtained before and after cortical laser ablation (COLA) performed on the actomyosin meshwork. The left image shows a schematic of COLA performed with a pulsed ultraviolet laser along a 6 μm line (light blue in both images) along the anterior-posterior (AP) axis, in the posterior of the cell. The center frames show the pre- (top) and post-cut image (bottom) of posterior COLA. The image to the right shows the tension measurement in the zygote's actomyosin cortex upon laser ablation along the blue line. The black arrows are the displacements between precut (purple) and postcut images (green). The average speed of this initial recoil measured in a direction orthogonal to the cut line is proportional to the normal component of the 2D tension tensor. The white bar is 4 μm. Adapted from Mayer *et al.*, 2010.

Finally, Fig. 32 shows polarized actin waves propagating around the periphery of a Drosophila cell that has been fixed to a substrate, preventing it from moving, under condition of enhanced actin polymerization (Asano *et al.*, 2009). In this case the hydrodynamic theory was used to model the cortical actin network as an active polar gel coupled to a stationary substrate and to determine the conditions under which wave propagation will occur. The theory predicts the existence of a critical value of polarity associated with filament treadmilling above which the polarization waves will occur as observed in experiments.

V. DERIVATION OF HYDRODYNAMICS FROM MICROSCOPIC MODELS OF ACTIVE MATTER

A. Microscopic models

While the macroscopic equations of motion of active matter can be obtained from general considerations of

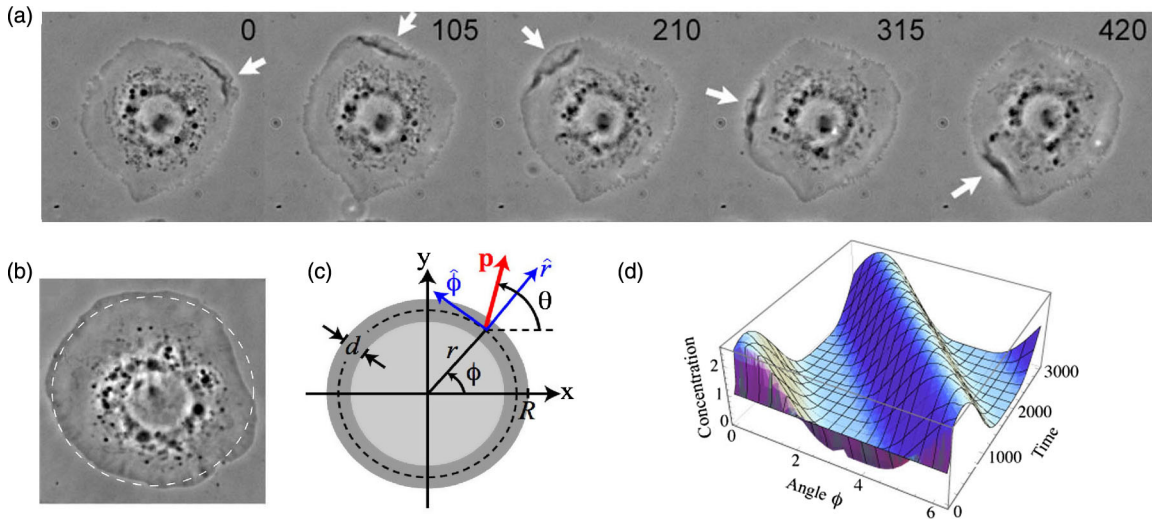

FIG. 32 (color online). (a) A circular actin wave in the lamellipodium in a Drosophila cell fixed to a substrate and treated to enhance polarization of actin filaments. The wave travels along the cell's periphery, with the arrows marking the regions of maximum actin density at various times. (b) Phase contrast microscopy picture of a control Drosophila cell fixed to a substrate with a typical circular shape. (c) In the theoretical model, the cell perimeter is represented by a circle of radius R. (d) The calculated concentration of active filaments as a function of the polar angle ϕ and time. Adapted from Asano *et al.*, 2009.

symmetry, determination of the magnitude and often even the sign of the coefficients requires additional physical assumptions. Unlike for systems near equilibrium, the assumptions are not easily identified. Furthermore the relaxation of the constraints required by equilibrium allows the possibility of a much larger number of terms. Physical insight can be provided by using the tools and methods of nonequilibrium statistical mechanics (Zwanzig, 2001) to derive the continuum equations via systematic coarse graining of simplified microscopic models of the active processes driving the system (Kruse and Jülicher, 2000; Kruse, Camalet, and Jülicher, 2001; Liverpool, Maggs, and Ajdari, 2001; Liverpool, 2003; Aranson and Tsimring, 2005; Bertin, Droz, and Grégoire, 2006, 2009; Kraikivski, Lipowsky, and Kierfeld, 2006; Baskaran and Marchetti, 2008a). While a comprehensive review of such approaches is beyond the scope of this paper, we present some specific examples that highlight one possible path for carrying out such a coarse graining. One approach is to start from stochastic equations for the microscopic dynamics and then systematically project the microscopic degrees of freedom on to macroscopic variables, such as the density $\rho(\mathbf{r}, t)$ and polarization $\mathbf{p}(\mathbf{r}, t)$, defined in Eqs. (1a) and (1b). This procedure yields hydrodynamic equations for the macroscopic variables on length scales long compared to the size ℓ of the individual active elements. For simplicity, we restrict ourselves to overdamped systems, where the medium through which the active particles may move (fluid or substrate) is inert and provides only friction. In this case the momentum of the active particles is not conserved and the microscopic degrees of freedom are the positions $\mathbf{r}_n(t)$ and orientations $\hat{\boldsymbol{\nu}}_n(t)$ of the active elements, plus possibly other microscopic degrees of freedom describing internal active processes. Of course medium-mediated hydrodynamic interactions can play a crucial role in controlling the dynamics of collections of swimmers. To incorporate such effects one needs to consider a two-component system and explicitly describe the exchange of momentum between particles and solvent. Both the translational and rotational velocities of each particle must be incorporated in the microscopic model, as well as the solvent degrees of freedom. This more general case is outlined briefly in Sec. V.B.4. In general, approximations are required both to identify a tractable microscopic model and to carry out the coarse-graining procedure to derive equations for the macroscopic variables. The form of the resulting equations is general, as it is dictated by symmetry, and the microscopic description allows a calculation of the phenomenological parameters and transport coefficients involved in the hydrodynamic equations. This is important, for example, for biological systems because it allows one to predict the variation of the transport coefficients with the biological parameters that can be changed in the experiments.

The purpose of this section is to review a number of such derivations and summarize their similarities and differences. In equilibrium statistical mechanics there is a long tradition of simplified microscopic descriptions which have eventually led to a number of paradigmatic minimal models (Ising, XY, Heisenberg) that capture the essentials of the behavior of a variety of equilibrium systems. Similarly we describe some minimal microscopic descriptions of active matter that have provided insight into the complex physics of these systems. An interesting aspect of these microscopic realizations is that they allow one to identify the common behavior of different experimental systems. Two examples we focus on are (1) mixtures of cross-linking motor constructs and protein filaments (Nédélec *et al.*, 1997; Nédélec, 1998; Surrey *et al.*, 2001) and (2) collections of self-propelled particles. Experimental realizations of the latter may be actin filaments in motility assays (Kron and Spudich, 1986; Butt *et al.*, 2010; Schaller *et al.*, 2010) or suspensions of swimming microorganisms (Dombrowski *et al.*, 2004; Zhang *et al.*, 2010).

1. Self-propelled particles

A microscopic realization of active systems is provided by interacting self-propelled particles (SPP). While these can be

thought of as simplified agent-based models of flocks of birds and shoals of fish (Vicsek *et al.*, 1995), they can also act as realistic models for less complex systems, such as polar protein filaments (e.g., *F* actin) in gliding motility assays on surfaces decorated with molecular motors (e.g., myosin) (Kron and Spudich, 1986; Schaller *et al.*, 2010), suspensions of swimming microorganisms (Dombrowski *et al.*, 2004; Zhang *et al.*, 2010), or even layers of vibrated granular rods (Narayan, Ramaswamy, and Menon, 2007). It should be stressed, however, that there have been suggestions that hydrodynamic interactions may be important in motility assays at high filament density (Schaller, Weber, Hammerich *et al.*, 2011).

Each self-propelled particle has a position and an orientation. It also has an individual self-propulsion velocity of magnitude v_0 and direction specified by the particle's orientation. SPPs interact with neighboring particles via either a local rule (Vicsek *et al.*, 1995) or physical (steric or other) interactions (Baskaran and Marchetti, 2008a, 2008b, 2009; Leoni and Liverpool, 2010). Mean-field models for the stochastic dynamics of the particles can be expressed in terms of the one-particle density $c(\mathbf{r}, \hat{\boldsymbol{\nu}}, t)$. This measures the probability of finding a self-propelled particle with position $\mathbf{r}$ and orientation $\hat{\boldsymbol{\nu}}$ at time t. The equation of motion for $c(\mathbf{r}, \hat{\boldsymbol{\nu}}, t)$ takes into account the interplay of fluctuations (diffusion), interactions, and self-propulsion. These mean-field models are valid in the regime of weak interactions, low density, and weak density correlations. The kinetic equation for the one-particle density can then be solved directly either analytically or numerically for specific geometries and initial condition (Saintillan, 2012). Alternatively, to describe macroscopic behavior, the kinetic theory can also be further coarse grained by projecting on to macroscopic fields such as $\rho(\mathbf{r}, t)$ and $\mathbf{p}(\mathbf{r}, t)$ to obtain the equivalent of Eq. (5), where the parameters α, β, K, v_1, and $\lambda_{1,2,3}$ are expressed in terms of the microscopic parameters of the system (Bertin, Droz, and Grégoire, 2006, 2009; Baskaran and Marchetti, 2008a, 2010; Ihle, 2011). A concrete example of this procedure is given in Sec. V.B.3.

2. Motors and filaments

Another microscopic realization of active matter is provided by suspensions of polar protein filaments cross-linked by active cross-links consisting of clusters of molecular motors (Nédélec *et al.*, 1997; Nédélec, 1998; Surrey *et al.*, 2001; Backouche *et al.*, 2006; Mizuno *et al.*, 2007). The motivation for this *in vitro* work is to provide an understanding of the mechanics of the eukaryotic cell cytoskeleton from the bottom up. Molecular motors are proteins that are able to convert stored chemical energy into mechanical work by hydrolyzing ATP molecules. The mechanical work is done by the motors moving in a unidirectional manner along the polar filaments. Particular motor proteins are associated with specific polar filaments, e.g., kinesins "walk" on microtubules while myosins "walk" on filamentous actin. Since the filaments are polar, they can be characterized by a position and an orientation. Some workers (Kruse and Jülicher, 2000, 2003, 2006; Liverpool, 2003; Liverpool and Marchetti, 2005; Ahmadi, Marchetti, and Liverpool, 2006) modeled the motor clusters as active cross-linkers (see Fig. 33) capable of walking along the filaments and exchange forces and torques

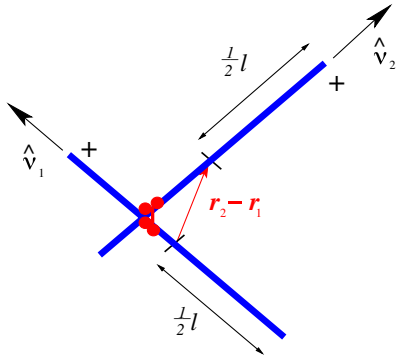

FIG. 33 (color online). A schematic of a pair of filaments of length ℓ with midpoint positions and orientations $\mathbf{r}_1$, $\hat{\boldsymbol{\nu}}_1$ and $\mathbf{r}_2$, $\hat{\boldsymbol{\nu}}_2$ driven by an active cross-link.

among filament pairs, hence yielding additional, active, contributions to the translational and rotational velocities of filaments. Another model was proposed by Aranson and Tsimring (2005, 2006) who described the filament dynamics via a stochastic master equation for polar rigid rods interacting via instantaneous inelastic "collisions." Both models express the stochastic dynamics of the active system in terms of the one-particle density of filaments $c(\mathbf{r}, \hat{\boldsymbol{\nu}}, t)$. The kinetic equation for $c(\mathbf{r}, \hat{\boldsymbol{\nu}}, t)$ takes account of the interplay of diffusion and active contributions induced by the cross-linking motor clusters or the inelastic collisions. The kinetic equations can again be further coarse grained by projecting on the continuum fields, such as $\rho(\mathbf{r}, t)$ and $\mathbf{p}(\mathbf{r}, t)$ to obtain the equivalent of Eq. (5), with microscopic expressions for all parameters. Although the parameter values depend on the specific microscopic model, the continuum equations obtained by these two approaches have the same structure. The work by Aranson and Tsimring (2005, 2006) incorporates, however, terms of higher order in the gradients of the continuum fields neglected in Kruse and Jülicher (2000, 2003), Liverpool (2003), and Ahmadi, Marchetti, and Liverpool (2006). These models give rise to contracted states and propagating density-polarization waves in both one (Kruse and Jülicher, 2000; Kruse, Camalet, and Jülicher, 2001) and higher dimensions (Liverpool, 2003; Liverpool and Marchetti, 2005), as well as aster and spiral patterns (Aranson and Tsimring, 2005, 2006). Finally, a number of other mean-field implementations of the dynamics of motor-filament suspensions, some including explicitly motor dynamics or additional passive cross-linkers, have been used by others to understand pattern formation in these systems (Lee and Kardar, 2001; Sankararaman, Menon, and Kumar, 2004; Ziebert and Zimmermann, 2004, 2005; Ziebert, Aranson, and Tsimring, 2007).

In the next sections we briefly outline one procedure for going from the fluctuating microscopic dynamics to the macroscopic equations of motion. We restrict our discussion to dry systems. For wet systems, see published work (Liverpool and Marchetti, 2006; Marchetti and Liverpool, 2007; Baskaran and Marchetti, 2009; Leoni and Liverpool, 2010).

B. From stochastic dynamics to macroscopic equations

We consider a collection of N identical (a simplification) anisotropic particles, each described by a position $\mathbf{r}_n(t)$ and

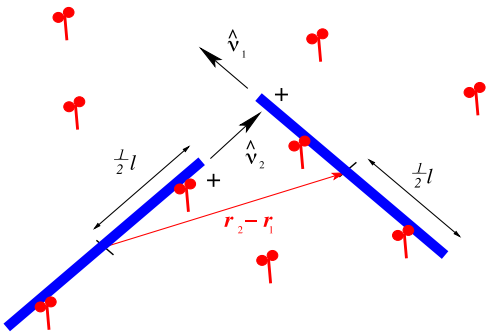

FIG. 34 (color online). An example of self-propelled particles: cartoon of a motility assay with filaments of length ℓ with positions and orientations $\mathbf{r}_1, \hat{\boldsymbol{\nu}}_1$ and $\mathbf{r}_2, \hat{\boldsymbol{\nu}}_2$ driven by motors tethered to a plane.

orientation $\hat{\boldsymbol{\nu}}_n(t)$, for particle n (see Fig. 34). The microscopic stochastic equations of motion for the positions and orientations are given by

$$\partial_t \mathbf{r}_n = \mathbf{v}_n(\mathbf{r}_n, \hat{\boldsymbol{\nu}}_n) + \boldsymbol{\xi}_n(t), \tag{75a}$$

$$\partial_t \hat{\boldsymbol{\nu}}_n = \boldsymbol{\omega}_i(\mathbf{r}_n, \hat{\boldsymbol{\nu}}_n) \times \hat{\boldsymbol{\nu}}_n + \Theta_n(t). \tag{75b}$$

The first terms on the rhs are the deterministic contributions to the motion arising from both passive interactions (e.g., steric repulsion, attractive interactions, etc.) and active velocities. Their specific form depends on the particular model system considered. The second terms on the rhs of Eqs. (75) are stochastic forces arising from a variety of noise sources, including but not limited to thermal noise. They are assumed to be Gaussian and white, with zero mean and correlations[7]

$$\langle \xi_{n\alpha}(t)\xi_{m\beta}(t')\rangle = 2\Delta_{\alpha\beta}(\hat{\boldsymbol{\nu}}_n)\delta_{nm}\delta(t-t'), \tag{76a}$$

$$\langle \Theta_{n\alpha}(t)\Theta_{m\beta}(t')\rangle = 2\Delta_R\delta_{nm}\delta_{\alpha\beta}\delta(t-t'). \tag{76b}$$

The translational noise correlation tensor is of the form $(\hat{\boldsymbol{\nu}}) = \Delta_\parallel \hat{\boldsymbol{\nu}}\,\hat{\boldsymbol{\nu}} + \Delta_\perp(\boldsymbol{\delta} - \hat{\boldsymbol{\nu}}\,\hat{\boldsymbol{\nu}})$. In a thermal system $\Delta_\parallel = D_\parallel$ and $\Delta_\perp = D_\perp$, with $D_\parallel$ and $D_\perp$ describing Brownian diffusion along the long direction of the particle and normal to it, respectively. Also in this case $\Delta_R = D_R$, where D_R is the rotational diffusion rate. In an active system the noise strengths are in general independent quantities.

For particles with fixed self-propulsion speed v_0 along their long axis the deterministic part of the velocities in Eqs. (75) has the form

$$\mathbf{v}_n(\mathbf{r}_n, \hat{\boldsymbol{\nu}}_n) = v_0\hat{\boldsymbol{\nu}}_n + [\boldsymbol{\zeta}(\hat{\boldsymbol{\nu}}_n)]^{-1} \cdot \sum_m \mathbf{f}(\mathbf{r}_n, \mathbf{r}_m; \hat{\boldsymbol{\nu}}_n, \hat{\boldsymbol{\nu}}_m), \tag{77a}$$

$$\boldsymbol{\omega}_n(\mathbf{r}_n, \hat{\boldsymbol{\nu}}_n) = \zeta_R^{-1} \sum_m \boldsymbol{\tau}(\mathbf{r}_n, \mathbf{r}_m; \hat{\boldsymbol{\nu}}_n, \hat{\boldsymbol{\nu}}_m), \tag{77b}$$

with $\boldsymbol{\zeta}(\hat{\boldsymbol{\nu}}) = \zeta_\parallel \hat{\boldsymbol{\nu}}\,\hat{\boldsymbol{\nu}} + \zeta_\perp(\boldsymbol{\delta} - \hat{\boldsymbol{\nu}}\,\hat{\boldsymbol{\nu}})$ a friction tensor and ζ^R a rotational friction coefficient. Again, in a Brownian system in thermal equilibrium at temperature T friction and diffusion (which in this case is also the strength of the noise) are related by the Stokes-Einstein relation $D_{\alpha\beta} = k_B T[\boldsymbol{\zeta}^{-1}]_{\alpha\beta}$ and $D_R = k_B T/\zeta_R$. In active systems these relations do not in general hold and noise and friction should be treated as independent.

The pairwise forces and torques in Eqs. (77) can be expressed in term of the total passive and active interactions in the system. The case of particles propelled by internal torques has also been considered in the literature, but will not be discussed here (Fily, Baskaran, and Marchetti, 2012).

1. Smoluchowski dynamics

For simplicity, we again restrict ourselves to the case of particles with overdamped dynamics. Starting from the Langevin equations (75) for the individual filaments, standard techniques can be used to derive an equation for the one-particle probability distribution function (Zwanzig, 2001). One first obtains an infinite hierarchy of equations for the $M(\leq N)$ particle distribution functions $c_M(\mathbf{r}_1, \hat{\boldsymbol{\nu}}_1, \mathbf{r}_2, \hat{\boldsymbol{\nu}}_2, \ldots, \mathbf{r}_M, \hat{\boldsymbol{\nu}}_M, t)$, the probability of finding M particles with positions and orientations $\{\mathbf{r}_1, \hat{\boldsymbol{\nu}}_1, \mathbf{r}_2, \hat{\boldsymbol{\nu}}_2, \ldots, \mathbf{r}_M, \hat{\boldsymbol{\nu}}_M\}$ at time t, regardless of the position and orientation of the other $N - M$ particles (Baskaran and Marchetti, 2010). A closure approximation is then required to truncate the hierarchy. This is implemented by expressing a higher order distribution function in terms of the lower ones. The traditional method is to write the two-particle distribution function as a product of two one-particle densities (Kruse and Jülicher, 2000; Liverpool, 2003; Aranson and Tsimring, 2005; Bertin, Droz, and Grégoire, 2006, 2009), as in the familiar molecular chaos approximation used to obtain the Boltzmann equation.

This procedure gives a nonlinear equation for the one-particle density $c(\mathbf{r}, \hat{\boldsymbol{\nu}}, t) = \sum_n \langle \delta(\mathbf{r} - \mathbf{r}_n)\delta(\hat{\boldsymbol{\nu}} - \hat{\boldsymbol{\nu}}_n)\rangle$, where the bracket denotes a trace over all other degrees of freedom and an average over the noise, in the form of a conservation law, given by

$$\partial_t c + \boldsymbol{\nabla} \cdot \mathbf{J}_c + \mathcal{R} \cdot \mathcal{J}_c = 0, \tag{78}$$

where $\mathcal{R} = \hat{\boldsymbol{\nu}} \times \partial_{\hat{\boldsymbol{\nu}}}$ is the rotation operator. The translational probability current $\mathbf{J}_c(\mathbf{r}, \hat{\boldsymbol{\nu}}, t)$ and the rotational probability current $\boldsymbol{J}_c(\mathbf{r}, \hat{\boldsymbol{\nu}}, t)$ are given by (Doi and Edwards, 1986)

$$\mathbf{J}_c = \mathbf{v}c - \boldsymbol{\Delta} \cdot \nabla c, \qquad \mathcal{J}_c = \boldsymbol{\omega}c - \Delta_R \mathcal{R}_c,$$

where $\mathbf{v}$ and $\boldsymbol{\omega}$ are given in Eqs. (77) and $\boldsymbol{\Delta}$ and Δ_R are, respectively, the translational and rotational noise strengths introduced in Eqs. (76).

It should be stressed that this closure scheme may yield different physical approximations for different classes of microscopic dynamics (Bialké, Speck, and Löwen, 2012; Fily and Marchetti, 2012). An illustrative example can be found in Baskaran and Marchetti (2010), which systematically derives a kinetic equation for self-propelled hard rods starting with a microscopic Langevin dynamics that includes inertia by first obtaining a Fokker-Planck equation for the joint probability distribution of both position and orientation and velocities, and finally derive the Smoluchowski limit where friction is large relative to inertia at the level of the kinetic equation by making a nonthermal assumption on the local distribution of velocities. This procedure yields a different Smoluchowski equation from that obtained by simply taking the overdamped limit at the level of the Langevin equation. While the structure of the hydrodynamic equations obtained by coarse graining the one-particle kinetic equation

[7]Note that one must also enforce that $\hat{\boldsymbol{\nu}} \cdot \Theta = 0$.

is the same in both cases (as it is dictated by symmetry considerations), the values of the parameters in the continuum equations and particularly their dependence on v_0 and noise strength depend on whether the overdamped limit is taken right at the outset, i.e., at the level of the microscopic dynamics, or at the level of the kinetic equation. Much work remains to be done to understand this subtle point and therefore we will not discuss it further in this review. A further interesting open question is how to systematically obtain a stochastic equation for the one-particle density which properly includes the noisy dynamics of the density fluctuations for active systems (Dean, 1996).

We leave some of these interesting open questions and discuss how to use the Smoluchowski dynamics as described by Eqs. (78) in the derivation of hydrodynamic equations.

2. From Smoluchowski to hydrodynamics

One approach, explored extensively by Saintillan and Shelley (2007, 2008a, 2008b), is to directly solve the Smoluchowski equations, either analytically or numerically. This work has been used to investigate the stability of both aligned and isotropic suspensions of active particles with hydrodynamic interactions (see also below) and has revealed a rich dynamics with strong density fluctuations. This approach will not be discussed further here. A recent review can be found in Saintillan (2012).

Here we focus instead on obtaining the description of the dynamics of the system in terms of a few macroscopic fields introduced phenomenologically in the first part of this review. A crucial assumption in deriving this continuum or hydrodynamic theory is the choice of the continuum fields as those whose fluctuations are long lived on large length scales. They include fields associated with conserved quantities and possible broken symmetries of the system. In a collection of active particles with no momentum conservation, the only conserved quantity is the number of particles and hence the density, defined in Eq. (1a), is a slow variable. In addition, to allow for the possibility of broken orientational order, with either polar or nematic symmetry, we consider the dynamics of a polarization field [Eq. (1b)] and an alignment tensor [Eq. (21)]. The fields are defined as moments of the one-particle distribution function as

$$\rho(\mathbf{r}, t) = \int d\hat{\boldsymbol{\nu}} c(\mathbf{r}, \hat{\boldsymbol{\nu}}, t), \tag{79a}$$

$$\rho(\mathbf{r}, t)\mathbf{p}(\mathbf{r}, t) = \int d\hat{\boldsymbol{\nu}}\, \hat{\boldsymbol{\nu}}\, c(\mathbf{r}, \hat{\boldsymbol{\nu}}, t), \tag{79b}$$

$$\rho(\mathbf{r}, t)\mathbf{Q}(\mathbf{r}, t) = \int d\hat{\boldsymbol{\nu}}\, \hat{\mathbf{Q}}(\hat{\boldsymbol{\nu}}) c(\mathbf{r}, \hat{\boldsymbol{\nu}}, t), \tag{79c}$$

with $\hat{\mathbf{Q}}(\hat{\boldsymbol{\nu}}) = \hat{\boldsymbol{\nu}}\,\hat{\boldsymbol{\nu}} - \frac{1}{d}\mathbf{1}$ and d the system's dimensionality. In general one could write an exact expansion of $c(\mathbf{r}, \hat{\boldsymbol{\nu}}, t)$ in terms of all its moments and transform the Smoluchowski equation into an infinite hierarchy of equations for the moments. The hydrodynamic description is obtained by assuming that higher order moments relax quickly on the time scales of interest and by truncating this expansion to include only conserved quantities and order parameter fields. Equivalently, considering for simplicity the case of $d = 2$, one can write

$$c(\mathbf{r}, \hat{\boldsymbol{\nu}}, t) = \frac{\rho(\mathbf{r}, t)}{2\pi}\{1 + 2\mathbf{p}(\mathbf{r}, t)\cdot\hat{\boldsymbol{\nu}} + 4\mathbf{Q}(\mathbf{r}, t)\colon \hat{\mathbf{Q}}(\hat{\boldsymbol{\nu}})\}, \tag{80}$$

insert this ansatz into the Smoluchowski equation, Eq. (78), and obtain the hydrodynamic equations for filament concentration, polarization, and alignment tensor. For details of the calculation, which also involves using a gradient expansion for the filament probability distribution and evaluating angular averages, see the literature (Liverpool, 2003; Ahmadi, Marchetti, and Liverpool, 2006; Baskaran and Marchetti, 2008a; Bertin, Droz, and Grégoire, 2009; Ihle, 2011). The result is a set of coupled equations for the hydrodynamic variables $\rho(\mathbf{r}, t)$, $\mathbf{p}(\mathbf{r}, t)$, and $\mathbf{Q}(\mathbf{r}, t)$ that has the form given in Sec. II, with parameter values that are calculated explicitly in terms of microscopic properties of the system.

In particular, one finds that the continuum equations governing the dynamics of motor-filament systems and collections of self-propelled particles have the same structure, with quantitative differences of the hydrodynamic parameters. In models of SPP the activating internal processes drive each individual unit and active contributions arise even at the single-particle level. In cell extracts of cytoskeletal filaments and associated motor proteins activity arises from interactions among the filaments mediated by motor clusters that act as active cross-linkers, exchanging forces among the filaments. As a result, the active parameters in the hydrodynamic equations are proportional to the square of the density of filaments, resulting in different behavior at large scales. For this reason motor-filament suspensions have also been referred to as systems of "mutually propelled particles" (Giomi *et al.*, 2012) to distinguish them from SPPs.

3. An example: Derivation of continuum equations for aligning Vicsek-type particles

To illustrate the method, we show in this section the derivation of the continuum equations for a simple model of self-propelled point particles on a substrate in two dimensions with a polar angular interaction that tends to align particles as in the Vicsek model. We consider N particles with polarity defined by an axis $\hat{\boldsymbol{\nu}}_n = (\cos\theta_n, \sin\theta_n)$. The dynamics is governed by Eqs. (75) that now take the explicit form

$$\partial_t \mathbf{r}_n = v_0\hat{\boldsymbol{\nu}}_n - \zeta^{-1}\sum_m \frac{\partial V}{\partial \mathbf{r}_n} + \boldsymbol{\xi}_n(t), \tag{81a}$$

$$\partial_t \theta_n = \zeta_R^{-1}\sum_m \frac{\partial V}{\partial \theta_n} + \Theta_n(t), \tag{81b}$$

where v_0 is the fixed self-propulsion speed and we have taken $\zeta_{\alpha\beta} = \zeta\delta_{\alpha\beta}$. The noise is Gaussian and white, with zero mean, as given in Eqs. (76) and $\Delta_{\alpha\beta} = \Delta\delta_{\alpha\beta}$. Forces and torques in Eq. (81a) are expressed as derivatives of a pair potential, given by

$$\zeta_R^{-1}V(x_n, x_m) = -\frac{\gamma}{\pi R^2}\Theta(R - |\mathbf{r}_n - \mathbf{r}_m|)\cos(\theta_m - \theta_n),$$

that tends to align particles of the same polarity, with $\Theta(x)$ the Heaviside step function and R the range of the interaction. Here we use the shorthand $x_n = (\mathbf{r}_n, \theta_n)$ and γ is the

interaction strength with dimensions of length squared over time. As we are interested in a hydrodynamic model that describes spatial variations on length scales large compared to the range R of the interaction, we assume the interaction to be local. This polar aligning interaction was used recently in Farrell *et al.* (2012) in a related model that highlights the role of caging effects. As outlined in Sec. V.B.1, one can then use standard methods (Zwanzig, 2001) to transform the coupled Langevin equations into a Smoluchowski equation for the one-particle distribution $c(\mathbf{r}, \theta, t)$ given by

$$\begin{aligned}\partial_t c + v_0 \boldsymbol{\nu}_1 \cdot \boldsymbol{\nabla}_1 c &= \Delta \nabla_1^2 c + \Delta_R \partial_{\theta_1}^2 c + \frac{1}{\zeta} \boldsymbol{\nabla}_1 \cdot c(x_1, t) \\ &\times \int_{x_2} \boldsymbol{\nabla}_1 V(x_1, x_2) c(x_2, t) + \Delta_R \partial_{\theta_1}^2 c \\ &+ \frac{1}{\zeta_R} \partial_{\theta_1} c(x_1, t) \int_{x_2} \partial_{\theta_1} V(x_1, x_2) c(x_2, t). \end{aligned} \tag{82}$$

To obtain hydrodynamic equations, we now proceed as outlined in Sec. V.B.2 and transform the kinetic equation into a hierarchy of equations for the angular moments of the one-particle probability density c. In two dimensions the moments are simply written by introducing an angular Fourier transform (Bertin, Droz, and Grégoire, 2009) in terms of the Fourier components $f_k(\mathbf{r}, t) = \int_0^{2\pi} c(\mathbf{r}, \theta, t) e^{ik\theta} d\theta$. By comparing with Eqs. (79) it is easy to see that $f_0 = \rho$, $f_1 = w_x + i w_y$, with $\mathbf{w} = \rho \mathbf{p}$ the polarization density, and the real and imaginary parts of f_2 are proportional to the two independent components of the alignment tensor $\mathbf{Q}$. Using $2\pi c(\mathbf{r}, \theta, t) = \sum_k f_k e^{-ik\theta}$ and retaining for simplicity only terms up to linear order in the gradients, we obtain a hierarchy of equations

$$\begin{aligned}\partial_t f_k + \frac{v_0}{2} \partial_x (f_{k+1} + f_{k-1}) + \frac{v_0}{2i} \partial_y (f_{k+1} - f_{k-1}) \\ = -k^2 \Delta_R f_k + \frac{ik\gamma}{2\pi} \sum_q f_q V_{-q} f_{k-q} + \mathcal{O}(\nabla^2), \end{aligned} \tag{83}$$

where all discrete sums run from $-\infty$ to $+\infty$ and $V_q = \int d\theta e^{iq\theta} \sin\theta = i\pi(\delta_{q,1} - \delta_{q,-1})$. We consider equations for f_0 and f_1, assume that f_2 is a fast variable, so that $\partial_t f_2 \simeq 0$, and neglect all higher order Fourier components, i.e., assume $f_k = 0$ for $k \geq 3$. Eliminating f_2 in favor of f_0 and f_1, it is then straightforward to obtain (Bertin, Droz, and Grégoire, 2006, 2009; Farrell *et al.*, 2012)[8]

$$\partial_t \rho + v_0 \boldsymbol{\nabla} \cdot (\rho \mathbf{p}) = 0, \tag{84a}$$

$$\begin{aligned}\partial_t \mathbf{p} + \lambda_1 (\mathbf{p} \cdot \boldsymbol{\nabla}) \mathbf{p} = -[a(\rho) + \beta |\mathbf{p}|^2] \mathbf{p} - \mathbf{v}_1 \cdot \boldsymbol{\nabla} \rho \\ + \frac{\lambda_3}{2} \boldsymbol{\nabla} |\mathbf{p}|^2 + \lambda_2 \mathbf{p} (\boldsymbol{\nabla} \cdot \mathbf{p}) + \mathcal{O}(\nabla^2), \end{aligned} \tag{84b}$$

with

$$a(\rho) = \Delta_R - \tfrac{1}{2}\gamma\rho, \tag{85a}$$

$$\beta = \frac{\gamma^2 \rho^2}{8\Delta_R}, \tag{85b}$$

$$\lambda_1 = \frac{3 v_0 \gamma \rho}{16 \Delta_R}, \tag{85c}$$

$$\lambda_2 = -\lambda_3 = -\frac{5 v_0 \gamma \rho}{16 \Delta_R}, \tag{85d}$$

$$\mathbf{v}_1 = \frac{v_0}{2\rho}\left(1 - \frac{5\gamma\rho}{8\Delta_R} p^2\right)\boldsymbol{\delta} - \frac{v_0}{\rho}\left(1 - \frac{\gamma\rho}{2\Delta_R}\right)\mathbf{p} \cdot \mathbf{p}. \tag{85e}$$

Equations (84) have the same structure as Eq. (5), although noise has been neglected here. The various coefficients are expressed in terms of microscopic parameters and are in general found to depend on density and order parameter. In particular, the coefficient $\mathbf{v}_1$ of the $\boldsymbol{\nabla}\rho$ term is now a tensor, describing anisotropic pressure gradients that can play a role in the ordered state. These effects were neglected for simplicity in the phenomenological model. We also stress that there is an important difference between the parameter values obtained in the present model and those obtained by Bertin, Droz, and Grégoire (2006, 2009) and Baskaran and Marchetti (2008a) as in the latter models the effective interaction strength (here γ) depends linearly on v_0. As a result, Baskaran and Marchetti (2008a) and Bertin, Droz, and Grégoire (2009) found that $\lambda_i \sim v_0^2$, while here $\lambda_i \sim v_0$. This difference arises because in Baskaran and Marchetti (2008a) and Bertin, Droz, and Grégoire (2009) they systematically described binary collisions, yielding an instantaneous change of direction with probability one in a small time interval, while the model of Farrell *et al.* (2012) presented here (and chosen for illustrative purpose because of its simplicity) considers a continuous evolution of the position due to the application of a force in the Langevin equation. These differences may of course be important for large values of v_0.

This example shows how the derivation of hydrodynamics from a microscopic model yields explicit values for the various parameters in the continuum equations in terms of microscopic parameters. Of course, as stressed, these values are model dependent. In addition, there is a price to be paid in that in the derivation one has made two important assumptions. The first is the assumption of low density that allows us to replace the two-particle probability distribution by the product of two one-particle distribution functions in the kinetic equation. The second is effectively an assumption of weak interaction that enters in the moment closure approximation. The two assumptions are not independent and essentially amount to the so-called assumption of "molecular chaos" used for instance in the derivation of the familiar Boltzmann equation.

4. Hydrodynamic interactions

The examples presented ignore the momentum exchange between the active particles and the solvent that one would have for instance in suspensions of swimming organisms. This physical effect is important for understanding the properties of a wide variety of experiments and should be included for a complete microscopic description of active matter.

[8] Microscopic derivations of continuum equations of the type presented naturally yield an equation for the polarization density $\mathbf{w} = \rho \mathbf{p}$ rather than the order parameter field $\mathbf{p}$. Of course it is straightforward to use the density equation to transform one into the other.

The coupling to the solvent has been treated in the literature in at least two ways.

One approach is to include an additional equation for the solvent velocity field $\mathbf{v}(\mathbf{r}, t)$ which is coupled to the microscopic equations of motion (Liverpool and Marchetti, 2006; Marchetti and Liverpool, 2007) or to the corresponding Smoluchowski equation (Saintillan and Shelley, 2008a; Pahlavan and Saintillan, 2011). The active particles are convected and rotated by the local fluid flow while also imparting additional forces (stresses) onto the fluid. This gives rise to a coupled equation of motion for the concentration of filaments $c(\mathbf{r}, \hat{\boldsymbol{\nu}}, t)$ and the velocity field $\mathbf{v}(\mathbf{r}, t)$ which can be solved directly (Saintillan and Shelley, 2008a; Pahlavan and Saintillan, 2011) or coarse grained as described above to give coupled equations for $\rho(\mathbf{r}, t)$, $\mathbf{p}(\mathbf{r}, t)$, $\mathbf{Q}(\mathbf{r}, t)$, and $\mathbf{v}(\mathbf{r}, t)$. For the case where the suspension is incompressible ($\rho = \text{const}$), the momentum ($\mathbf{v}$) equation has the form $\rho(\partial_t + \mathbf{v}\cdot\boldsymbol{\nabla})\mathbf{v} = \boldsymbol{\nabla}\cdot\boldsymbol{\sigma}$ with $\boldsymbol{\nabla}\cdot\mathbf{v} = 0$. This equation may also be often treated in the Stokes approximation $\boldsymbol{\nabla}\cdot\boldsymbol{\sigma} = 0$, appropriate for systems at low Reynolds number. The active forces due to the swimmers are incorporated as an additional (active) contribution to the stress tensor, so that $\sigma_{\alpha\beta} = \sigma^p_{\alpha\beta} + \sigma^a_{\alpha\beta}$, where the passive contribution $\sigma^p_{\alpha\beta}$ has the form obtained in equilibrium liquid crystals (de Gennes and Prost, 1993). The active contribution $\sigma^a_{\alpha\beta}$ is evaluated by noting that, in the absence of external body forces, the force distribution exerted by the active particles on the fluid can be written as a multipole expansion with lowest order nonvanishing term being a dipole. The active stress $\sigma^a_{\alpha\beta}$ can then be identified with the active reactive fluxes proportional to $\zeta\Delta\mu$ [see Eq. (42)]. To leading order in a gradient expansion it contains two additive contributions. The first term $\sigma^{a1}_{\alpha\beta} \propto \zeta\Delta\mu q_{\alpha\beta}$ has nematic symmetry and is present in both polar and nematic systems, where it is written as $\sigma^{a1}_{\alpha\beta} \propto \zeta\Delta\mu Q_{\alpha\beta}$. In addition, for polar systems only, the active stress also contains terms $\sigma^{a2}_{\alpha\beta} \propto \zeta'\Delta\mu\partial_\alpha p_\beta + \zeta''\Delta\mu\partial_\beta p_\alpha$ (Liverpool and Marchetti, 2006; Marchetti and Liverpool, 2007). When the hydrodynamic equations are written on the basis of the entropy production formulation discussed in Sec. III.B, this term is discarded as one of higher order in the driving forces. It is also of higher order in the gradients as compared to $\sigma^{a1}_{\alpha\beta}$, although only of first order, rather than quadratic, in the polarization field. Finally, it is the leading nonvanishing contribution to the active stress that has polar (as opposed to nematic) symmetry and it plays a role in controlling the onset of oscillatory states in these systems (Giomi, Marchetti, and Liverpool, 2008; Giomi and Marchetti, 2012).

Alternatively, one may integrate out the solvent velocity field to generate effective hydrodynamic interactions at the two-body level which give rise to additional long-range pairwise contributions to the deterministic velocities and angular velocities $\mathbf{v}_n$, $\boldsymbol{\omega}_n$ in Eqs. (75) (Baskaran and Marchetti, 2009; Leoni and Liverpool, 2010). These interactions arise from the forces generated on the fluid by the active particles. The local force distribution due to the active elements can be expanded in a multipole expansion. The lowest nonvanishing term in this expansion is a dipole, which also gives the longest range interactions. The simplest static models of swimming organisms then are force dipoles which can be characterized as contractile or extensile depending on the direction of the forces making up the dipole. Coarse graining the equations leads to a set of coupled integral equations for $\rho(\mathbf{r}, t)$, $\mathbf{p}(\mathbf{r}, t)$, and $\mathbf{Q}(\mathbf{r}, t)$ which in extended domains can be used to obtain generalized linear hydrodynamic modes whose behavior is identical to those obtained when keeping an explicit velocity field. Hydrodynamic equations for collections of static force dipoles have been obtained (Baskaran and Marchetti, 2009) which show the phenomenology described before. Swimming objects, however, are dynamic, undergoing an internal cyclical motion that leads to self-propulsion. The collective behavior of simplified dynamic models of swimmers with such internal cycles has also been studied and used to generate effective hydrodynamic equations (Leoni and Liverpool, 2010). Averaged over an internal cycle such dynamic models have an average force distribution that also has a multipolar expansion whose lowest term is generically a force dipole. The hydrodynamic equations obtained are then similar to those obtained for static dipoles. However, by tuning internal parameters one can also study self-propelled swimmers whose average force distribution starts at quadrupolar order. Here the symmetry broken between contractile and extensile objects is restored and, in the absence of any other interactions, only nematic phases are possible (Leoni and Liverpool, 2010, 2012).

C. Current status of microscopic theories of active matter

Perhaps the most important open question in deriving active theories from microscopic or mesoscopic models concerns understanding the nature of the noise. Thermal noise is often negligible in active systems at low frequency, but noise is nonetheless ubiquitous and plays a crucial role in controlling the large-scale behavior, as it can both act to destroy large-scale coherence or drive synchronization, depending on the specific situation. So far practically all work on active systems has either neglected noise or modeled it as a Gaussian, white random force, akin to thermal noise, but of unknown strength. In general one expects the noise to depend on activity. Multiplicative or non-Markovian random forces could also be at play in active systems. For instance, the multiplicative character of the noise introduces (Mishra, 2009; Mishra *et al.*, 2012; Bertin *et al.*, 2013) singular features into the fluctuation-driven phase separation (Mishra and Ramaswamy, 2006) that characterizes a stable active nematic. Microscopic models are needed that attempt to take into account the stochastic nature of active forces and to derive a coarse-grained model where the effective noise amplitude is expressed in terms of local nonequilibrium processes that may lead to temporal or spatial correlations at large scales. An example is the work of Lacoste and Lau (2005) that couples the shot noise associated with the on and off switching of energy-dissipating pumps in active membranes to the membrane curvature and demonstrates that pump stochasticity plays a crucial role in controlling superdiffusive behavior in the membrane.

Of great interest is also the detailed understanding of hydrodynamic interactions in bacterial suspensions and their role in controlling the large-scale behavior. Recent

experiments probed for the first time the flow fields induced by swimming unicellular organisms. Measurements on Chlamydomonas revealed qualitative differences as compared to the puller stresslet configuration that had been used in the literature (Drescher *et al.*, 2010) and have further shown complex time-dependent oscillatory patterns. In contrast it was found that the flow field of E. coli is well described by a pusher stresslet, but its strength is very small and it is washed out by rotational diffusion of the swimming direction (Drescher *et al.*, 2011). These results have important implications for the behavior of microorganisms near surfaces and open the way to new quantitative investigations of the role of hydrodynamic interactions.

Finally, an area that is receiving increasing attention is the study of active matter at high density, where active glassy or solid states may emerge. As mentioned in Sec. II.C the collective dynamics of confluent layers of epithelial cells has been likened to that of glassy and supercooled systems. Mesoscopic models of interacting cell layers and tissues are beginning to emerge (Henkes, Fily, and Marchetti, 2011), although much more work remains to be done to understand the complex interplay of contractile stresses and substrate adhesion in controlling the buildup of cellular stresses in collective cell migration.

VI. CONCLUSIONS, OUTLOOK, AND FUTURE DIRECTIONS

In this review we discussed two-dimensional and three-dimensional active systems that are maintained out of equilibrium by a permanent energy consumption that takes place locally in each active unit. In these systems local polarity, when present, yields spontaneous motion. Typically, models of active matter describe the collective behavior of systems like fish shoals, birds flock, or animals herds as well as vibrated granular matter, bacterial colonies, or the cellular cytoskeleton. From a spatial symmetry point of view these systems are not different from ferroelectric and nematic liquid crystals. The fundamental difference stems from the fact that active systems consume and dissipate energy at all times. This feature has a number of profound consequences which we have addressed in this review:

- Polar flocks on a substrate, e.g., animal herds or keratocytes on a glass slide, display long-range order in two dimensions. This behavior is fundamentally different from that of equilibrium systems that are bound to obey the Mermin-Wagner theorem and can at best exhibit quasi-long-range order.
- Nematic as well as polar ordered phases of systems on a substrate exhibit giant density fluctuations, breaking the familiar $\sqrt{N}$ equilibrium scaling of number fluctuations in subregions with N particles on average.
- The uniform ordered state of bulk momentum-conserving systems of polar and nematic symmetry is generically unstable in the Stokesian regime.
- The end result of this instability for the typical active suspension appears to be turbulence at low Reynolds number (Dombrowski *et al.*, 2004; Wolgemuth, 2008) driven by the competition between forcing by active stress and relaxation by orientational diffusion.
- All these systems can support a new type of soundlike propagating waves with different propagation laws in opposite directions due to polarity.

We described how the macroscopic hydrodynamic equations for active systems can be obtained either from symmetry arguments, from generalized thermodynamics close to equilibrium, or from microscopic models. In each case we presented the simplest description that highlights the generic features uniquely associated with activity. Our analysis is restricted to two and three dimensions and we deliberately left aside one-dimensional and quasi-one-dimensional systems, which have already been extensively investigated (Helbing, 2001; Reichenbach, Franosch, and Frey, 2006). We note, however, that the mechanisms leading to the onset of traffic jams are probably related to the giant density fluctuations predicted in active systems in two dimensions [see also Yang, Marceau, and Gompper (2010) and Fily, Baskaran, and Marchetti (2012)].

All these unusual features have been either observed experimentally or confirmed in careful numerical simulations. It is difficult to establish the existence of long-range order experimentally, but simulations with a large number of active particles show unambiguously its existence. This is an important result that the statistical physics community was not inclined to believe. Giant density fluctuations have now been observed ubiquitously in systems with both polar and nematic interactions via simulations (Chaté, Ginelli, and Montagne, 2006; Chaté, Ginelli, Grégoire, Peruani, and Raynaud, 2008; Ginelli and Chaté, 2010), experimentally in vibrated granular media (Narayan, Ramaswamy, and Menon, 2007; Deseigne, Dauchot, and Chaté, 2010), and in bacterial suspensions (Zhang *et al.*, 2010). These observations confirmed the theoretically predicted scaling. We note, however, that this scaling was recently questioned by Toner (2012b). These large fluctuations are also present in the cellular cytoskeleton and their role is starting to be recognized (Gowrishankar and Rao, 2012) and their potential physiological relevance is beginning to be explored (Goswami *et al.*, 2008; Chaudhuri *et al.*, 2011; Gowrishankar *et al.*, 2012).

The long-wavelength instability of momentum-conserving systems is confirmed by numerical simulation and in fact can give rise to ''low Reynolds number turbulence'' in some instances (Dombrowski *et al.*, 2004). It is a good paradigm for explaining bacterial swirls but also the rotating microtubule spindles observed both *in vivo* and *in vitro* (Nédélec *et al.*, 1997; Nédélec, 1998). Furthermore, the existence of ''low Reynolds number'' waves have also been predicted in crystals moving without inertia through a dissipative medium, such as sedimenting colloids (Lahiri and Ramaswamy, 1997) or drifting Abrikosov lattices (Balents, Marchetti, and Radzihovski, 1998; Ling, Berger, and Prober, 1998; Simha and Ramaswamy, 1999), and also observed and understood in microfluidic drifting drop arrays (Beatus, Tlusty, and Bar-Ziv, 2006; Beatus, Bar-Ziv, and Tlusty, 2007). Such waves propagating in only one direction have been observed in cell lamellipodia as expected from active gel theory (Giannone *et al.*, 2004).

Eventually, one may be able to discuss with order of magnitude accuracy phenomena such as cell wound healing Petitjean *et al.* (2010), cell division (Salbreux, Prost, and

Joanny, 2009), and cell oscillations (Salbreux *et al.*, 2007). One can thus say that we currently have a good qualitative understanding of active systems. What do we need to get to the next stage, that is, to get to real quantitative understanding? One ingredient which we omitted on purpose up to now is signaling: biochemical signaling for cell biology or bacterial colonies external factors like food, smell, or sun in flocks, shoals, and herds. Such factors have been discussed in bacterial colonies and shown to give rise to ordered structures (Cates *et al.*, 2010). A direction that looks particularly promising is the coupling of active gel physics and chemical reactions in the context of cells and tissues, resulting, for instance, in increasing considerably the range of existence of Turing structures (Giomi, Liverpool, and Marchetti, 2010; Bois, Jülicher, and Grill, 2011; Giomi *et al.*, 2012), and in the spatiotemporal control and enhancement of chemical reaction rates in signaling and sorting (Chaudhuri *et al.*, 2011). A complete understanding of cell mechanics will require including detailed biochemical signaling networks. However, this cannot be achieved without extensive experimental input. Symmetry considerations and conservation laws are no longer sufficient, and this task requires the cooperation of several disciplines. It is worth the effort though, since it could be extended to tissue dynamics and developmental biology.

Another natural extension in the case of herds, flocks, and shoal is the investigation of a putative leader role (Couzin *et al.*, 2011; Leonard *et al.*, 2012). Up to now, completely "democratic" rules have been assumed. Within this approach, a leader could appear like a delta function, and its role involve the response function of the collection of individuals. In another promising direction, Guttal and Couzin (2010) treated the parameters in a Vicsek-style model of flocking and migration as heritable, selectable attributes, and studied their dynamics on evolutionary time scales, finding a remarkable range of evolutionarily stable strategies including coexistence of distinct behaviors in a herd.

Another frontier concerns active quantum systems. A classical imitation was recently introduced (Couder and Fort, 2006) and some Al-Ga-Se heterostructures gave rise to zero resistivity behavior described by equations similar to those of Toner and Tu (Alicea *et al.*, 2005). A general investigation of the type we present here would be very useful.

Eventually working with living systems is necessary and important, but it is often difficult. Artificial systems such as provided by layers of vibrated granular matter (Narayan, Ramaswamy, and Menon, 2007; Kudrolli *et al.*, 2008; Deseigne, Dauchot, and Chaté, 2010; Kumar, Ramaswamy, and Sood, 2011), noisy walkers (Kumar, Ramaswamy, and Rao, 2008), artificial swimmers (Dreyfus *et al.*, 2005; Bartolo and Lauga, 2010), and colloids propelled by catalytic reactions (Paxton *et al.*, 2004; Golestanian, Liverpool, and Ajdari, 2005, 2007; Howse *et al.*, 2007; Golestanian, 2009; Palacci *et al.*, 2010; Gibbs and Zhao, 2011; Golestanian, 2012; Theurkauff *et al.*, 2012) are useful but are often restricted to two dimensions (granular layers) or have been studied only at relatively low density (artificial self-propelled particles). A remarkable system of light-controlled active colloids was recently engineered that exhibits collective effects such as the formation of crystalline clusters (Palacci *et al.*, 2013). It would be nice to have three-dimensional active systems driven by light or chemical reactions (Buttinoni *et al.*, 2012). Attempts have been made (Prost, 2010) to raise interest among chemists, but so far progress toward realizing artificial active gels has been limited. Such systems would allow one to vary parameters over a wide range and in a controlled manner and would therefore provide extremely valuable artificial realizations of active matter.

ACKNOWLEDGMENTS

We thank many colleagues for invaluable discussions, suggestions and collaboration on some of the work summarized here, including Tapan Adhyapak, Shiladitya Banerjee, Aparna Baskaran, Andrew Callan-Jones, Yaouen Fily, Kripa Gowrishankar, Yashodhan Hatwalne, Silke Henkes, Frank Jülicher, Norio Kikuchi, Karsten Kruse, Marco Leoni, Ananyo Maitra, Satyajit Mayor, Gautam Menon, Narayanan Menon, Shradha Mishra, Vijay Narayan, Suropriya Saha, Guillaume Salbreux, Sumithra Sankararaman, Ken Sekimoto, John Toner, and Rafael Voituriez. M. C. M. was supported by the National Science Foundation Grants No. DMR-0806511, No. DMR-1004789, and No. DGE-1068780. J. F. J., J. P., S. R., and M. R. acknowledge support from Grant No. 3504-2 of CEFIPRA, the Indo-French Centre for the Promotion of Advanced Research. T. B. L. acknowledges support of the EPSRC under Grant No. EP/G026440/1. S. R. was supported in part by a J. C. Bose Fellowship. J. F. J. and J. P. acknowledge the support of the European Network Mitosys.

REFERENCES

Adhyapak, T. C., S. Ramaswamy, and J. Toner, 2013, Phys. Rev. Lett. **110**, 118102.

Ahmadi, A., M. C. Marchetti, and T. B. Liverpool, 2005, Phys. Rev. E **72**, 060901(R).

Ahmadi, A., M. C. Marchetti, and T. B. Liverpool, 2006, Phys. Rev. E **74**, 061913.

Aldana, M., V. Dossetti, C. Huepe, V. M. Kenkre, and H. Larralde, 2007, Phys. Rev. Lett. **98**, 095702.

Alicea, J., L. Balents, M. P. A. Fisher, A. Paramekanti, and L. Radzihovsky, 2005, Phys. Rev. B **71**, 235322.

Angelani, L., R. DiLeonardo, and R. Giancarlo, 2009, Phys. Rev. Lett. **102**, 048104.

Angelini, T. E., E. Hannezo, X. Trepat, J. J. Fredberg, and D. A. Weitz, 2010, Phys. Rev. Lett. **104**, 168104.

Angelini, T. E., E. Hannezo, X. Trepat, M. Marquez, J. J. Fredberg, and D. A. Weitz, 2011, Proc. Natl. Acad. Sci. U.S.A. **108**, 4714.

Aranson, I. S., A. Snezhko, J. S. Olafsen, and J. S. Urbach, 2008, Science **320**, 612.

Aranson, I. S., A. Sokolov, J. O. Kessler, and R. E. Goldstein, 2007, Phys. Rev. E **75**, 040901(R).

Aranson, I. S., and L. S. Tsimring, 2005, Phys. Rev. E **71**, 050901(R).

Aranson, I. S., and L. S. Tsimring, 2006, Phys. Rev. E **74**, 031915.

Asano, Y., A. Jiménez-Dalmaroni, T. Liverpool, M. Marchetti, L. Giomi, A. Kiger, T. Duke, and B. Baum, 2009, HFSP J. **3**, 194.

Backouche, F., L. Haviv, D. Groswasser, and A. Bernheim-Groswasser, 2006, Phys. Biol. **3**, 264.

Baglietto, G., and E. V. Albano, 2009, Phys. Rev. E **80**, 050103(R).

Balents, L., M. Marchetti, and L. Radzihovski, 1998, Phys. Rev. B **57**, 7705.

Balland, M., N. Desprat, D. Icard, S. Fereol, A. Asnacios, J. Browaeys, S. Henon, and F. Gallet, 2006, Phys. Rev. E **74**, 021911.

Ballerini, M., *et al.*, 2008, Proc. Natl. Acad. Sci. U.S.A. **105**, 1232.

Banerjee, S., and M. C. Marchetti, 2011, Soft Matter **7**, 463.

Bartolo, D., and E. Lauga, 2010, Phys. Rev. E **81**, 026312.

Baskaran, A., and M. C. Marchetti, 2008a, Phys. Rev. Lett. **101**, 268101.

Baskaran, A., and M. C. Marchetti, 2008b, Phys. Rev. E **77**, 011920.

Baskaran, A., and M. C. Marchetti, 2009, Proc. Natl. Acad. Sci. U.S.A. **106**, 15 567.

Baskaran, A., and M. C. Marchetti, 2010, J. Stat. Mech. P04019.

Baskaran, A., and M. C. Marchetti, 2012, Eur. Phys. J. E **35**, 95.

Basu, A., J.-F. Joanny, F. Jülicher, and J. Prost, 2008, Eur. Phys. J. E **27**, 149.

Basu, A., J.-F. Joanny, F. Jülicher, and J. Prost, 2012, New J. Phys. **14**, 115001.

Batchelor, G. K., 2000, *An Introduction to Fluid Dynamics* (Cambridge University Press, Cambridge, England).

Beatus, T., R. Bar-Ziv, and T. Tlusty, 2007, Phys. Rev. Lett. **99**, 124502.

Beatus, T., T. Tlusty, and R. Bar-Ziv, 2006, Nat. Phys. **2**, 743.

Bees, M., P. Andresen, E. Mosekilde, and M. Givskov, 2000, J. Math. Biol. **40**, 27.

Bees, M., P. Andresen, E. Mosekilde, and M. Givskov, 2002, Bull. Math. Biol. **64**, 565.

Bendix, P. M., G. H. Koenderink, D. Cuvelier, Z. Dogic, B. N. Koeleman, W. M. Briehera, C. M. Fielda, L. Mahadevan, and D. A. Weitz, 2008, Biophys. J. **94**, 3126.

Ben-Jacob, E., I. Cohen, and H. Levine, 2000, Adv. Phys. **49**, 395.

Bertin, E., H. Chate, F. Ginelli, S. Mishra, A. Peshkov, and S. Ramaswamy, 2013, arXiv:1305.0772.

Bertin, E., M. Droz, and G. Grégoire, 2006, Phys. Rev. E **74**, 022101.

Bertin, E., M. Droz, and G. Grégoire, 2009, J. Phys. A **42**, 445001.

Bialké, J., T. Speck, and H. Löwen, 2012, Phys. Rev. Lett. **108**, 168301.

Bois, J. S., F. Jülicher, and S. Grill, 2011, Phys. Rev. Lett. **106**, 028103.

Brennen, C., and H. Winet, 1977, Annu. Rev. Fluid Mech. **9**, 339.

Butt, T., T. Mufti, A. Humayun, P. B. Rosenthal, S. Khan, S. Khan, and J. E. Molloy, 2010, J. Biol. Chem. **285**, 4964.

Buttinoni, I., G. Volpe, F. Kümmel, and C. Bechinger, 2012, J. Phys. Condens. Matter **24**, 284129.

Callan-Jones, A. C., and F. Jülicher, 2011, New J. Phys. **13**, 093027.

Cates, M. E., 2012, Rep. Prog. Phys. **75**, 042601.

Cates, M. E., S. M. Fielding, D. Marenduzzo, E. Orlandini, and J. M. Yeomans, 2008, Phys. Rev. Lett. **101**, 0618102.

Cates, M. E., D. Marenduzzo, I. Pagonabarraga, and J. Tailleur, 2010, Proc. Natl. Acad. Sci. U.S.A. **107**, 11 715.

Chaikin, P., and T. Lubensky, 2000, *Principles of Condensed Matter Physics*, new edition (Cambridge University Press, Cambridge, England).

Chaté, H., F. Ginelli, and G. Grégoire, 2007, Phys. Rev. Lett. **99**, 229601.

Chaté, H., F. Ginelli, G. Grégoire, F. Peruani, and F. Raynaud, 2008, Eur. Phys. J. B **64**, 451.

Chaté, H., F. Ginelli, G. Grégoire, and F. Raynaud, 2008, Phys. Rev. E **77**, 046113.

Chaté, H., F. Ginelli, and R. Montagne, 2006, Phys. Rev. Lett. **96**, 180602.

Chaudhuri, A., B. Bhattacharya, K. Gowrishankar, S. Mayor, and M. Rao, 2011, Proc. Natl. Acad. Sci. U.S.A. **108**, 14 825.

Chen, D. T. N., A. W. C. Lau, L. A. Hough, M. F. Islam, M. Goulian, T. C. Lubensky, and A. G. Yodh, 2007, Phys. Rev. Lett. **99**, 148302.

Couder, Y., and E. Fort, 2006, Phys. Rev. Lett. **97**, 154101.

Couzin, I. D., C. C. Ioannou, G. Demirel, T. Gross, C. J. Torney, A. Hartnett, L. Conradt, S. A. Levin, and N. E. Leonard, 2011, Science **334**, 1578.

Das, D., and M. Barma, 2000, Phys. Rev. Lett. **85**, 1602.

Dean, D. S., 1996, J. Phys. A **29**, L613.

de Gennes, P. G., and J. Prost, 1993, *The Physics of Liquid Crystals* (Clarendon Press, Oxford).

de Groot, S. R., and P. Mazur, 1984, *Non-Equilibrium Thermodynamics* (Dover, New York).

Deseigne, J., O. Dauchot, and H. Chaté, 2010, Phys. Rev. Lett. **105**, 098001.

DiLeonardo, R., L. Angelani, D. dell'Arciprete, G. Ruocco, V. Iebba, S. Schippa, M. P. Conte, F. Mecarini, F. D. Angelis, and E. D. Fabrizio, 2010, Proc. Natl. Acad. Sci. U.S.A. **107**, 9541.

Doi, M., and S. F. Edwards, 1986, *The Theory of Polymer Dynamics* (Clarendon Press, Oxford).

Dombrowski, C., L. Cisneros, S. Chatkaew, R. E. Goldstein, and J. O. Kessler, 2004, Phys. Rev. Lett. **93**, 098103.

Drescher, K., J. Dunkel, L. H. Cisneros, S. Ganguly, and R. E. Goldstein, 2011, Proc. Natl. Acad. Sci. U.S.A. **108**, 10 940.

Drescher, K., R. E. Goldstein, N. Michel, M. Polin, and I. Tuval, 2010, Phys. Rev. Lett. **105**, 168101.

Dreyfus, R., J. Baudry, M. L. Roper, M. Fermigier, H. A. Stone, and J. Bibette, 2005, Nature (London) **437**, 862.

Dzyaloshinskii, I., and G. Volovick, 1980, Ann. Phys. (N.Y.) **125**, 67.

Edwards, C. M., and U. S. Schwarz, 2011, Phys. Rev. Lett. **107**, 128101.

Edwards, S. A., and J. M. Yeomans, 2009, Europhys. Lett. **85**, 18008.

Einstein, A., 1906, Ann. Phys. (Berlin) **324**, 289.

Einstein, A., 1911, Ann. Phys. (Berlin) **339**, 591.

Elgeti, J., and G. Gompper, 2009, Europhys. Lett. **85**, 38 002.

Enculescu, M., and H. Stark, 2011, Phys. Rev. Lett. **107**, 058301.

Fabry, B., G. N. Maksym, J. P. Butler, M. Glogauer, D. Navajas, and J. J. Fredberg, 2001, Phys. Rev. Lett. **87**, 148102.

Farrell, F., M. C. Marchetti, D. Marenduzzo, and J. Tailleur, 2012, Phys. Rev. Lett. **108**, 248101.

Fielding, S. M., D. Marenduzzo, and M. E. Cates, 2011, Phys. Rev. E **83**, 041910.

Fily, Y., A. Baskaran, and M. C. Marchetti, 2012, Soft Matter **8**, 3002.

Fily, Y., and M. C. Marchetti, 2012, Phys. Rev. Lett. **108**, 235702.

Finlayson, B. A., and L. E. Scriven, 1969, Proc. R. Soc. A **310**, 183.

Foffano, G., J. S. Lintuvuori, A. N. Morozov, K. Stratford, M. E. Cates, and D. Marenduzzo, 2012, Eur. Phys. J. E **35**, 98.

Forster, D., 1974, Phys. Rev. Lett. **32**, 1161.

Forster, D., 1975, *Hydrodynamic Fluctuations, Broken Symmetry, and Correlation Functions*, Frontiers in Physics, a lecture note and reprint series (W. A. Benjamin, New York), Advanced Book Program.

Furthauer, S., M. Neef, S. W. Grill, K. Kruse, and F. Jülicher, 2012, New J. Phys. **14**, 023001.

Galajda, P., J. Keymer, P. Chaikin, and R. Austin, 2007, J. Bacteriol. **189**, 8704.

Gardel, M., J. Shin, F. MacKintosh, L. Mahadevan, P. Matsudaira, and D. Weitz, 2004, Science **304**, 1301.

Giannone, G., B. J. Dubin-Thaler, H. G. Döbereiner, N. Kieffer, A. R. Bresnick, and M. P. Sheetz, 2004, Cell **116**, 431.
Gibbs, J., and Y. Zhao, 2011, Front Mat. Sci. **5**, 25.
Ginelli, F., and H. Chaté, 2010, Phys. Rev. Lett. **105**, 168103.
Ginelli, F., F. Peruani, M. Bär, and H. Chaté, 2010, Phys. Rev. Lett. **104**, 184502.
Giomi, L., T. B. Liverpool, and M. C. Marchetti, 2010, Phys. Rev. E **81**, 051908.
Giomi, L., L. Mahadevan, B. Chakraborty, and M. F. Hagan, 2011, Phys. Rev. Lett. **106**, 218101.
Giomi, L., L. Mahadevan, B. Chakraborty, and M. F. Hagan, 2012, Nonlinearity **25**, 2245.
Giomi, L., and M. C. Marchetti, 2012, Soft Matter **8**, 129.
Giomi, L., M. C. Marchetti, and T. Liverpool, 2008, Phys. Rev. Lett. **101**, 198101.
Golestanian, R., 2009, Phys. Rev. Lett. **102**, 188305.
Golestanian, R., 2012, Phys. Rev. Lett. **108**, 038303.
Golestanian, R., T. Liverpool, and A. Ajdari, 2005, Phys. Rev. Lett. **94**, 220801.
Golestanian, R., T. B. Liverpool, and A. Ajdari, 2007, New J. Phys. **9**, 126.
Gönci, B., M. Nagy, and T. Vicsek, 2008, Eur. Phys. J. Special Topics **157**, 53.
Gopinath, A., M. F. Hagan, M. C. Marchetti, and A. Baskaran, 2012, Phys. Rev. E **85**, 061903.
Goswami, D., K. Gowrishankar, S. Bilgrami, S. Ghosh, R. Raghupathy, R. Chadda, R. Vishwakarma, M. Rao, and S. Mayor, 2008, Cell **135**, 1085.
Gowrishankar, K., S. Ghosh, S. Saha, C. Ruma, S. Mayor, and M. Rao, 2012, Cell **149**, 1353.
Gowrishankar, K., and M. Rao, 2012, "Nonequilibrium phase transitions in active contractile polar filaments," arXiv:1201.3938.
Grégoire, G., and H. Chaté, 2004, Phys. Rev. Lett. **92**, 025702.
Grill, S. W., 2011, Current Opinion in Genetics & Development **21**, 647.
Gruler, H., U. Dewald, and M. Eberhardt, 1999, Eur. Phys. J. B **11**, 187 [http://link.springer.com/article/10.1007%2FBF03219164#page-1].
Guasto, J. S., K. A. Johnson, and J. P. Gollub, 2010, Phys. Rev. Lett. **105**, 168102.
Günther, S., and K. Kruse, 2007, New J. Phys. **9**, 417.
Guttal, V., and I. D. Couzin, 2010, Proc. Natl. Acad. Sci. U.S.A. **107**, 16 172.
Haines, M., A. Sokolov, I. S. Aranson, L. Berlyand, and D. A. Karpeev, 2009, Phys. Rev. E **80**, 041922.
Hatwalne, Y., S. Ramaswamy, M. Rao, and R. A. Simha, 2004, Phys. Rev. Lett. **92**, 118101.
Head, D. A., W. J. Briels, and G. Gompper, 2011, BMC Biophysics **4**, 18.
Helbing, D., 2001, Rev. Mod. Phys. **73**, 1067.
Henkes, S., Y. Fily, and M. C. Marchetti, 2011, Phys. Rev. E **84**, 040301(R).
Hohenberg, P. C., 1967, Phys. Rev. **158**, 383.
Howse, J. R., R. A. L. Jones, A. J. Ryan, T. Gough, R. Vafabakhsh, and R. Golestanian, 2007, Phys. Rev. Lett. **99**, 048102.
Ihle, T., 2011, Phys. Rev. E **83**, 030901(R).
Ishikawa, T., 2009, J. R. Soc. Interface **6**, 815.
Joanny, J. F., F. Julicher, K. Kruse, and J. Prost, 2007, New J. Phys. **9**, 422.
Joanny, J.-F., and J. Prost, 2009a, HFSP J. **3**, 94.
Joanny, J.-F., and J. Prost, 2009b, in *Poincaré Seminar 2009*, edited by B. Duplantier, and V. Rivasseau (Birkhauser, Boston).
Joanny, J.-F., and S. Ramaswamy, 2012, J. Fluid Mech. **705**, 46
Jülicher, F., K. Kruse, J. Prost, and J.-F. Joanny, 2007, Phys. Rep. **449**, 3.
Jülicher, F., and J. Prost, 1997, Phys. Rev. Lett. **78**, 4510.
Kareiva, M., and N. Shigesada, 1983, Oecologia **56**, 234.
Kemkemer, R., D. Kling, D. Kaufmann, and H. Gruler, 2000, Eur. Phys. J. E **1**, 215.
Keren, K., Z. Pincus, G. Allen, E. Barnhart, A. Marriott, A. Mogilner, and J. Theriot, 2008, Nature (London) **453**, 475.
Kikuchi, N., A. Ehrlicher, D. Koch, J. A. Käs, S. Ramaswamy, and M. Rao, 2009, Proc. Natl. Acad. Sci. U.S.A. **106**, 19 776.
Koch, D. L., and G. Subramanian, 2011, Annu. Rev. Fluid Mech. **43**, 637.
Koenderink, G. H., Z. Dogic, F. Nakamura, P. M. Bendix, F. C. MacKintosh, J. H. Hartwig, T. P. Stossel, and D. A. Weitz, 2009, Proc. Natl. Acad. Sci. U.S.A. **106**, 15 192.
Kraikivski, P., R. Lipowsky, and J. Kierfeld, 2006, Phys. Rev. Lett. **96**, 258103.
Kron, S. J., and J. Spudich, 1986, Proc. Natl. Acad. Sci. U.S.A. **83**, 6272.
Kruse, K., S. Camalet, and F. Jülicher, 2001, Phys. Rev. Lett. **87**, 138101.
Kruse, K., F. Joanny, F. Jülicher, J. Prost, and K. Sekimoto, 2004, Phys. Rev. Lett. **92**, 078101.
Kruse, K., J. F. Joanny, F. Jülicher, and J. Prost, 2006, Phys. Biol. **3**, 130.
Kruse, K., J. F. Joanny, F. Jülicher, J. Prost, and K. Sekimoto, 2005, Eur. Phys. J. E **16**, 5.
Kruse, K., and F. Jülicher, 2000, Phys. Rev. Lett. **85**, 1778.
Kruse, K., and F. Jülicher, 2003, Phys. Rev. E **67**, 051913.
Kruse, K., and F. J. Jülicher, 2006, Eur. Phys. J. E **20**, 459.
Kudrolli, A., 2010, Phys. Rev. Lett. **104**, 088001.
Kudrolli, A., G. Lumay, D. Volfson, and L. S. Tsimring, 2008, Phys. Rev. Lett. **100**, 058001.
Kumar, K. V., S. Ramaswamy, and M. Rao, 2008, Phys. Rev. E **77**, 020102.
Kumar, N., S. Ramaswamy, and A. K. Sood, 2011, Phys. Rev. Lett. **106**, 118001.
Kung, W., M. C. Marchetti, and K. Saunders, 2006, Phys. Rev. E **73**, 031708.
Lacoste, D., and A. W. C. Lau, 2005, Europhys. Lett. **70**, 418.
Lahiri, R., and S. Ramaswamy, 1997, Phys. Rev. Lett. **79**, 1150.
Landau, L. D., and E. M. Lifshitz, 1998, *Fluid Mechanics* (Butterworth-Heinemann, Stoneham, MA).
Larson, R., 1988, *Constitutive Equations for Polymer Melts and Solutions* (Butterworths, London).
Lau, A. W. C., B. D. Hoffman, A. Davies, J. C. Crocker, and T. C. Lubensky, 2003, Phys. Rev. Lett. **91**, 198101.
Lau, A. W. C., and T. C. Lubensky, 2009, Phys. Rev. E **80**, 011917.
Lauga, E., and T. R. Powers, 2009, Rep. Prog. Phys. **72**, 096601.
Lebwohl, P., and G. Lasher, 1973, Phys. Rev. A **7**, 2222.
Lee, H. Y., and M. Kardar, 2001, Phys. Rev. E **64**, 056113.
Leonard, N. E., T. Shen, B. Nabet, L. Scardovi, I. D. Couzin, and S. A. Levin, 2012, Proc. Natl. Acad. Sci. U.S.A. **109**, 227.
Leoni, M., and T. B. Liverpool, 2010, Phys. Rev. Lett. **105**, 238102.
Leoni, M., and T. B. Liverpool, 2012, Phys. Rev. E **85**, 040901(R).
Levine, A. J., and F. C. MacKintosh, 2009, J. Phys. Chem. B **113**, 3820.
Ling, X. S., J. E. Berger, and D. E. Prober, 1998, Phys. Rev. B **57**, R3249.
Lingwood, D., and K. Simons, 2010, Science **327**, 46.
Liverpool, T. B., 2003, Phys. Rev. E **67**, 031909.
Liverpool, T. B., A. C. Maggs, and A. Ajdari, 2001, Phys. Rev. Lett. **86**, 4171.

Liverpool, T. B., and M. C. Marchetti, 2005, Europhys. Lett. **69**, 846.
Liverpool, T. B., and M. C. Marchetti, 2006, Phys. Rev. Lett. **97**, 268101.
Liverpool, T. B., M. C. Marchetti, J.-F. Joanny, and J. Prost, 2009, Europhys. Lett. **85**, 18 007.
MacKintosh, F. C., and A. J. Levine, 2008, Phys. Rev. Lett. **100**, 018104.
Makris, N. C., P. Ratilal, D. T. Symonds, S. Jagannathan, S. Lee, and R. W. Nero, 2006, Science **311**, 660.
Manneville, J.-B., P. Bassereau, S. Ramaswamy, and J. Prost, 2001, Phys. Rev. E **64**, 021908.
Marchetti, M. C., 2012, Nature (London) **491**, 340.
Marchetti, M. C., and T. B. Liverpool, 2007, in *Cell Motility*, edited by P. Lenz (Springer-Verlag, Berlin).
Marenduzzo, D., E. Orlandini, and J. M. Yeomans, 2007, Phys. Rev. Lett. **98**, 118102.
Martin, P. C., O. Parodi, and P. Pershan, 1972, Phys. Rev. A **6**, 2401.
Mayer, M., M. Depken, J. S. Bois, F. Jülicher, and S. W. Grill, 2010, Nature (London) **467**, 617.
McCandlish, S. R., A. Baskaran, and M. F. Hagan, 2012, Soft Matter **8**, 2527.
Mermin, N. D., and H. Wagner, 1966, Phys. Rev. Lett. **17**, 1133.
Mertz, A. F., S. Banerjee, Y. Che, G. K. German, Y. Xu, C. Hyland, M. C. Marchetti, V. Horsley, and E. R. Dufresne, 2012, Phys. Rev. Lett. **108**, 198101.
Milner, S. T., 1993, Phys. Rev. E **48**, 3674.
Milošević, S., L. Sasvári, and B. Tadić, 1978, Z. Phys. B **29**, 139.
Mishra, S., 2009, Ph.D. thesis (Indian Institute of Science, Bangalore).
Mishra, S., A. Baskaran, and M. C. Marchetti, 2010, Phys. Rev. E **81**, 061916.
Mishra, S., F. Ginelli, S. Puri, E. Bertin, H. Chate, and R. Ramaswamy, 2012 (unpublished).
Mishra, S., and S. Ramaswamy, 2006, Phys. Rev. Lett. **97**, 090602.
Mizuno, D., C. Tardin, C. F. Schmidt, and F. C. MacKintosh, 2007, Science **315**, 370.
Mogilner, A., and G. Oster, 1996, Biophys. J. **71**, 3030.
Mogilner, A., and G. Oster, 1999, Eur. Biophys. J. **28**, 235.
Muhuri, S., M. Rao, and S. Ramaswamy, 2007, Europhys. Lett. **78**, 48 002.
Murray, J. D., 2003, *Mathematical Biology Vol. II: Spatial Models and Biomedical Applications* (Springer, New York), 3rd ed.
Narayan, V., S. Ramaswamy, and N. Menon, 2007, Science **317**, 105.
Narayan, V., S. Ramaswamy, and N. Menon, 2008, Science **320**, 612.
Nédélec, F., 1998, Ph.D. thesis (Université Paris 11), http://www.cytosim.org/reprints/these/index.html.
Nédélec, F., T. Surrey, A. Maggs, and S. Leibler, 1997, Nature (London) **389**, 305.
Onsager, L., 1949, Ann. N.Y. Acad. Sci. **51**, 627.
Oron, A., S. H. Davis, and S. G. Bankoff, 1997, Rev. Mod. Phys. **69**, 931.
Pahlavan, A. A., and D. Saintillan, 2011, Phys. Fluids **23**, 011901.
Palacci, J., B. Abécassis, C. Cottin-Bizonne, C. Ybert, and L. Bocquet, 2010, Phys. Rev. Lett. **104**, 138302.
Palacci, J., S. Sacanna, A. P. Steinberg, D. J. Pine, and P. M. Chaikin, 2013, Science **339**, 936.
Palffy-Muhoray, P., M. A. Lee, and R. G. Petschek, 1988, Phys. Rev. Lett. **60**, 2303.
Parrish, J. K., and W. M. Hamner, 1997, *Animals Groups in Three Dimensions: How Species Aggregate* (Cambridge University Press, Cambridge, England).
Paxton, W. F., K. C. Kistler, C. C. Olmeda, A. Sen, S. K. S. Angelo, Y. Cao, T. E. Mallouk, P. E. Lammert, and V. H. Crespi, 2004, J. Am. Chem. Soc. **126**, 13 424.
Pedley, T. J., and J. O. Kessler, 1992, Annu. Rev. Fluid Mech. **24**, 313.
Peruani, F., A. Deutsch, and M. Bär, 2006, Phys. Rev. E **74**, 030904.
Peruani, F., A. Deutsch, and M. Bär, 2008, Eur. Phys. J. Special Topics **157**, 111.
Peruani, F., J. Starruss, V. Jakovljevic, L. Sogaard-Anderseng, A. Deutsch, and M. Bär, 2012, Phys. Rev. Lett. **108**, 098102.
Peshkov, A., I. S. Aronson, E. Bertin, H. Chaté, and F. Ginelli, 2012, arXiv:1207.5751.
Petitjean, L., M. Reffay, E. Grasland-Mongrain, M. Poujade, B. Ladoux, A. Buguin, and P. Silberzan, 2010, Biophys. J. **98**, 1790.
Pinot, M., F. Chesnel, J. Z. Kubiak, I. Arnal, F. J. Nedelec, and Z. Gueroui, 2009, Curr. Biol. **19**, 954.
Poujade, M., E. Grasland-Mongrain, A. Hertzog, J. Jouanneau, P. Chavrier, B. Ladoux, A. Buguin, and P. Silberzan, 2007, Proc. Natl. Acad. Sci. U.S.A. **104**, 15 988.
Prevost, A., P. Melby, D. A. Egolf, and J. S. Urbach, 2004, Phys. Rev. E **70**, 050301(R).
Prost, J., 2010, in *From Non-covalent Assemblies to Molecular Machines*, edited by J. Sauvage, and P. Gaspard, Solvay Conference in Chemistry (Wiley, New York), Vol. 21.
Prost, J., and R. Bruinsma, 1996, Europhys. Lett. **33**, 321.
Prost, J., J.-F. Joanny, P. Lenz, and C. Sykes, 2007, *The Physics of Listeria Propulsion in Cell Motility*, edited by P. Lenz (Springer-Verlag, New York).
Rafaï, S., L. Jibuti, and P. Peyla, 2010, Phys. Rev. Lett. **104**, 098102.
Ramaswamy, S., 2010, Annu. Rev. Condens. Matter Phys. **1**, 323.
Ramaswamy, S., and G. F. Mazenko, 1982, Phys. Rev. A **26**, 1735.
Ramaswamy, S., and M. Rao, 2001, C. R. Acad. Sci. Paris, Série IV **2**, 817.
Ramaswamy, S., and M. Rao, 2007, New J. Phys. **9**, 423.
Ramaswamy, S., R. A. Simha, and J. Toner, 2003, Europhys. Lett. **62**, 196.
Ramaswamy, S., J. Toner, and J. Prost, 2000, Phys. Rev. Lett. **84**, 3494.
Ranft, J., M. Basan, J. Elgeti, J.-F. J. Joanny, J. Prost, and F. Jülicher, 2010, Proc. Natl. Acad. Sci. U.S.A. **107**, 20 863.
Reichenbach, T., T. Franosch, and E. Frey, 2006, Phys. Rev. Lett. **97**, 050603.
Reynolds, C. W., 1987, Computer Graphics **21**, 25 (SIGGRAPH '87 Conference Proceedings).
Romanczuk, P., M. Bär, W. Ebeling, B. Lindner, and L. Schimansky-Geier, 2012, Eur. Phys. J. Special Topics **202**, 1.
Saintillan, D., 2010, Exp. Mech. **50**, 1275.
Saintillan, D., 2012, in *Natural Locomotion in Fluids and on Surfaces: Swimming, Flying, and Sliding*, edited by S. Childress, A. Hosoi, W. W. Schultz, and Z. J. Wang (Springer, New York).
Saintillan, D., and M. J. Shelley, 2007, Phys. Rev. Lett. **99**, 058102.
Saintillan, D., and M. J. Shelley, 2008a, Phys. Rev. Lett. **100**, 178103.
Saintillan, D., and M. J. Shelley, 2008b, Phys. Fluids **20**, 123304.
Salbreux, G., J. F. Joanny, J. Prost, and P. Pullarkat, 2007, Phys. Biol. **4**, 268.
Salbreux, G., J. Prost, and J. F. Joanny, 2009, Phys. Rev. Lett. **103**, 058102.

Sanchez, T., D. N. Chen, S. J. DeCamp, M. Heymann, and Z. Dogic, 2012, Nature (London) **491**, 431.
Sankararaman, S., G. I. Menon, and P. B. S. Kumar, 2004, Phys. Rev. E **70**, 031905.
Sankararaman, S., and S. Ramaswamy, 2009, Phys. Rev. Lett. **102**, 118107.
Sarkar, J., and A. Sharma, 2010, Langmuir **26**, 8464.
Sarkar, N., and A. Basu, 2011, Eur. Phys. J. E **34**, 1.
Schaller, V., C. Weber, E. Frey, and A. R. Bausch, 2011, Soft Matter **7**, 3213.
Schaller, V., C. Weber, C. Semmrich, E. Frey, and A. R. Bausch, 2010, Nature (London) **467**, 73.
Schaller, V., C. A. Weber, B. Hammerich, E. Frey, and A. R. Bausch, 2011, Proc. Natl. Acad. Sci. U.S.A. **108**, 19183.
Schwarz-Linek, J., C. Valeriani, A. Cacciuto, M. E. Cates, D. Marenduzzo, A. N. Morozov, and W. C. K. Poon, 2012, Proc. Natl. Acad. Sci. U.S.A. **109**, 4052.
Schweitzer, F., 2003, *Brownian Agents and Active Particles: Collective Dynamics in the Natural and Social Sciences* (Springer, Berlin).
Serra-Picamal, X., V. Conte, R. Vincent, E. Anon, D. T. Tambe, E. Bazellieres, J. P. Butler, J. J. Fredberg, and X. Trepat, 2012, Nat. Phys. **8**, 628.
Shi, X., and Y. Ma, 2010, arXiv:1011.5408.
Simha, R. A., and S. Ramaswamy, 1999, Phys. Rev. Lett. **83**, 3285.
Simha, R. A., and S. Ramaswamy, 2002a, Phys. Rev. Lett. **89**, 058101.
Simha, R. A., and S. Ramaswamy, 2002b, Physica (Amsterdam) **306A**, 262.
Small, J. V., T. Stradal, E. Vignal, and K. Rottner, 2002, Trends Cell Biol. **12**, 112.
Sokolov, A., M. Apadoca, B. A. Grzybowski, and I. S. Aranson, 2010, Proc. Natl. Acad. Sci. U.S.A. **107**, 969.
Sokolov, A., and I. S. Aranson, 2009, Phys. Rev. Lett. **103**, 148101.
Stone, H., 2005, Chem. Eng. Sci. **60**, 4838.
Sumino, Y., K. H. Nagai, Y. Shitaka, D. Tanaka, K. Yoshikawa, H. Chaté, and K. Oiwa, 2012, Nature (London) **483**, 448.
Surrey, T., F. J. Nédélec, S. Leibler, and E. Karsenti, 2001, Science **292**, 1167.
Szabó, B., G. J. Szolosi, B. Gonci, Z. Juranyi, D. Selmeczi, and T. Vicsek, 2006, Phys. Rev. E **74**, 061908.
Tailleur, J., and M. E. Cates, 2008, Phys. Rev. Lett. **100**, 218103.
ten Hagen, B., S. van Teeffelen, and H. Löwen, 2009, Condens. Matter Phys. **12**, 725.
Theurkauff, I., C. Cottin-Bizonne, J. Palacci, C. Ybert, and L. Bocquet1, 2012, Phys. Rev. Lett. **108**, 268303.
Tjhung, E., M. E. Cates, and D. Marenduzzo, 2011, Soft Matter **7**, 7453.
Toner, J., 2009, online lecture notes, Institut Henri Poincaré.
Toner, J., 2012a, Phys. Rev. Lett. **108**, 088102.
Toner, J., 2012b, Phys. Rev. E **86**, 031918.
Toner, J., and Y. Tu, 1995, Phys. Rev. Lett. **75**, 4326.
Toner, J., and Y. Tu, 1998, Phys. Rev. E **58**, 4828.
Toner, J., Y. Tu, and S. Ramaswamy, 2005, Ann. Phys. (Amsterdam) **318**, 170.
Trepat, X., M. R. Wasserman, T. E. Angelini, E. Millet, D. A. Weitz, J. P. Butler, and J. J. Fredberg, 2009, Nat. Phys. **5**, 426.
Vallotton, P., G. Danuser, S. Bohnet, J.-J. Meister, and A. Verkhovsky, 2005, Mol. Biol. Cell **16**, 1223.
Verkhovsky, A. B., T. M. Svitkina, and G. B. Borisy, 1999, Curr. Biol. **9**, 11.
Vicsek, T., A. Czirók, E. Ben-Jacob, I. Cohen, and O. Shochet, 1995, Phys. Rev. Lett. **75**, 1226.
Voituriez, R., J. F. Joanny, and J. Prost, 2005, Europhys. Lett. **70**, 404.
Voituriez, R., J. F. Joanny, and J. Prost, 2006, Phys. Rev. Lett. **96**, 28102.
Wan, M., C. O. Reichhardt, Z. Nussinov, and C. Reichhardt, 2008, Phys. Rev. Lett. **101**, 018102.
Wensink, H., J. Dunkel, S. Heidenreich, K. Drescher, R. Goldstein, H. L en, and J. Yeomans, 2012, Proc. Natl. Acad. Sci. U.S.A. **109**, 14 308.
Wensink, H. H., and H. Löwen, 2008, Phys. Rev. E **78**, 031409.
Wolgemuth, C., E. Hoiczyk, D. Kaiser, and G. Oster, 2002, Curr. Biol. **12**, 369.
Wolgemuth, C. W., 2008, Biophys. J. **95**, 1564.
Wu, X.-L., and A. Libchaber, 2000, Phys. Rev. Lett. **84**, 3017.
Wu, Y., Y. Jiang, A. D. Kaiser, and M. Alber, 2011, Phys. Biol. **8**, 055003.
Yamada, D., T. Hondou, and M. Sano, 2003, Phys. Rev. E **67**, 040301.
Yang, Y., V. Marceau, and G. Gompper, 2010, Phys. Rev. E **82**, 031904.
Yoshinaga, N., J. F. Joanny, J. Prost, and P. Marcq, 2010, Phys. Rev. Lett. **105**, 238103.
Zhang, H. P., A. Be'er, E.-L. Florin, and H. L. Swinney, 2010, Proc. Natl. Acad. Sci. U.S.A. **107**, 13 626.
Ziebert, F., I. S. Aranson, and L. S. Tsimring, 2007, New J. Phys. **9**, 421.
Ziebert, F., and W. Zimmermann, 2004, Phys. Rev. E **70**, 022902.
Ziebert, F., and W. Zimmermann, 2005, Eur. Phys. J. E **18**, 41.
Zwanzig, R., 2001, *Nonequilibrium Statistical Mechanics* (Oxford University Press, Oxford, UK).